UNIVERSITÀ DEGLI STUDI DI MILANO

GRADUATE SCHOOL IN PHARMACOLOGICAL SCIENCES

Department of Pharmacological and Biomolecular Sciences

PhD. in Pharmacological Sciences,

XXVI° cycle

THE ROLE OF THE ACTIN CAPPING PROTEIN EPS8 IN EXCITATORY SYNAPSE FORMATION AND FUNCTION

BIO/14

Stefania Zambetti

R09296

Tutor: Prof. Michela Matteoli

Co-tutor: Dr. Elisabetta Menna

Director: Prof. Alberto Panerai

Academic year 2012-2013

Table of contents

Abbreviation list

Abi1, abl-interactor 1

AKT, AKT8 virus oncogene cellular homologue

AMPA, α-Amino-3-hydroxy-5-methyl-4-isoxazolepropionic acid

Arp2/3, Actin-related protein 2/3

BDNF, Brain-derived neurotrophic factor

CAMK, Ca2+/calmodulin-dependent protein kinase

CapZ, capping protein muscle Z-line

Cdc42, Cell division control protein 42 homolog

Cp, capping protein

Ena/VASP, enabled/vasodilator-stimulated phosphoprotein

Eps8, epidermal growth factor receptor pathway substrate 8

ERK, extracellular regulated MAP kinase

FMRP, fragile X mental retardation protein

FRAP, fluorescence recovery after photobleaching

FRET, Förster resonance energy transfer

GABA, gamma-aminobutyric acid

GAP, GTPase-Activating Protein

GEF, GTPase-exchange factor

GEFT, GTPase-exchange factor

GFP, green fluorescence protein

JNK, c-Jun N-terminal kinase

LIMK, LIM domain kinase 2

MAPK, mitogen-activated protein kinase

mDia2, diaphanous-related formin 3

MDM2, mouse double minute 2 homolog

MEF2, myocyte enhancer factor-2

mEPSC, miniature excitatory postsynaptic current

MLCK, myosin light-chain kinase

mTOR, mammalian target of rapamycin

PAK, p21 protein (Cdc42/Rac)-activated kinase 1

PIX, phosphatidylinositol kinase

PSD95, postsynaptic density 95

RAS, Rat sarcoma

RND1, Rho family GTPase 1

RFP, red fluorescence protein

SHANK, SH3 and multiple ankyrin repeat domains protein

siRNA, small interference RNA

SNARE, SNAP (soluble NSF attachment protein) receptor proteins

Tiam1, T-cell lymphoma invasion and metastasis-inducing protein 1

TTX, tetrodotoxin

vGLUT1, vesicular glutamate transporter 1

WAVE, Wiskott–Aldrich syndrome protein

SUMMARY

Our group has previously demonstrated the role of Eps8 (epidermal growth factor receptor pathway substrate 8) in regulating the formation of synapse-precursor structures in cultured hippocampal neurons. Indeed, neurons lacking Eps8 showed an increased number of axonal and dendritic filopodia, whereas the overexpression of this protein induced the formation of flat structures resembling lamellipodia. Moreover, we have demonstrated that the capping activity of Eps8 is regulated by BDNF. Indeed, upon BDNF stimulation, Eps8 is phoshorylated by MAPK, pEps8 detaches from the barbed ends of actin filaments, thus allowing the growth of new filopodia. Accordingly, Eps8 null neurons are no longer able to increase filopodia density upon BDNF stimulation [1].

Within the mouse brain Eps8 acts mainly as a capping protein [1]. Its role in the formation of filopodia –synapse-precursor structures- and in the BDNF pathway prompted us to further investigate the involvement of Eps8 in synaptic contact formation and function. To this aim, wt and null animals were subjected to learning and memory tasks. Eps8 KO mice showed a serious impairment in spatial, episodic memory and social behavior; these defects were associated also with an increased density of excitatory synapses and alteration of dendritic spine morphology of CA1 hippocampal pyramidal neurons. Moreover, the formation of new dendritic spines which normally occurs during memory formation was completely absent in mutated mice. In order to elucidate the molecular and cellular basis of such defects, cultured hippocampal neurons were established from both wt and Eps8 KO mice. Null cultures displayed an increase density of excitatory synapses and dendritic spines, which also presented immature features when compared with aged-matched wt cultures. In addition Eps8 null cultures were not able to undergo synaptic potentiation upon stimulation with a chemical LTP protocol. Transfection

of neurons with cDNAs encoding for Eps8 wt or for a capping mutant (named Eps8H1) allowed us to dissect the involvement of capping activity in the process of synapse formation and maturation. In fact neurons expressing wt protein displayed an increased number of synapses and bigger spines; conversely, such modifications were not induced by the H1 capping mutant expression. We also showed that the capping activity of Eps8 is necessary for the expression of LTP. Indeed, the injection of a synthetic peptide which inhibits the Eps8 capping activity into the postsynaptic neuron via the patch pipette prevented synaptic potentiation. Finally, we found that Eps8 levels were significantly decreased in the brain of autistic patients suggesting that Eps8 may be involved in the pathogenesis of autism.

INTRODUCTION

NEUROPSYCHIATRIC DISORDERS AS SYNAPSE DISEASES

Neuropsychiatric and neurodegenerative disorders – such as autism spectrum disorders (ASD), intellectual disabilities (ID), schizophrenia (SZ) and Alzheimer's diseases (AD) – deeply compromise the quality of life of both patients and their relatives, posing an immense burden to society. The above-mentioned disorders are characterized by a severe impairment on information processing and cognition, associated with abnormal neuronal connectivity and plasticity [2, 3].

ASD patients present disrupted social interaction, delayed or absent verbal communication and repetitive behaviors [2-6]. Moreover, these patients are often suffering of ID and/or epilepsy [7-11]. ASD affect 0.9% of children, with a diagnosis occurring around 2-3 years of age [4, 12], the time of human synapse formation and maturation [5]. Interestingly, recent studies have revealed an increased spine density and abnormal spine morphology in frontal, temporal and parietal lobes of ADS patients (Fig.1) [13, 14]. Furthermore, several mutations in synaptic molecules including neuroligin [15], neurexin [16] and Shank [17-19] have been identified in autistic subjects.

ID affect about 2-3% of children and young adults and are commonly classified as mild (50<QI<70) to severe (QI<70) [3, 20]. ID are an extremely heterogeneous conditions that may result from both non-genetic (such as maternal intoxication, prematurity, ischemia or infection) and genetic factors that overall affect cognitive functions [20], [3]. Several mutated genes causing both syndromic and non-syndromic

ID have been identified and most of them are located on X chromosome [3, 20]. Despite the diverse factors that could lead to ID, these pathologies have been consistently associated with abnormal dendrites and dendritic spines, the postsynaptic specialization of excitatory synapses [21-23].

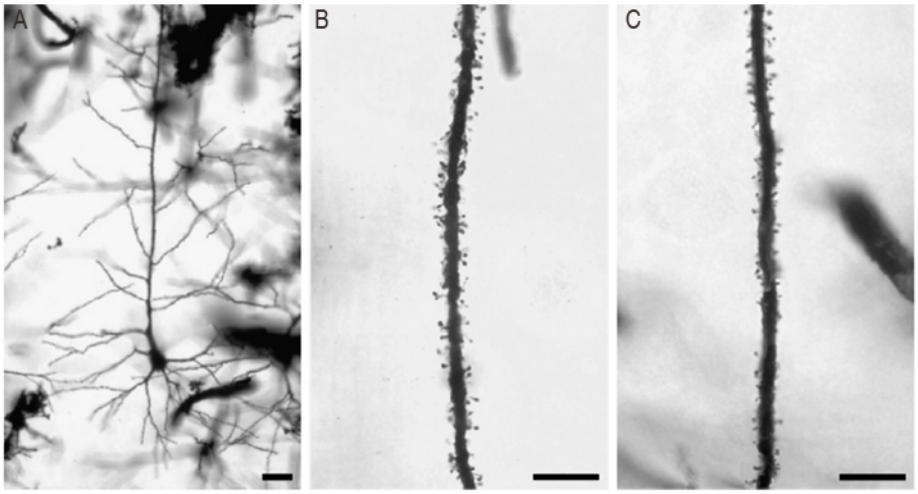

Figure 1. ***Alteration of dendritic spines morphology in ADS***. *(A) An example of a Golgi-impregnated pyramidal cell in layer III of the superior frontal gyrus in an ASD case. (B and C) Apical dendrite segments showing spine densities of layer V pyramidal cells in the superior frontal gyrus of ASD (B) and control subjects (C). Both examples are approximately 300 μm from the cell soma. Scale bare in (A) 25 μm; in (B and C) 20 μm. From Hutsler and Zhang (2009).*

SZ is a complex developmental psychiatric disorder affecting thought, perception of reality, emotion and cognition, which affects approximately 0.5-1% of the population [3, 12]. It is generally characterized by positive (i.e. hallucination, delusion, disorganized thoughts) and negative (i.e. reduced affect and social withdrawal) symptoms, associated with abnormal executive functions [24, 25]. Typically positive symptoms rise in late adolescence or early adulthood; whereas negative ones and cognitive dysfunction could be observed earlier in the development [3]. Alterations of glutamate, GABA and dopamine transmission have been implicated in the development of SZ [26-30].

Alzheimer disease is a neurodegenerative pathology with typically onset of age 65, characterized by a progressive loss of memory, critical thought and impairment in cognitive functions [31]. Dementia affects an estimated 35.6 million of people, and AD represents the most common form of dementia [2]. Although amyloid plaques, neurofibrillary tangles and cell death are well described AD hallmarked, recent data strongly implicate synapse dysfunction as a central player in AD pathology, providing evidence that synaptic alterations precede cell death [2, 31, 32].

Together, these disorders span the entire human life and deeply compromise human cognitive functions and everyday life. Despite their differences in symptoms, emerging evidences in the last decade strongly indicate a common substrate for all of those disorders: a dysfunction of synaptic contacts (Fig.2) and, as a consequence, of neuronal circuits [2, 3]. Given a single neuron usually receives hundreds or thousands of excitatory and inhibitory inputs which impact the firing activity of the receiving neuron following a complex process of synaptic integration, defects in synaptic proteins and in synapse formation would lead to abnormal synaptic transmission, disrupting the excitatory/inhibitory (E/I) balance in the postsynaptic neurons and altering the normal information processing and circuit function [6]. Indeed, alterations of E/I balance has been involved in many neuropsychiatric disorders, such as autism spectrum disorders and schizophrenia [33-36]. Consistently, it has been recently demonstrated that a shift of E/I balance toward excitation in the mouse medial prefrontal cortex (mPFC) induced by optogenetic stimulation causes social impairment in mice [37].

Intriguingly, the majority of neuropsychiatric disorder-related genes codify for synaptic proteins or factors that control synaptic protein

expression or their function [3, 4, 38]. Moreover, numerous animal models in which those genes are mutated or deleted closely reproduce human pathologies. For example mutations of SHANK proteins, a family of postsynaptic scaffolds, have been described in autistic and ID subjects [17, 19, 39-41]. Studies in mice in which mutations or deletions of SHANK genes have been induced have clearly

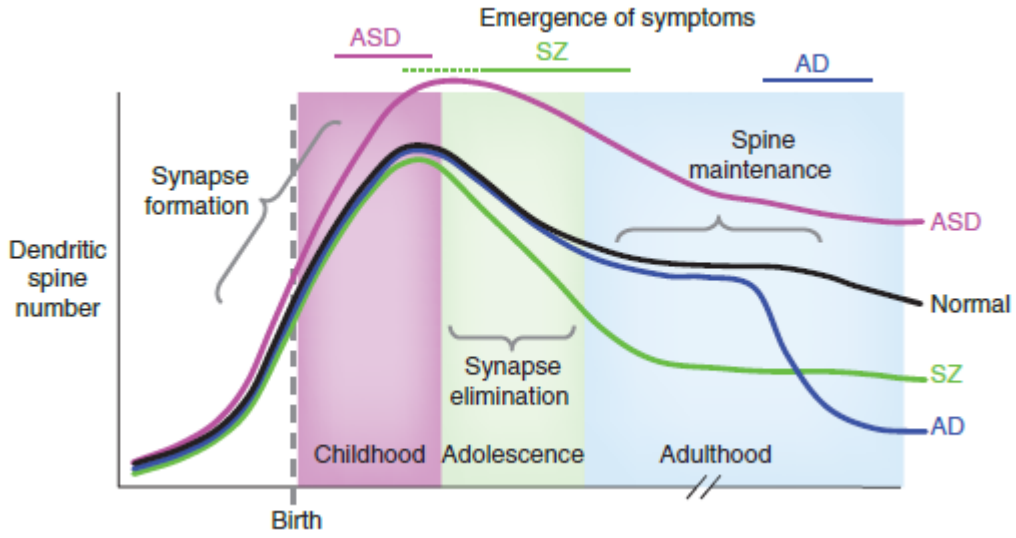

Figure 2. Dendritic spines alterations are a common feature of neuropsychiatric disorders. *Putative lifetime trajectory of dendritic spine number in a normal subject (black), in ASD (pink), in SZ (green) and in AD (blue). Bars across the top indicate the period of emergence of symptoms and diagnosis. In normal subjects, spine numbers increase before and after birth; spines are selectively eliminated during childhood and adolescence to adult levels. In ASD, exaggerated spine formation or incomplete pruning may occur in childhood leading to increased spine numbers. In SZ, exaggerated spine pruning during late childhood or adolescence may lead to the emergence of symptoms during these periods. In AD, spines are rapidly lost in late adulthood, suggesting perturbed spine maintenance mechanisms that may underlie cognitive decline. From Penzes et al. (2011).*

demonstrated abnormal synaptic structure and function, as well as cognitive impairment and behavior alterations, such as reduced social interaction and hyperactivity [6, 42-47]. Indeed, *Shank3* heterozygouse mice display reduced miniature excitatory postsynaptic current (mEPSC) amplitude and basal synaptic transmission [42]; whereas mice with deletion of exon 4-9 of *Shank3* are socially impaired and exhibit alteration in dendritic spine morphogenesis and defective synaptic plasticity [44].

Furthermore aberrant levels of LIMK1, an important synaptic signaling protein controlling the spine cytoskeleton [48], is implicated in Williams syndrome, a mental disorder with severe defects in visuospatial cognition [49]. LIMK1 is a serine kinase highly enriched in the synaptic compartment and it is activated downstream Rac pathway activation. Once activated LIMK1 phosphorylates and inhibits cofilin, an actin depolymerizing and serving factor, leading to accumulation of actin filaments (F-actin) [48, 50]. The structure of presynaptic terminals and postsynaptic spines is determined by a number of factors, the best established of which is the actin cytoskeleton. The dynamic assembly and disassembly of the actin cytoskeleton is tightly regulated by a variety of actin binding proteins (ABPs) and by synaptic activity [38, 51]. Indeed it is not surprising that LIMK1 mutated neurons show alteration of dendritic spine morphology and defects of synaptic plasticity [52, 53]. In addition, protochaderin10 (Pcdh10), an ASD associated gene, was recently implicated in the activity dependent synapse elimination through PSD-95 ubiquitination. In fact, upon MEF2 activation, PSD-95 is ubiquitinated by Mdm2 and then binds to Pcdh10, which links it to proteasome for degradation [54]. MEF2 cooperates with FMRP to regulates the expression of Pcdh10. Inhibition of the interaction between Pcdh10 and the proteasome blocks PSD-95 degradation and synapse elimination [54], suggesting a possible mechanism involved in the abnormal synapse refinement occurring in fragile X syndrome (XFra). PSD-95 not only is a key component of excitatory synapses but also plays a fundamental role during the process of synapse formation [55, 56]. As a consequence, the content of PSD-95 at the synaptic level is tightly regulated. Interleukin 1 receptor associated protein-like 1 (IL1RAPL1) is an ASD associated gene that encodes for a synaptic transmembrane protein [57]. Interestingly, IL1RAPL1 is involved in formation and

stabilization of excitatory synapses by recruiting PSD-95 at the synaptic level through JNK signaling pathway [58]. In addition, IL1RAPL1 induced the presynaptic differentiation through its trans-synaptic interaction with protein tyrosine phosphatases δ [59, 60]. As a consequence of this interaction RhoGAP2 is recruited to excitatory synapses thus promoting dendritic spine formation [59]. Furthermore IL1RAPL1 is involved in the development of inhibitory circuits in the cerebellum, an ASD-related brain region [6], regulating the E/I balance as determined by a study using *il1rapl1-/-* mice [61]. Finally, primary hippocampal neurons from mice carrying the hemizygose deletion of the chromosome 22, where the IL1RAPL1 gene is located, display reduced spine density and size [62]. The 22q11.2 microdeletion syndrome is the most common copy number variation associated with SZ [63]. Interestingly, the loss of the two genes within this region is sufficient to compromise dendritic spine morphology, thus suggesting that genetic information encoded in this chromosomic region is crucial for spine formation. Notably, one of the two genes is ZDHHC8 which encodes for a palmitoyl transferase responsible for PSD-95 palmitoylation [62], a posttranslational modification responsible for PSD-95 synapse targeting [64].

From this point of view ADS, ID, SZ and AD could be described as different faces of a same disease in which the specific symptoms and age of onset derive from the specific synaptic pathway affected (Fig.2) [2, 3]. As a consequence, important effort has been made to understand the mechanisms that govern synapse formation and function, in order to determine pathways in which risk proteins are involved, with the aim to identify new candidate genes and innovative therapeutic approaches. In fact, emerging evidence suggest that it is possible improve cognitive function of patients suffering of neuropsychiatric disorders modulating

the affected pathway or different pathways which play a redundant role [2, 65-68].

EXCITATORY SYNAPSES AND DENDRITIC SPINES

Human brain consists of more than 10^{11} neurons, which process and transmit information via electrical signals. Communication between neurons occurs at specialized cellular junctions, the majority of which are chemical synapses [69, 70]. The precise control of synaptic contact formation and function is critical for maintaining proper neuronal network connectivity and activity, and ultimately for normal brain function [5]. Furthermore, it is widely accepted that information in the brain is stored by formation and elimination of synaptic contacts and/or in form of structural and biochemical modifications of the preexistent ones [71-77].

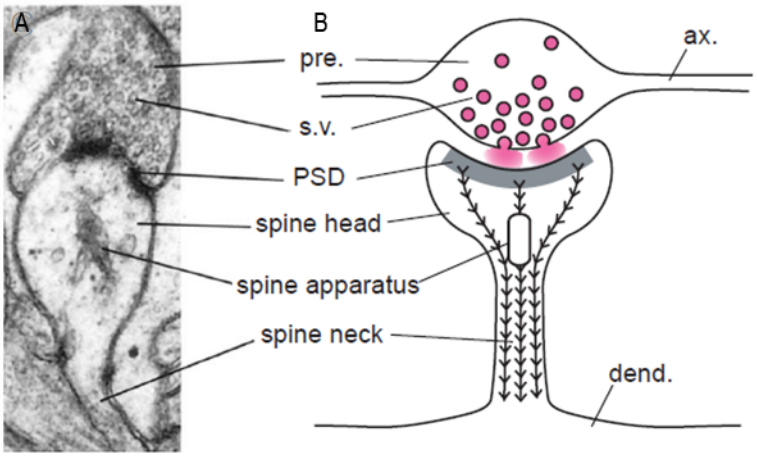

Figure 3. Excitatory synapse structure. *(A) A single spine synapse seen by electron microscopy, and (B) a diagram of a spine structure. The neurotransmitter glutamate (pink) is stored within synaptic vesicles*

and released into the synaptic cleft where it activates receptors located in the postsynaptic density (PSD). Actin filaments are represented by the barbed lines. ax., axon; pre., presynaptic bouton; dend., shaft of dendrite; s.v., synaptic vesicle. From Matus (2000).

Chemical synapses are asymmetrical junctions consisting of a presynaptic axon terminal harboring synaptic vesicles and a postsynaptic compartment enriched in neurotransmitter receptors (Fig.3) [69, 78, 70, 79, 80]. Pre-and postsynaptic sites are separated by a narrow gap (20-25 nm) named synaptic cleft, in which the neurotransmitters are released [70, 81]. A variety of synaptic adhesion and extracellular matrix proteins hold pre- and postsynaptic membrane together at the appropriate separation (Fig.9B) [69, 71] and cooperate to maintain the proper synaptic function [82-84].

The presynaptic compartment is an axon specialization in which electrical signals carried by action potential are transduced into a chemical signals through the release of neurotransmitter (Fig.4) [73, 85]. Synaptic vesicles (SVs) are the most prominent feature of presynaptic sites (Fig.4B,C) [80, 86, 87]. They are specialized organelles containing

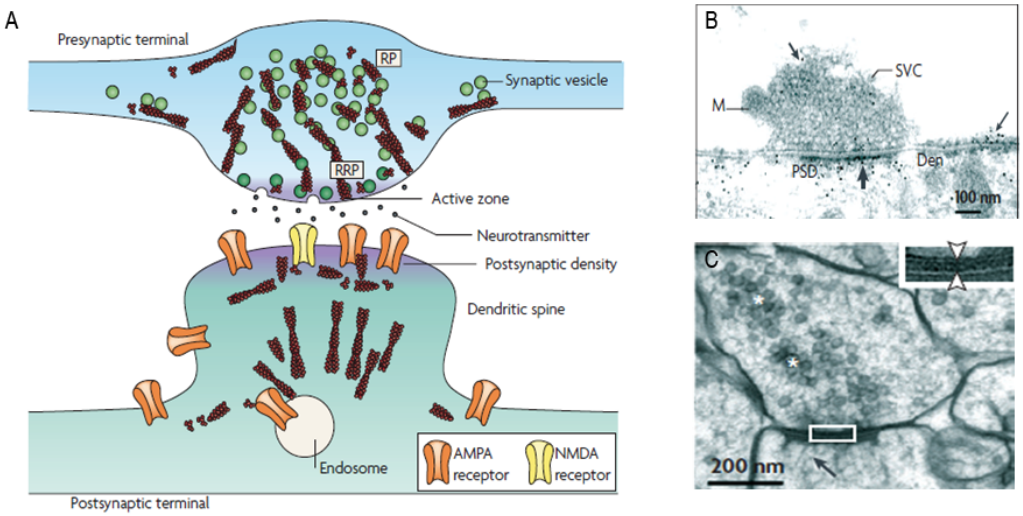

***Figure 4. The presynaptic compartment**. (A) Structure of presynaptic compartment. At the presynaptic terminal some SVs (readily releasable pool, RRP) are docked at the AZ, where they undergo exocytosis to release neurotransmitters. Numerous vesicles that belong to the reserve pool (RP) are located centrally, where they are interlinked by short actin filaments. The subgroups are linked by longer filaments to the plasma membrane and to the AZ. Postsynaptically, the spine harbors AMPA and NMDA receptors at the*

PSD, which lies opposite the presynaptic AZ. (B) Electron micrograph of a lamprey reticulospinal synapse, showing actin localization by immunogold labelling. The arrows indicate label actin. Actin is present scattered within the synaptic vesicle cluster (SVC) (intermediate-thickness arrow) and below the PSD (thickest arrow) in the dendrite (Den). It is also present at the endocytic zone that surrounds the AZ (thinnest arrow). M=mitochondrion. (C) Electron micrograph of a hippocampal synapse from a sample that was subjected to high-pressure freezing. Synaptic vesicles are interlinked by small filaments and are grouped into smaller clusters (asterisks). Long filaments extend from the PSD (arrow). From Cingolani and Goda (2008).

neurotransmitter molecules and localized nearby the thickening of plasma membrane, named active zone (AZ), where SVs fused and neurotransmitter exocytosis take places [80, 86, 88, 89]. SVs are organized by a complex cytomatrix composed by actin filaments and regulatory proteins which furthermore act synergically to regulate SVs availability (Fig.4C) [80, 86, 88]. Probably, the better characterized of those regulatory proteins belong to the SNARE complex, which regulates the docking and the calcium dependent fusion of SVs at the presynaptic plasma membrane [86, 89, 90]. The complex molecular mechanism underlying SV exocytosis has been largely elucidated by the seminal contribution of Thomas Sudhof which has been awarded with the Nobel Prize this year.

The neurotransmitters released from the presynaptic terminal act on appropriate neurotransmitter receptors localized on plasma membrane of postsynaptic neurons [78]. Whether a synapse is excitatory or inhibitory is a function of the type of receptors and neurotransmitters operating at the synapse, which ultimately determine the postsynaptic current displayed. Synaptic receptors are classically subdivided in two groups: the inotropic receptors mediating fast synaptic response and the G protein-coupled receptors responsible of the metabotropic signaling [91-93]. The excitatory synaptic transmission is mainly regulated by AMPA and NMDA glutamate receptor activation [94-96]; whereas the

activation of inotropic $GABA_A$ receptors provides the prominent inhibitory transmission in mature neurons [34, 97].

The inhibitory and excitatory synapses of the CNS express a different array of specific proteins. Synaptic vesicles, which contain GABA or glutamate neurotransmitters, fuse with the plasma membrane at the active zone. Numerous adhesion proteins span the synaptic cleft, holding the pre- and postsynaptic membranes close and in fixed positions. Neurotransmitter receptors are located on the postsynaptic membrane, opposite the sites of fusion of synaptic vesicles, where they arrange in macromolecular complexes which also encompass a large number of structural (scaffold, gephyrin, homer, PSD-95, shank) and signaling (like CaMKII) proteins. These components account for the postsynaptic density, which has the main function of receiving and transmitting signals. In the CNS, glutamatergic excitatory synapses typically form on dendritic spines, while inhibitory GABAergic synapses can be found on the dendritic branch or on the soma. The presence of a prominent postsynaptic complex, named postsynaptic density (PSD, Fig.5), is an hallmark of the excitatory synapses [78, 98, 99], whereas inhibitory synapses does not show such electron dense thickness within the postsynaptic compartment [81, 99, 100, 101].

The PSD contains, therefore, a huge number of molecules including glutamate receptors (NMDA-, AMPA- and KA- type), scaffold proteins such as PSD-95 and Shank [102, 103], signaling molecules as CaMK and MAP kinase [104-107], and finally actin filaments and actin regulatory proteins (Fig.5A) [38, 98, 108, 109]. The latter play a fundamental role either in maintaining synaptic structure and function, thus regulating the dynamic changes that ultimately are at the base of cognitive functions such as learning and memory (Fig.5B) [108, 110, 51, 98, 111-114].

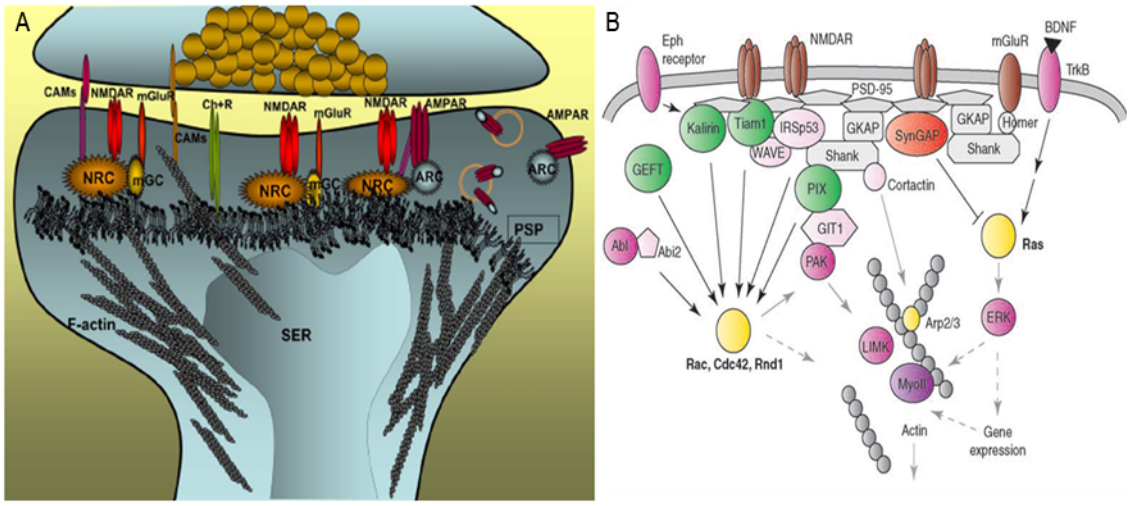

Figure 5. The postsynaptic compartment. *(A) PSD organization. ProSAP/Shank molecules create a dense platform (ProSAP/Shank platform, PSP) within the PSD by self-association. PSP is attached to the actin cytoskeleton and, if present, with the smooth endoplasmic reticulum (SER). The synaptic backbone structure co-clusters NMDAR complexes (NRC) and mGluR complexes (mGC). AMPARs are targeted and recycled within the PSD/spine compartment by proteins of the AMPAR complex (ARC). The pre- and postsynaptic membrane is held in register by cell adhesion molecules (CAMs). Several different channels and receptors (Ch+R), are directly clustered by ProSAP/Shank molecules. From Boeckers (2006). (B) Example of ABPs within dendritic spines. The GTPase Rac1, Cdc42, Rnd1 and Ras promote spine formation and growth. Cell surface receptors (EphR and NMDAR) activate GEF (GEFT, kalirin, Tiam1, PIX) to stimulate Rac1, Cdc42 and/or Rnd1. Rac and Cdc42 regulate actin cytoskeleton, in part by stimulating PAK and myosin II activity. IRSp53, Abi2 and WAVE are adaptor proteins involved in signaling to Rac and Cdc42. WAVE and cortactin regulate the Arp2/3 complex and actin branching. NMDAR and TrkB stimulate the Ras-ERK MAP kinase pathway, which is inhibited by the RasGAP SynGAP. From Tada and Sheng (2006).*

In projection neurons of mammalian brain, the postsynaptic sites of glutamatergic synapses are typically housed within specialized cellular compartments called dendritic spines (Fig6A,B) [72, 115]. Dendritic spines (Fig.5A and Fig6C, bottom) are small membranous protrusions that rise from dendrites [72, 115] and contain glutamate receptors and ion channels [78], the PSD [99], actin filaments and actin binding proteins [109, 116, 117], a variety of membrane bound organelles such as smooth endoplasmatic reticulum, mitochondria [118] and finally ribosomes [119].

Typically dendritic spines are characterized by a bulbous head and are connected to parental dendrites by a narrow neck (Fig.6C, bottom)

[72, 111, 120]. Given their morphological appearance spines mainly allow a spatial and functional compartmentalization of synaptic signaling [114, 121-123]. One of the most striking characteristic of dendritic spines is the morphological diversity [99, 109]. Indeed, morphological studies have identified several categories of spines based on their shape and size: thin, stubby and mushroom spines (Fig.6C, top) [99, 109]. However, it is thought that this variety is not due to the existence of different types of spines, but instead reflects a temporal snapshot of a dynamic phenomenon [20]. In fact, live imaging studies have demonstrated that dendritic spines are remarkably dynamic, changing shape and size over timescale of seconds to minutes and of hours to days [72, 120].

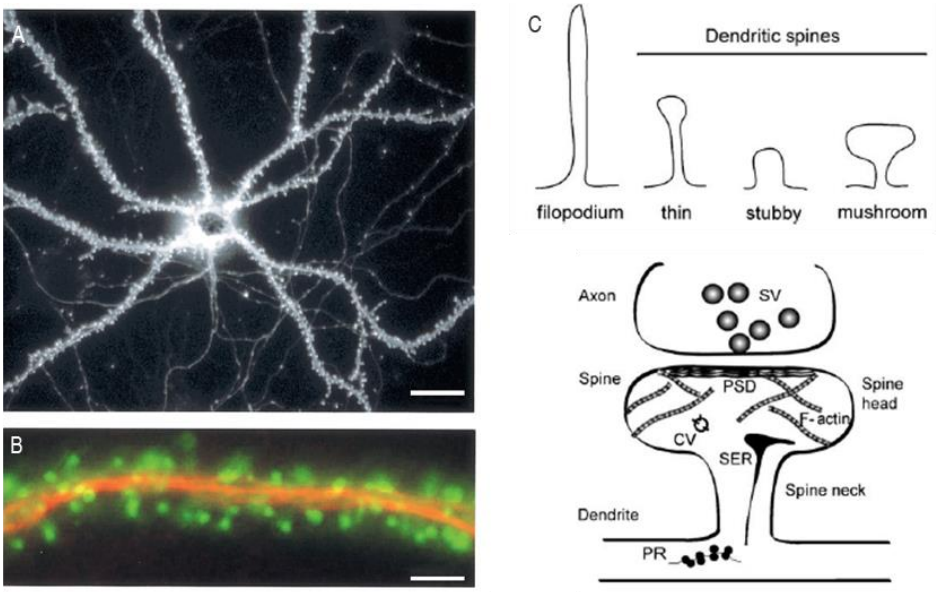

Figure 6. Principal neurons are spangled by dendritic spines. *(A) A living hippocampal neuron in cell culture expressing G-actin tagged with GFP. The myriad fluorescent dots on the dendrites are spine heads where actin accumulates. (B) Part of a dendrite from a GFP-actin expressing cell that was fixed and then stained with antibodies against the dendrite-specific microtubule protein MAP2 (red). MAP2 labeling shows microtubules concentrated in the shaft of the dendrite compared to green actin-GFP labeling of actin present in dendritic spine heads. From Matus (2000). (C, top) Schematic representation of a filopodium and the three most common types of dendritic spine morphologies. (C, bottom) Dendritic spine ultrastructure. CV, coated vesicles; PSD, postsynaptic density; PR, polyribosome; SER, smooth endoplasmic reticulum; SV, synaptic vesicles. From Ethell and Pasquale (2005). Scale bare in (A) 15 µm, in (B) 5 µm.*

This structural plasticity is thought to be essential for synaptic strength changes, thus providing a link between spine shape and functional state of synaptic contacts [72, 120, 122]. Actually it has been demonstrated the formation of new dendritic spines [124, 125] and the enlargement of preexistent ones upon induction of long term potentiation (LTP) [126-128], a protocol that mimics synaptic plasticity during learning process (Fig.7A). In contrast, low frequency stimulation used to induced long term depression (LTD) is associated with spine head shrinkage [126, 129, 130] and spine loss [126, 130]. Moreover the dimension of spine head is correlated to the size of postsynaptic density, and then to the number of AMPA receptors which are inserted in the postsynaptic membrane and to synaptic strength (Fig.7A) [51, 73, 108, 131]. Finally, recent *in vivo* studies using two photon microscopy have demonstrated that formation of new memories is striking associated with the growth of new spines (Fig.7) followed by a period of synaptic pruning [75-77] and with changes of spine shape and size [75]. Interestingly, alteration of dendritic spine density and morphology have been reported in several neuropsychiatric and neurodegenerative disorders [22], such as ASD (Fig.1) [13, 14], [132], SZ [133-135] and AD [31].

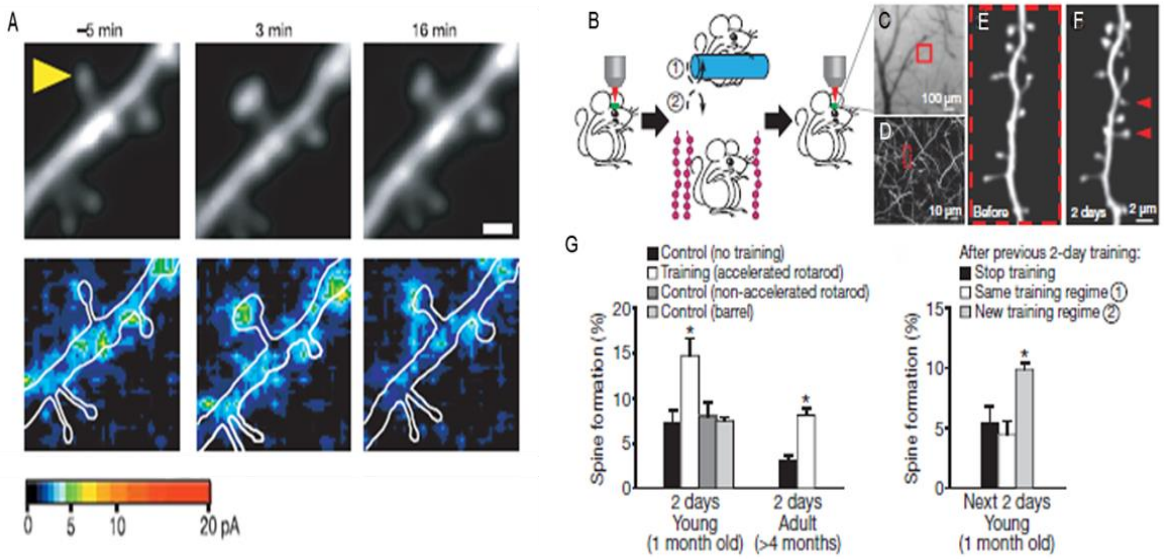

Figure 7. Structural changes of dendritic spines are tightly linked to synaptic function. *(A) Colocalization of enlargement of spine heads and potentiation of AMPAR-mediated currents. Examples of small spines that showed transient enlargement (upper panel) and potentiation of AMPA currents (lower panel). The amplitude of AMPA currents is pseudocolour coded. The neurons were depolarized to 0 mV and the small spines, indicated by the arrowheads, were stimulated by two photon uncaging of glutamate at 2 Hz between times 0 and 60 s. White lines in the lower panels indicate contours of dendrites. From Matsuzaki et al. (2004). (B) Motor learning and novel sensory experience promote rapid dendritic spine formation. Transcranial two-photon imaging of spines before and after rotarod training or sensory enrichment. (C) CCD camera view of the vasculature of the motor cortex. (D) Two-photon image of apical dendrites from the boxed region. A higher magnification view of a dendritic segment in (D) is shown in (E). (E,F) Repeated imaging of a dendritic branch before (E) and after rotarod training (F). Arrowheads indicate new spines formed over 2 days. (G) The percentage of new spines formed within 2 days in the motor cortex was significantly higher in young or adult mice after training as compared with controls with no training or running on a non-accelerated rotarod. No increase in spine formation was found in the barrel cortex after training.. After previous 2-day training, only a new training regime (reverse running) caused a significant increase in spine formation. From Yang et al. (2009). Scale bars in (A) 1 μm.*

COUPLING ACTIN DYNAMICS TO SYNAPSE PLASTICITY

Structural changes of dendritic spines and functional modulation of synaptic strength are based on the architecture and flexibility of actin cytoskeleton at the synaptic level (Fig.9B) [112, 116, 126, 136]. Actin and its regulatory proteins are highly enriched in dendritic spines (Fig.8) [116, 117, 126] where they provide structural support and regulate

vesicular and molecular trafficking [136-139]. Moreover actin cytoskeleton is also required for proper synaptic function and for activity dependent synaptic plasticity [51, 139, 140]. Indeed myosin, the actin motor protein of muscular contraction and nonmuscle motility, regulates both AMPA and NMDA receptors function. In fact it has been demonstrated that Myoisin Vb is involved in the recycling of AMPA receptor during synaptic plasticity [141] and that MLCK positively regulates NMDAR-mediated synaptic currents in an actin dependent manner [142]. Moreover, the displacement of α-actinin, an actin binding proteins that link NMDAR to actin cytoskeleton, is involved in the receptor inactivation upon calcium influx [143, 144], suggesting that alteration of actin architecture may affect the functional property of synaptic contacts and dendritic spines.

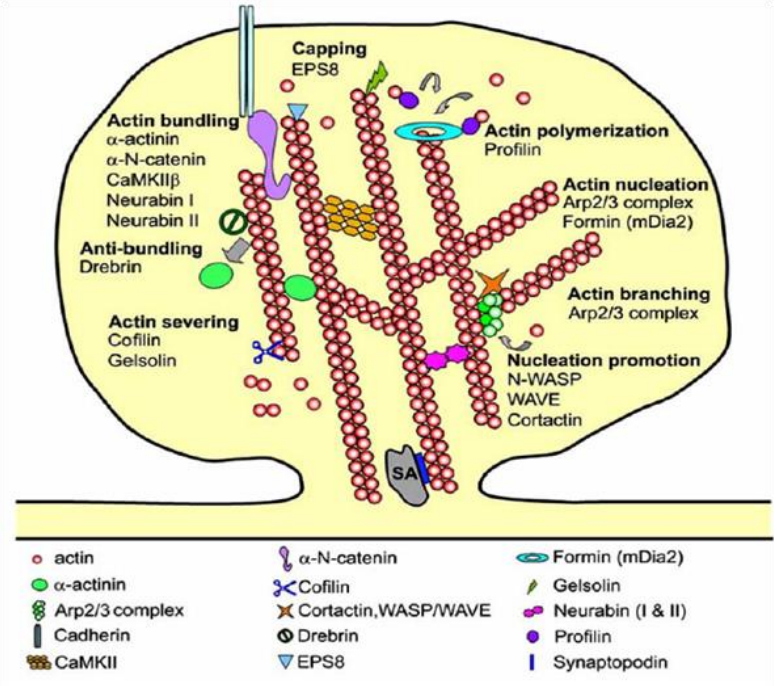

Figure 8. Schematic diagram of actin-binding proteins in dendritic spines*. Dendritic spines are enriched in actin, which is organized into branched and unbranched filaments. Reorganization and turnover of actin filaments are modulated by actin binding proteins, which regulate spine and synaptic function. The actin binding proteins shown here regulate actin capping, polymerization, nucleation, branching, severing, and bundling. SA (spine apparatus). From Lin and Webb (2009).*

Actin filaments exist in two distinct pools within dendritic spines [128]. A dynamic pool is localized at the tip of the dendritic spine and is characterized by a fast treadmilling toward the center of the spine head [116], thus providing an expansive force in order to maintain spine shape [145-147]. A stable pool is instead localized at the base of the spine. It has been proposed that its size depends on the volume of dendritic spines [116]. Moreover, during two photon glutamate uncaging at single spine level a third pool, named enlargement pool, appears and its stabilization is necessary for the long term increase of spine head [116], then supporting the involvement of actin remodeling in structural plasticity. Consistently, actin dynamics are regulated by synaptic activity and actin polymerization and depolymerization have been associated respectively with potentiation and depression of synaptic transmission (Fig.9B) [112, 126, 136, 148, 149]. Within dendritic spines actin exists in a dynamic equilibrium between globular actin (G-actin) and F-actin, which is regulated by the rate of actin polymerization [150]. A shift of this equilibrium toward F-actin occurs during tetanic stimulation [126]. Conversely, low frequency stimulation increases the G-actin content, thus promoting actin depolymerization and dendritic spine shrinking [126]. Pharmacological interfering with actin dynamics or ablation of actin binding proteins seriously affects both spine morphology and the establishment of synaptic potentiation [112, 149-154]. Consistently, a variety of actin regulatory proteins are known to be relocalized within dendritic spine in an activity dependent manner [148, 155-162] or during memory formation [163]. In addition, animal models in which actin binding and regulatory proteins are mutated show alteration of dendritic spines [164-166] and impairment in cognitive functions [167-170]. Therefore it is not surprising that a variety of actin regulators have

found to be altered or mutated in neuropsychiatric disorders [18, 38, 171-175].

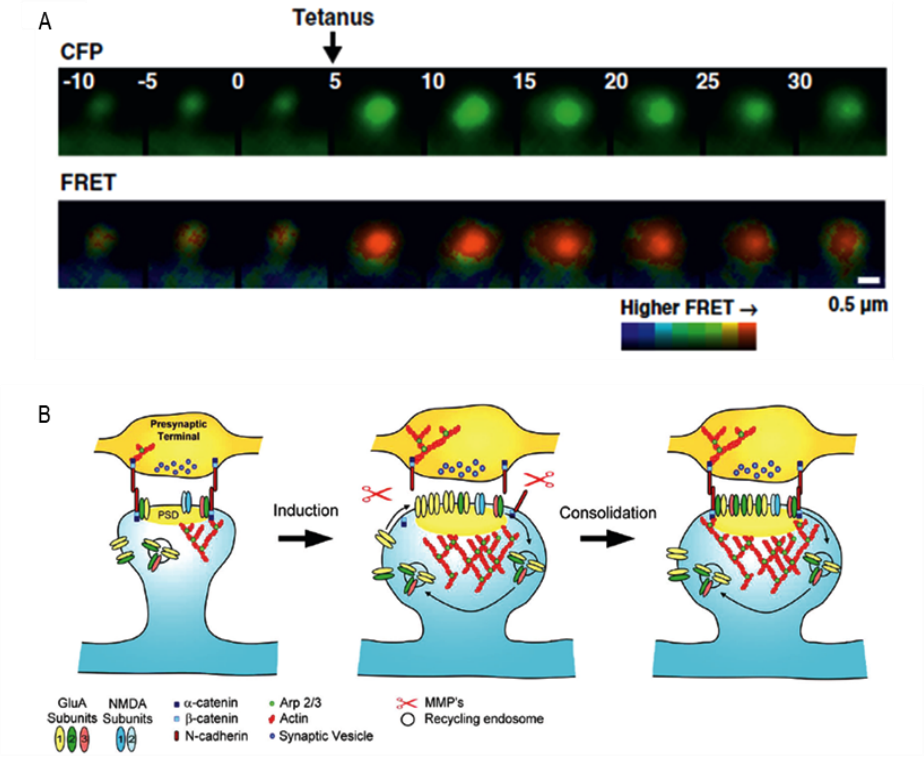

Figure 9. Actin involvement in dendritic spines remodeling. *(A) Expansion of the dendritic spine and rapid polymerization of actin by local tetanic stimulation. Actin polymerization was visualized by FRET-based imaging method, which detects the proximity of actin molecules. From Okamoto et al. (2004). (B) Model of activity-dependent spine expansion. During NMDAR–dependent LTP, GluA2-lacking AMPAR (yellow) are transiently trafficked into the synapse (middle). Activation of these Ca-permeable AMPAR then promotes actin polymerization. Actin network reorganization then sustains spine head expansion and anchors the new PSD molecules that have been recruited. In addition, matrix metalloproteinases (MMPs) are released from the postsynaptic terminal and cleave N-cadherin complexes, allowing structural modifications to take place. GluA2-lacking receptors are then replaced by GluA2-containing AMPAR (far right), and the newly potentiated synapse is then subsequently stabilized by N-cadherins. From Fortin et al. (2011). Scale bare in (A) 0,5 µm.*

Actin cytoskeleton is not only important for structural and functional plasticity, but rather it is also involved in synaptic contact formation and spine maturation [51]. In fact, during synaptogenesis filopodia emerging from dendritic shaft and axon make the first contact between the future pre- and postsynaptic compartments (Fig.10A,B) [176-180]. Then, rapid and considerable actin cytoskeleton reorganization [82, 181, 182] induced by synapse inducing factors allows

synaptic contact stabilization and the coordinate recruitment of pre- and postsynaptic machineries [71]. At the same time, the highly motile dendritic filopodia switch to a more stable structure (Fig.10B,C), the dendritic spines [177, 183]. Dendritic filopodia are distinguished from conventional filopodia [184, 185], since they contain an actin filament network consisting of branched and intersecting linear filaments (Fig.10C) [117] and are immunoposive for Arp2/3 complex and capping proteins, as well as myosin II, a component of contractile actin network [117]. On the contrary, the cross-linking protein fascin, a marker of conventional filopodia, is absent although it is present in growth cone filopodia [117, 186]. These unconventional structures would be conserved in the dendritic spine neck (Fig.10C and Fig.11)[117]. Furthermore, dendritic filopodia seem to rise from spots of branched actin filaments present within dendritic shaft (Fig.10C) [117].

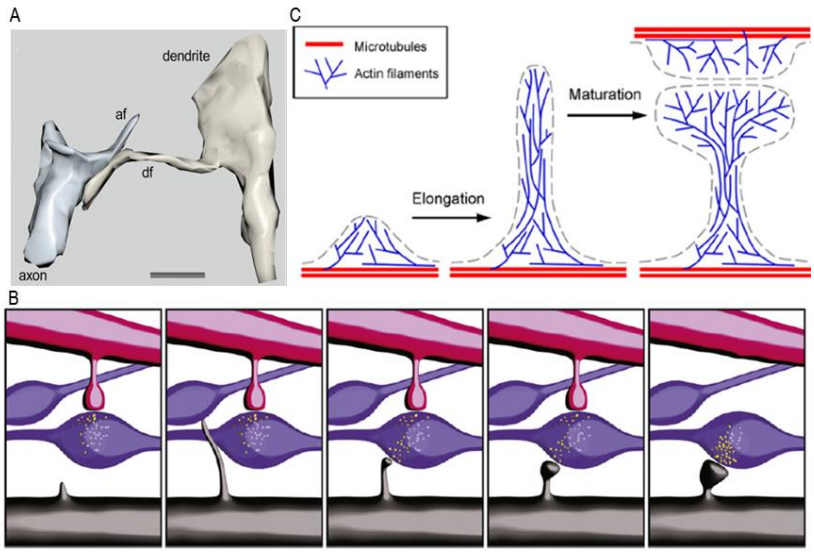

Figure 10. Model for actin cytoskeleton organization in dendritic protrusions and for spine morphogenesis. *(A) Three-dimensional interacting filopodium. From Fiala et al. (1998). (B) Schematic drawings showing the formation of a dendritic spine occurring through the initial formation of a filopodium (grey) that contacts an already-present axonal bouton (blue) connected to dendritic spine (red). From Knott and Holtmaat (2008). (C) The process of spine formation probably begins with the formation of a dendritic patch, which then elongates into a dendritic filopodium. On receiving of appropriate signals, filopodium undergoes maturation into a spine; this process probably involves the formation of a dense branched actin network, which drives the expansion of the filopodial tip into a spine*

head. Membrane is shown in gray, actin filament in blue and microtubule in red. From Korobova and Svitkina (2010). Scale bars in (A), 1 μm.

Recently, it has been demonstrated that the elongation of dendritic filopodia takes place not only from the tip but also from the roof of actin filaments and it requires the small GTPase Rif and its effector mDia2 formin (Fig.11) [166], which catalyses the nucleation and elongation of linear actin filaments by insertional assembly of monomers to the fast growing barbed ends [184]. The transition from filopodia to mature spines either during development or plasticity phenomena appears to be regulated by the GTPase Cdc42 and its effector Arp2/3 (Fig.11) [166], which nucleates branched actin filaments form preexistent ones [145, 187]. Moreover, Arp2/3 and its regulators, such as WAVE and profilins, are highly enriched in dendritic spines [113, 154, 165] (Fig.11).

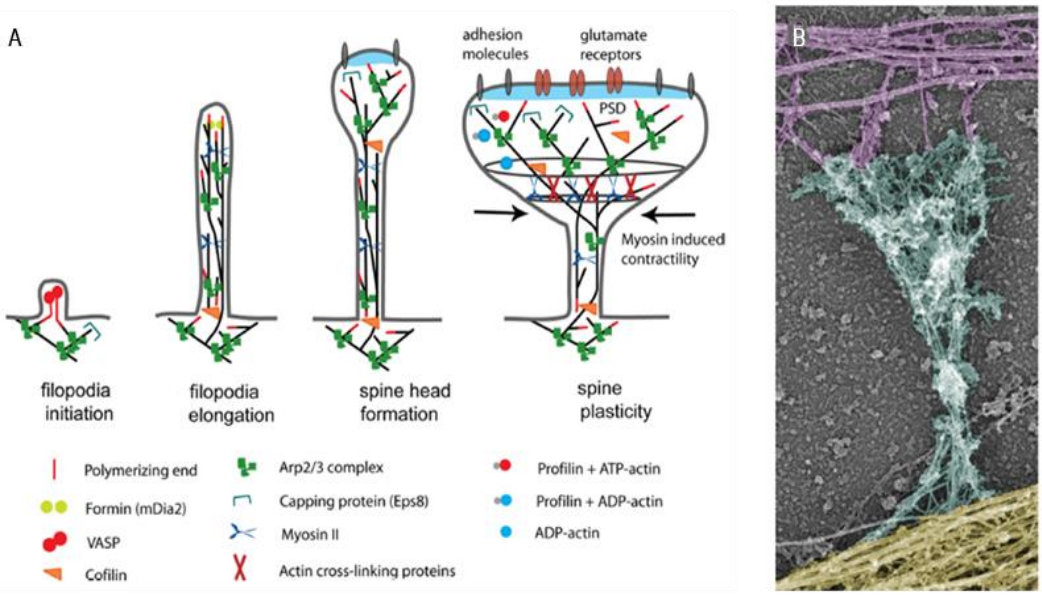

Figure 11. Actin regulatory mechanisms during spine development and plasticity. *(A) Filopodium growth, left panel. Eps8 inhibits filopodium initiation by its capping activity, whereas Ena/VASP proteins promote its elongation from branched filaments by anti-capping activity. mDia2 promotes actin filament polymerization in the filopodium tip, then Ena/VASP and myosin X could promote filopodia elongation. Extensive actin branching occurs at the filopodium tip and the spine head begins to form. Arp2/3-nucleated branched actin filaments lead to enlargement of the spine head. ADF/cofilins replenishes the actin monomer pool and controls the proper length of actin filaments, preventing formation of abnormal protrusions. Synaptic potentiation, right panel. During LTP, coordinate regulation and recruitments of*

actin binding proteins orchestrate functional and morphological changes of dendritic spines. (B) Actin and microtubule cytoskeleton organization in a mature dendritic spine from cultured hippocampal neurons visualized by platinum replica electron microscopy (EM). Axonal cytoskeleton, purple; dendritic shaft, yellow; dendritic spine, cyan. The spine head typically contains a dense network of short cross-linked branched actin filaments, whereas the spine neck contains loosely arranged longitudinal actin filaments, both branched and linear. The base of the spine also contains branched filaments, which frequently reside directly on the microtubule network in the dendritic shaft. From Hotulainen and Hoogenraad (2010).

Given the established role of Arp2/3 in the growth of lamellipodia in nonneuronal cells [145, 187], it has been recently proposed that spine formation and enlargement may be driven by the same process taking place during lamellipodium formation (Fig.11) [154]. Besides Arp2/3 activity, the latter process requires the concerted activity of capping and anti-capping proteins. Capping proteins bind the barbed ends of actin filaments thus blocking actin monomer addition; whereas anti capping proteins bind to the barbed ends of densely-packed, plasma membrane-localized actin filaments, protecting them from capping [188]. Indeed, when capping activity is high the newly nucleated actin branches become quickly capped, thus leading to a local increase of available actin monomers, which further feeds Arp2/3 complex activity. As a consequence, the formation of a dense and highly branched actin array of short actin filaments is favored (Fig.12). Conversely, when capping activity is low or anti-capping activity operated by Ena/VASP proteins is high, G-actin became rapidly incorporated into long and uncapped actin filaments (Fig.12) [186, 188, 189]. In agreement with this hypothesis, it has been demonstrated recently that a large amount of capping proteins are localized at the level of the spine head [117]. However, a direct demonstration of the role of capping activity in spine formation and enlargement is still lacking [56].

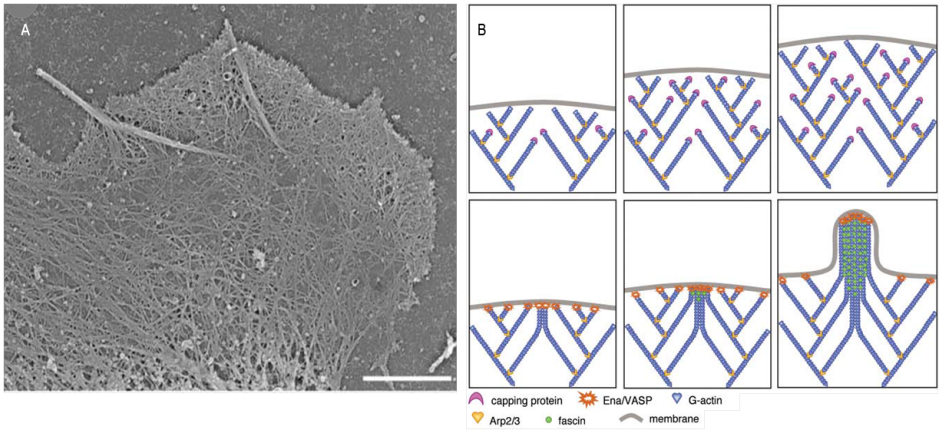

Figure 12. Structural organization of lamellipodium and filodium. *(A) Platinum replica EM shows few peripherally located filopodia embedded into highly branched actin network that characterized lamellipodial protrusions. Deeper cytoplasm shows sparser filament network. (B) Formation of lamellipodia or filopodia is regulated by capping activity. Top panel: high capping activity. Bottom panel: low capping activity. Scale bare in (A), 5 µm. From Mejillano et al. (2004).*

ACTIN REGULATION: THE ROLE OF EPS8

Eps8 is an actin binding and regulatory proteins discovered in tumor cells as substrate of EGF receptors in the mitogenic pathway [190]- It is characterized by a multimodular structure through which it regulates actin remodeling (Fig.13). In particular, Eps8 is able to activate Rac, which in turn regulates actin cytoskeleton [191-194]. Moreover, Eps8 is endowed with an actin capping and bundling activity [195-197] (Fig.13B). The capping and bundling functions of Eps8 have been recently dissected [197], the former lies in the H1 domain (Fig.13C) and mutations of two hydrophobic residues into Aspartate (V689D and L693D) are sufficient to completely abrogate barbed end-binding activity leaving other properties unaffected [197].

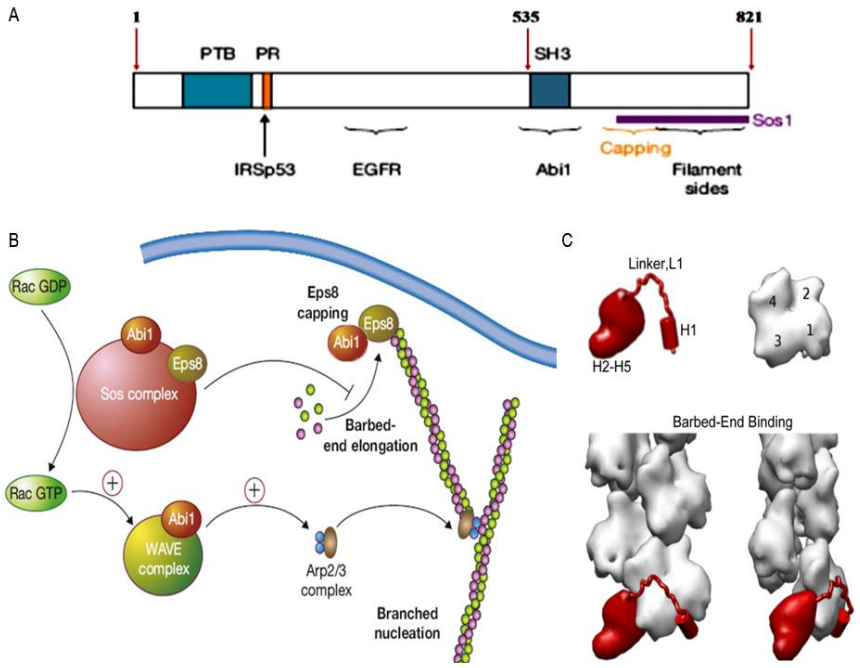

Figure 13. Eps8 structure and functions. *(A) Anatomy of human EPS8 protein. EPS8 is 821 residues long and contains several known regions of interest: a phospho-tyrosine-binding protein (PTB) domain; a proline-rich (PR) sequence, an EGF receptor-interacting region (EGFR); and a Src homology 3 (SH3) domain. Proteins known to interact with these regions are shown. (B) Cartoon of Eps8 function. Eps8 in complex with Abi1 and Sos1 regulates the activity of Rac. Moreover, Eps8-Abi1 binds the barbed end of actin filaments blocking the further incorporation of actin monomers. From Higg (2004). (C) Upper panel: a cartoon representation of Eps8 actin binding region and monomeric actin. The N-terminal amphipathic helix, H1, the connecting linker, L1, and the globular helical core, H2–H5, of Eps8 actin binding region are indicated. Monomeric actin is oriented with its barbed end downwards. Actin subdomains are numbered from 1 to 4. Bottom panel: at the barbed ends, the H1 binding site is fully accessible and H1 can bind within the hydrophobic pocket blocking further addition of monomeric actin. From Hertzog et al. (2010).*

The barbed-end capping activity of Eps8 resides in its conserved C-terminal effector domain, and it is functional when the protein is associated to Abi1 [195]. Conversely, Eps8 must associate with IRSp53 (insulin receptor tyrosine kinases substrate of 53 kDa) [198, 199] to efficiently cross-link actin filaments [196]. Interestingly, Abi1 is involved in synaptic contact formation and spine morphogenesis [134, 200, 201] These multiple actin regulatory roles of Eps8 *in vitro* are reflected by the observation that *in vivo* Eps8 is required for optimal actin-based motility, intestinal morphogenesis, and filopodial-like extension [195, 196, 202]. Eps8 is the prototype of a protein family with redundant biological

function (Eps8L1, 2 and 3) and widespread expression in most tissues and organs of the developing and adult mice with the notable exception of the brain where only Eps8 and Eps8L2, albeit at lower levels, was detectable [203].

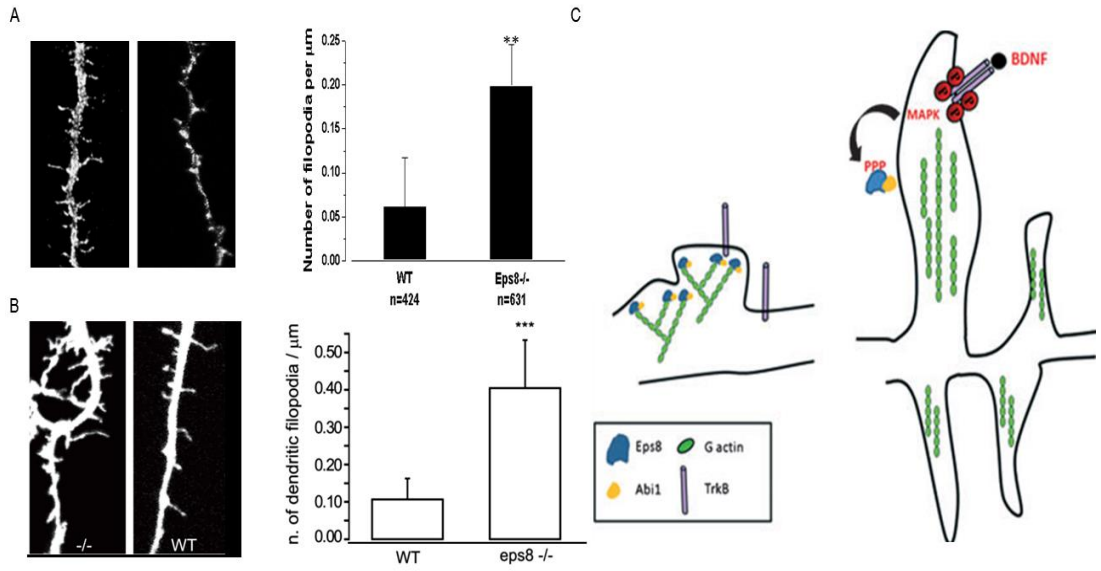

Figure 14. Eps8 controls synaptic precursor formation in hippocampal neurons. *(A,B) Eps8 negatively controls the formation of synaptic precursors. Eps8 null hippocampal neurons present an increase density of axonal (A) and dendritic (B) filopodia in early stage of developments. From Menna et al. (2009). (C) BDNF-MAP kinese-Eps8 pathway. In hippocampal neurons the stimulation with BDNF induced the formation of new filopodia. The growth of those actin based structures depends on the MAP kinese dependent inhibition of the capping activity of Eps8. In absence of this protein, in fact, the BDNF dependent formations of filopodia are abrogated. From Menna et al. (2011).*

In hippocampal neurons overexpression of Eps8 causes the formation of flat actin-rich protrusions along axons, which resemble lamellipodium extensions; on the other hand, protein silencing leads to an increased filopodium formation in the axonal and dendritic compartments ([1]; Fig.14A,B). Consistently, Eps8 has been localized postsynaptically in the dendritic articulations of cerebellar granule cells [203, 204], where it controls actin cytoskeleton stability and NMDA receptor-mediated current [203]. Interestingly, the capping activity of

Eps8 is also regulated by protein phosphorylation operated by activated MAPK upon the neurotrophic factor BDNF (Fig.14C) [1]. BDNF plays a pivotal role in building up neuronal networks, by affecting synaptogenesis and synaptic plasticity [205-207]. Intriguingly, BDNF is misregulated in autistic patients [208-210] and alterations of its expression lead to cognitive impairment and aberrant synaptic growth in animal models [168, 211-214].

AIM OF THE THESIS

Human brain contains around 10^{13}-10^{15} synapses which interconnect neurons creating a specialized network from which higher cognitive functions – such as learning, memory and consciousness – arise. Thus, synaptic contact formation and building up of brain circuits have to occur properly for a normal development and expression of cognitive functions. Perturbations of synaptogenesis process or synaptic contact dysfunction would then result in altered brain development and/or homeostasis, ultimately leading to neuropsychiatric or neurodegenerative disorders.

Actin is the main cytoskeletal components of synaptic contacts and its organization and dynamic changes, besides providing structural support, drive synaptic contact formation and remodeling during both development and plasticity processes (i.e spines maturation and enlargement). A variety of actin binding proteins play a role in the regulation of actin dynamics during these processes. In particular, capping and anti-capping proteins may regulate actin cytoskeletal

architecture and changes in dendritic spines similarly to their function in lamellipodia expansion in nonneuronal cells. Among them, Eps8 is crucial for the formation of neuronal filopodia during development by virtue of its actin capping activity [1]. Of note, the actin capping activity of Eps8 is likely to be predominant with respect to the function of Rac activation in neuronal cells because of the relative concentration of the other molecular partners of Eps8 [215]. However, a direct demonstration of the involvement of capping activity in spine formation and enlargement was not evident. In fact, whereas actin capping protein CP has been implicated in spine development [56], it forms a complex with other proteins, such as twinfilin [216], and mediates also membrane attachment of actin [217, 218].

We have previously demonstrated that the capping activity of Eps8 is regulated by protein phosphorylation operated by MAPK [1] which has a central role in synaptic plasticity [104, 105, 219-221]. Based on these considerations we intended to investigate the role of Eps8 in synaptic contacts development and to dissect the involvement of capping activity in spine morphogenesis and plasticity processes both *in vivo* and *in vitro*.

MATERIAL AND METHODS

Animals

All the experimental procedures that required the use of animals followed the guidelines established by the Italian Council on Animal Care and were approved by the Italian Government Decree No. 27/2010. All efforts were made to minimize the number of subjects used and their suffering. Eps8 wild-type (wt) and Eps8 knockout (KO) mice were housed in standard cages with free access to food and water at 22°C and with a 12-h alternating light/dark cycle. Genotyping was performed by PCR. Mice's tails were leaved 1-2 h shacking at 95°C in NaOH 50 mM. After that Tris HCl 1M pH8 was added and the samples were centrifugated. The surnatant-containg DNA was then used as a substrate for PCR, using the follow primers:

- A primer: CAGCGCATCGCCTTCTATCGC
- B primer: GCCCAGAACCCAAGTTACCTG
- C primer: AAGTAAAAGTTGACCAGTGCGTGG

Electrophoretic separation of PCR amplification products were then obtained on 2% agarose gel and UV-transilluminator was used to visualize a lower band around 200 kb (corresponding to the presence of wt gene) and a upper band around 500 kb (corresponding to Eps8 interrupt gene).

General health

In order to rule out that the lack of Eps8 may induce a worsening of general status of the animals, thus affecting behavioral analysis, general health of mice has been assessed (10 animals for each genotype) [222], [223]. The presence of normal neurological reflexes [224] and sensory abilities [226],[227],[228] were also verified. Motor function, coordination and muscle strength were also assessed [225]. Pain

sensitivity and aggression were tested as described in Corradini et al. (2012).

T maze Test

Before carrying out the test, mice were habituated to a black wooden T-maze composed of a stem (length 41 cm) and of an arm (length 91 cm), built with the same section (wide 11 cm, high 19 cm). Mice were then habituated to obtain food in the T-maze for 5 days [229].The task was composed by an acquisition phase and a reversal one. In the previous phase, in one of the two arms was placed Kellogg's cereal as reinforce for each of 10 daily trials (reinforce arm). Each mouse was then placed at the start point of the maze and given a free choice to enter either arm. In order to evaluate the abilities of the animals to learn the presence and the position of reinforcer, the number of days to reach the criterion was recorded. This parameter was defined as the ability to show 80% of correct choices for 3 days and was also used to select the mice that would be subject to the reversal phase. In the latter task the reinforcer was switched to the opposite arm in order to evaluate the cognitive flexibility of animals.

Radial maze Test

The radial maze consisted of eight arms (each 30 cm long, 7.5 cm wide, and with the enclosing walls 10 cm high), that extended radially from a central 30 cm wide octagonal platform that served as a starting base. Small plastic cups mounted at the end of each arm held 15 mg food pellets as reinforcers. Access to the arms was controlled by eight pneumatically operated sheet-metal guillotine doors. The entire maze was painted black, elevated 50 cm from the floor, and placed in the center of a small room (2.5m × 2.5m) lit by fluorescent lights and fitted with

several visual cues. Animal behaviour was monitored by a video camera (Model CCD, Securit Alarmitalia) whose signals were digitized and interfaced by a PF6PLUSPAL apparatus 512×512 pixels (Imaging Technology, Woburn, MA), and sent to a video monitor (Trinitron KX-14CP1, Sony, Japan). Image analysis and pattern recognition were done by a Delta System computer (Addonics) using software provided by Biomedica Mangoni (Pisa, Italy). Starting 2 weeks before the experiment, body weights were reduced by 10% by means of a restricted feeding schedule of standard chow (Harlan- Italy).The animals were kept at 90% of their free-feeding bodyweight for the duration of the experiment. After 3 days of free exploration the animals were trained to complete the maze. During each daily session, working memory was scored on the basis of the total number of errors (which corresponded to a re-entry into the arm just visited). Training continued, at the rate of one trial per day, until the mice reached the criterion of entering seven different arms in their first eight choices on 5 successive days, for a maximum of 30 days. The mean number of days taken to reach the criterion and the percentage of animals reaching the criterion were calculated.

Passive Avoidance

Animals, typically rodents, subject to passive avoidance learn to avoid an environment in which an aversive stimulus was previously delivered. The apparatus used for this task was made of two different compartments, one light and one dark, connected via a sliding door. In the acquisition trial, each mouse was placed in the light compartment and allowed to freely enter the dark one. The time (in s) taken to move from light compartment to the other was recorded. Once the mouse was in the dark compartment, the sliding door was closed and an unavoidable electric shock (0,8mA for 1 s) was delivered via the paws (aversive stimulus). At

the end of the acquisition phase, animals were placed back in the home cages. 24 h after retention trial was carried out. Mice were placed in the light compartment and the time taken to enter the dark compartment (retention latency, cut-off 180 s) was recorded. An increased retention latency indicates that the animal has learned the association between the shock and the dark compartment.

Novel Object Recognition test

Animals were habituated to the test arena for 10 min on the first day. The day after mice were subjected to familiarization (T1) and novel object recognition (T2). During T1 phase, two identical objects were placed in the center of the arena equidistant from the walls and from each other. Each mouse was placed in the center of the arena between the two objects for a maximum of 10 min or until it had completed 30 s of cumulative object exploration. Object recognition was scored when the animal was within 0.5 cm of an object with its nose toward the object. Exploration was not scored if a mouse reared above the object with its nose in the air or climbed on an object. Mice were returned to the home cage after familiarization and retested 120 min later, and in the arena a novel object (never seen before) took the place of one of the two familiar. Scoring of object recognition was performed in the same manner as during the familiarization phase. From mouse to mouse the role (familiar or new object) as well as the relative position of the two objects were counterbalanced and randomly permuted. Objects to discriminate consisted of white plastic cylinders, colored plastic Lego stacks of different shape and a metallic miniature car. The arena was cleaned with 70% ethanol after each trial. The basic measure was the time (in s) taken by the mice to explore the objects in the two trials. The performance was evaluated by calculating a discrimination index (N-F/N+F), where n=

time spent exploring the new object during T2, F= time spent exploring the familiar object during T2 [230].

Sociability

The apparatus was a rectangular, three-chamber transparent polycarbonate box (width=42.5 cm; height=22.2 cm; centre chamber, length=17.8; side chambers, length=19.1 cm). First of all habituation was carried out and animals were placed in the middle compartment, freely to explore all the chambers for 10 min. [228, 231]. Then an unfamiliar adult DBA/2J male mouse was placed in one side compartment whereas the opposite contained only empty wire cage. The time spent in and the number of entries into each chamber were recorded for 10 min. Data are expressed as time spent in each chamber or the difference score between the time spent to explore the compartment containing the conspecific and that spent in the empty compartment (for sociability test) [232].

EEG

Mice were anesthetized with intraperitoneal injection of 5% chloral hydrate dissolved in saline and given a volume of 10 ml/kg. Four screw electrodes (Bilaney Consultants GMBH, Dusseldorf, Germany) were inserted bilaterally through the skull over cortex (anteroposterior,+2.0–3.0 mm; left–right 2.0 mm from bregma) as previously described [233] according to brain atlas coordinates (Paxinos and Franklin, 2004); a further electrode was placed into the nasal bone as ground. The five electrodes were connected to a pedestal (Bilaney, Dusseldorf, Germany) and fixed with acrylic cement (Palavit, New Galetti and Rossi, Milan, Italy). The animals were allowed a week for recovery from surgery before the experiment. EEG traces were analyzed as [233] for spike activity. Basal cerebral activity was recorded continuously for 24 h in

freely moving mice. For each 24-h EEG recording, the mean number of spikes was evaluated in both genotypes. After the recordings, the EEG was analyzed for the incidence/amplitude of spontaneous cortical spike activity and the percentage of animals displaying spike activity, as previously described [233, 234].

Cell cultures

Primary cultures of mouse hippocampal neurons were established from E18 fetal, Eps8 KO or wild type (wt) littermates C57BL/6J mice as described by Banker and Cowan (1977) and Bartlett and Banker (1984) with slight modifications. Briefly, mouse hippocampi were extracted from embryos and dissociated by treatment with trypsin (0.125% for 15min at 37°C), followed by trituration with a fire-polished Pasteur pipette. The dissociated cells were plated onto 24 mm glass coverslips coated with poly-L-lysine (1 mg/ml, Sigma Chemical Co., St Louis, MO, USA) at density of 400 cells/mm2. The cells were maintained in Neurobasal (Invitrogen, San Diego, CA, USA) with B27 supplement and antibiotics, 2mM glutamine (Invitrogen, San Diego, CA, USA) and 12.5mM glutamate (Sigma-Aldrich, St. Louis, MO, USA) (neuronal medium). Neuronal cultures were then kept at constant temperature (37°C) in the presence of 5% CO_2. Part of the culture medium was replaced with fresh medium without glutamate after 3 days [235, 236] .

Quantitative RT-PCR analysis

Total RNA was isolated using the RNeasy® Mini Kit (Qiagen, Venlo, Limburg, Netherlands). 2 µg of RNA were processed in a reverse-transcription reaction with 100 ng of random examers, (SuperScript® VILO™ cDNA Synthesis Kit). 0.1 ng of cDNA was amplified, in triplicate, in a reaction volume of 25 µL with 10 pMol of each gene specific primer and

the SYBRgreen PCR MasterMix (Applied Biosystems, San Francisco, CA, USA). Real-time PCRmwas carried out on the 14 ABI/Prism 7700 Sequence Detector System (Perkin- Elmer/Applied Biosystems), using a pre-PCR step of 10 min at 95°C, followed by 40 cycles of 15 s at 95°C and 60s at 60°C. Specificity of the amplified products was confirmed by melting curve analysis (DISSOCIATION CURVE TM Perkin-Elmer/Applied Biosystems) and by 6% PAGE. Preparations with RNA template without reverse transcriptase were used as negative controls. Samples were amplified with primers for each genes (for details see Q-PCR primer list below) and rRNA GAPDH as a housekeeping gene. The Ct values were normalized to the GAPDH curve. The GAPDH gene was used as a control gene for normalization. Results were quantified using the 2- CT method [237]. PCR experiments were performed in triplicate, and standard deviations calculated and displayed as error bars.

Primer sequences used are listed below:

Assay ID Context Sequence Gene Symbol

Mm00519404_m1 ACCAGCTGGGCTGACTGGACAGGCA Eps8l3

Mm00509161_m1 GGTCAATGGTCAGCAAGATCCAGAA Eps8l1

Mm00519237_m1 ACATGCTAACAGGGGCTACCAGCCA Eps8l2

Determination of Rac activation

The levels of Rac-GTP were evaluated using G-LISA™ Rac Activation Assay Biochem Kit™ (Cytoskeleton, Denver, CO, USA). Results were normalized over the total level of Rac determined by western blot analysis. Monoclonal anti-Rac1 and anti-Eps8 antibodies (BD Transduction Laboratories, Franklin Lakes, NJ, USA). Monoclonal anti-Vinculin (Sigma-Aldrich, St. Louis, MO, USA).

Electron microscopy

Postnatal 90 days wt and Eps8KO mice were anesthetized with 4% chloralium hydrate. Animals were then perfused with 4% paraformaldehyde, 1% glutaraldehyde in Phosphate Saline Buffer (pH 7.4). Dissected brains were post-fixed in the same buffer for 2 hours. Coronal sections of 350 mm in thickness in the hippocampal region were then obtained by vibratome sectioning (Leica Microsystems, Wetzlar, Germany). From these sections, regions containing the CA1 and CA3 of the hippocampi were dissected and they were further processed for electron microscopy sample preparation. Briefly, the samples were fixed with glutaraldehyde (2% in cacodylate buffer 0.1M, pH 7.4), postfixed with 2% OsO_4 in the same buffer, en bloc stained with a saturated solution of uranyl acetate in 20% ethanol dehydrated and embedded in a mixture of Epon+Spurr epoxy resins. Ultra-thin sections were observed in a Philips CM10 microscope; images were collected at 28.500x and morphometric analysis was performed with Image J software.

cDNA constructs and expression

Neuronal cultures were co-transfected at 10-11DIV with 0.2 μg pSUPER-DsRed plasmid (obtained from pSUPER GFP, Oligoengine, Seattle, USA) and 0.5 μg of Eps8 WT or capping specific mutant H1 cDNAs [196, 197]. Acute down-regulation of the protein levels was achieved using two different double-strand small interfering RNA (siRNA) oligonucleotides (Invitrogen Stealth RNAi; called 1525 and 1158) against mouse Eps8 as previously described in Menna et al (2009). Mouse and rat hippocampal neurons were transfected by using Lipofectamine 2000 (Invitrogen, San Diego, CA).

Cell culture electrophysiology and chemical LTP

During recordings cells were bathed in a standard external solution containing (in mM): 125 NaCl, 5 KCl, 1.2 MgSO4, 1.2 KH2PO4, 2 CaCl2, 6 glucose, and 25 HEPES-NaOH, pH 7.4. Recording pipettes were fabricated from borosilicate glass capillary using an horizontal puller (Sutter Instruments, Novato, CA, USA) inducing tip resistances of 3-5 MΩ and filled with a standard intracellular solution containing (in mM): 130 K-gluconate, 10 KCl,1 EGTA, 10 HEPES- NaOH, 2 MgCl2, 4 MgATP, and 0.3 Tris-GTP. For miniature EPSC recordings 1μM tetrodotoxin, 20μM Bicuculline and 50μM AP5 (Tocris, Bristol, UK) were added to standard extracellular solution to block spontaneous action potentials propagation, GABA-A and NMDA receptors, respectively. Recordings were performed at room temperature in voltage clamp mode at holding potential of -70 mV using a Multiclamp 700B amplifier (Molecular Devices, Sunnyvale, CA, USA) and pClamp-10 software (Axon Instruments, Foster City, CA, USA). Series resistance ranged from 10 to 20 MΩ and was monitored for consistency during recordings. Cells in culture with leak currents >100 pA were excluded from the analysis. Signals were amplified, sampled at 10 kHz, filtered to 2 or 3 KHz, and analyzed using pClamp 10 data acquisition and analysis program.

For glycine-induced LTP experiments, recordings from each neuron lasted at least 60 min and each cell was continuously perfused (1ml/min) from a computer-controlled perfusion system with a solution containing (in mM) 125 NaCl, 5 KCl, 1.2 KH_2PO_4, 2 $CaCl_2$, 6 glucose, and 25 HEPES-NaOH, TTX 0.001, Strychnine 0.001 and bicuculline methiodide 0.02 (pH 7.4). Solution with glycine (100 μM) was applied for 3 min and then washed out for at least 45 min. The patch pipette electrode contained the following solution (in mM): 130 CsGluconate, 8 CsCl, 2 NaCl, 10 HEPES, 4

EGTA, 4 MgATP and 0.3 Tris-GTP. The Eps8-capping inhibitor peptide (blocking peptide, 10uM intracellular concentration) was dissolved in the intracellular solution and injected into neurons via the patch pipette. Glycine was applied at least 10 min after the injection of inhibitor peptide or its inactive control.

Immunofluorescence staining of dissociated neurons

Neuronal cultures were fixed with 4% paraformaldehyde and 4% sucrose (8-20 min.) or with 100% cold methanol (5 min.). The following antibodies were used: mouse anti-VAMP2 (1:1000; Synaptic System, Goettingen, Germany), guinea pig anti-Bassoon (1:300; Synaptic System, Goettingen, Germany), guinea pig anti-vGLUT1 (1:1000; Synaptic System, Germany), mouse anti-PSD-95 (1:400; UC Davis/NIH NeuroMab Facility, CA, USA), rabbit anti-GFP (1:400; Invitrogen, San Diego, CA), mouse anti-beta III tubulin (1:400; Promega Corporation, Madison, USA). Secondary antibodies were conjugated with Alexa-488, Alexa-555 or Alexa-633 fluorophores (Invitrogen, San Diego, CA, USA). Images were acquired using a Zeiss LSM 510 META confocal microscope. Image stacks (pixel size was 110 nm-110 nm) were then obtained keeping acquisition parameters (i.e., laser power, gain and offset) constant among different experimental settings. Analysis of synaptic puncta took in account only clusters lying along secondary dendritic branches. The detection threshold was set to 2.5-fold the level of background fluorescence referring to diffuse fluorescence within dendritic shafts. The minimum puncta size was set at four pixels (0.048 mm^2). Boolean function 'and' was used to evaluate the colocalization of two or three selected markers, usually PSD-95, vGLUT-1 and Bns. The resulting image was binarized and used as a colocalization mask to be subtracted to single channels. The number of the puncta resulting from colocalization mask subtraction was

measured for each marker. Colocalization ratio was defined as colocalizing puncta/total puncta number. The total area of the measured synaptic puncta represents synaptic area. For each cell, three or four dendrites were analyzed from maximum projection images. Filopodia were defined as thin protrusions without a distinguishable head, stubby spines as short protrusions without a neck, and mushroom spines as protrusions with a short neck and a distinguishable head [99]. Synapses were defined by the apposition of presynaptic and postsynaptic markers, such as vGLUT-1 or Bsn and PSD-95. Fluorescence images processing and analyses were performed with ImageJ Software (National Institutes of Health).

Live cell imaging and Fluorescence Recovery After Photobleaching (FRAP)

FRAP experiments were performed maintaining coverslips in a 37°C heated chamber with 5% CO2 in their own growth medium. The construct FU(PSD95:EGFP)W was a kind gift from Prof. Noam Ziv, Israel Institute of Technology, Haifa, Israel. Live cell imaging was performed with a confocal microscope Leica SP5 using a HCX PL APO 63X/ 1.4 oil immersion objective (Leica Microsystems, Wetzlar, Germany). Photobleaching was performed using a 488nm laser light at 100%. Images were collected every 500ms. The bleached region of interest (ROI) was put on the spine and has been used for both the photobleaching and the fluorescence recovery analysis. The fluorescence recovery was recorded and the analyses performed on the first 40 seconds after bleaching. Each image at each time point was corrected for the background and for the not-intended bleaching and normalized according to this formula: ((*Ft-Fb)/(Fr-Fb))/ (Fa-Fb),* where Ft is the fluorescence of a ROI at time t; Fb is the fluorescence of the background;

Fr is the fluorescence of the reference ROI at time t and Fa is the fluorescence of the ROI immediately before photobleaching. The data obtained were fitted with a single exponential using the LAS AF software (Leica Microsystems, Wetzlar, Germany).

Golgi staining

Mice were deeply anesthetized with avertin (0.2ml/10g body weight, i.p.) and Animals were perfused transcardially with 50-100 ml of saline solution (NaCl 0.9%). Brains were rapidly removed and incubated with Golgi-Cox impregnation solution (5 volumes of 5% $K_2Cr_2O_7$ solution, 5 volumes of 5% HgCl, 4 volumes of 5% K_2CrO_4 and 10 volumes of bidistillate water) for 1 weeek in the dark as described in in Glaser and Van der Loos (1982). Thus impregnation solution was removed and replaced with 30% sucrose solution for at least 2 days. Vibratome (VT1000S, Leica, Wetzlar, Germany) was used to obtain sections of 100µm thickness from the dorsal hippocampus. The vibratome reservoir should be filled with 6% sucrose and the blade is prepared for sectioning by immersion in xylene for 5 minutes. Sections were collected and kept in 6% sucrose solution until they would be placed in clean gelatinized microscope slides (2% gelatin, 1% $KCr(SO_4).12H_2O$). Coronal sections of 100µm thickness from the dorsal hippocampus were obtained using a vibratome (VT1000S, Leica, Wetzlar, Germany). Sections were then treated with ammonium hydroxide for 30 min, followed by 30 min in Kodak Film Fixer, and finally were rinsed with distilled water, dehydrated and mounted with a xilene-based medium [238].

Immunofluorescence staining on free-floating sections.

Immunofluorescent staining was carried out on free-floating sections as described in Frassoni et al., 2005. Free-floating sections were processed

for PSD-95 (rabbit policlonal antibody kindly provided by C. Sala; 1:400) and VAMP2 (Vesicle Associated Membrane Protein, Synaptic System, Gottingen, Germany 1:800), followed by incubation with secondary antibodies (Jackson Immunoresearch Laboratories, West Grove, PA, USA), indocarbocyanine (Cy) 2-conjugated goat anti-mouse (1:200) and Cy3-conjugated goat anti-rabbit (1:600), mounted in Fluorsave (Calbiochem, San Diego, CA, USA) [239]. Sections were examined by means of a Zeiss LSM 510 META confocal microscope (Leica Microsystems, Wetzlar, Germany). To resolve individual synaptic puncta, the images (512x512 pixels) were acquired using the x40 oil immersion lens (numerical aperture 1.0) with additional electronic zoom factor of up to 4. The gain and the offset were lower to prevent saturation in the brightest signals. The pinhole size was kept at the minimum setting (1.0-1.8). Analysis was carried out on each mice (Eps8 wt and KO) and three different sample from CA1 area were taken at two hippocampal coronal levels.

In vitro binding assay

In vitro binding assay was performed as previously described [196]. The antibodies used were: monoclonal anti-Eps8 (Transduction Laboratories, Lexington, KY); rabbit polyclonal anti-GST (Santa Cruz Biotechnology, Santa Cruz, CA, USA). Hs-Abi1 synthesized peptides (PPPPPVDYEDEE; AAAAAVAAEDEE) were from Mimotopes (Clayton Victoria, Australia). Recombinant purified His-Eps8 and GST-Abi1 were obtained as previously described [1, 195].

Analysis of human brain tissue samples

11 postmortem brain samples from subjects with autism and 13 control brain samples were provided to us by the Autism Speaks' Tissue Program

(Princeton, NJ, USA) via the Harvard Brain Bank (Belmont, MA, USA) and the University of Maryland Brain and Tissue Bank (Baltimore, MD, USA). Clinical information about each tissue sample was reported in the Autism Tissue Program online portal (http://www.atpportal.org). There were no statistically significant differences between groups for age at death or PMI (Peer-mediated instruction). Given that fusiform gyrus is hypoactivated during face discrimination tasks in autistic patients, this area was chosen for further analysis [240]. The diagnosis of autistic disorder was confirmed using the Autism Diagnostic Interview-Revised [241] postmortem through interviews with the parents and/or caregivers. Samples were stored at - 80°C before use. Protein extraction was performed as previously described [209, 242]. Around 100 mg of tissue was homogenized on ice without thawing using a sonic dismembrator in homogenization buffer (HB: 0.05M Tris pH 7.5, 0.5%Tween-20, 10mM EDTA, 1 complete, Mini, EDTA-free tablet (Roche, Cat. no. 11 836 170 001) per 10 ml of HB, 2 μg/ml pepstatin, 2 μg/ml aprotinin, 50mM sodium fluoride, 2mM sodium orthovanadate, 2.5mM sodium pyrophosphate, 1mM b-glycerophosphate, 0.5% sodium deoxycholate). The homogenate was incubated for 15 min on ice and then centrifuged at 12 000x g for 20min at 4°C. Supernatants containing solubilized protein were stored at -80°C before use. Protein concentrations were determined using a DC protein assay kit (Bio-Rad Laboratories, Mississauga, Ontario, Canada).

Western blotting analysis on human brain tissue samples

Western blotting was carried out as previously described with slight modifications [209, 242, 243]. Samples containing 35 μg protein were resolved in 10% sodium dodecyl sulphate-polyacrylamide gels under reducing conditions. After transfer onto polyvinylidene diflouride

membranes for 2 h at 250mA at 41C, blots were blocked for 1 h at room temperature in a 1:1 solution of phosphate-buffered saline (PBS) pH 7.4 and Odyssey Blocking Buffer (BB) (Cedarlane, Burlington, Ontario, Canada) and then incubated with rabbit polyclonal or mouse monoclonal Eps8 primary antibodies (dilution 1:1000) and b-actin antibodies (Sigma, diluted 1:5000) at 41C overnight in BB:PBS (1:1), 0.5% Tween-20 (PBS-T). Subsequently, membranes were washed and incubated for 1 h at room temperature in PBS-T with the secondary antibodies IRDye 680-conjugated goat anti-rabbit and IRDye 800CW-conjugated goat anti-mouse (LI-COR Biosciences, Lincoln, NE, USA; diluted 1:8000). All blots were scanned using an Odyssey Infrared Imaging System (LI-COR Biosciences). Blots were run twice with two different Eps8 antibodies. Each western blot contained a standard curve consisting of different amounts of protein per lane (from 5 to 80 mg) to ensure that the sample loading amount was in the linear range of detection for Eps8 [209, 242, 243]. The intensities of immunoreactive bands were measured using LI-COR Odyssey Software, version 2.0 with local background subtracted. Eps8 pixel values were normalized to b-actin values for each sample.

Statistical analysis

Morphological analysis of spine parameters and synapse density was performed using ImageJ software (NIH, Bethesda, MD, USA). n refers to the number of elements analysed. Statistical analysis was performed using SigmaStat 3.5 (Jandel Scientific) or PRISM 5 software (GraphPad, Software Inc., San Diego, CA,). After testing whether data were normallydistributed or not, the appropriate statistical test has been used, see figure legends. Data are presented as mean±s.e.m. from the indicated number of elements analyzed. For behaviour, the continuous data were analyzed using a paired Student's t-test and the categorical data were

analyzed using Fisher's exact probability test. The AUC was calculated for the total number of errors in completing the maze. The differences were considered to be significant if $P<0.05$ and are indicated by an asterisk; those at $P<0.01$ are indicated by double asterisks; those at $P<0.001$ are indicated by triple asterisks.

RESULTS

Eps8 knockout (Eps8 KO) mice are impaired in learning and memory

In collaboration with Dr. Marielvina Sala (University of Milan), Eps8 KO mice were subjected to a series of behavioral tests in order to characterize their cognitive function, with particular attention for learning and memory, with the aim to evaluate the potential involvement of Eps8 in such processes.

Spatial memory was evaluated by Radial- and T-maze and in both of them Eps8 KO mice performed worse compared to wild-type (wt) groups (Fig.15). Indeed, in Radial-maze task Eps8 KO mice exhibited a higher number of errors as indicated by the calculated area under the curve (AUC) and needed significantly more days than controls to reach the criterion (Fig.15A). Consistently, wt mice performed statistically better compared to Eps8 KO mice during the acquisition phase of T-maze test (Fig.15B, left). Conversely, no significant difference was detected in the reversal phase (Fig.15B, right).

When tested for novel object recognition (Fig.15C), no significant difference was detected in the amount of the time that mice spent exploring the two object during the familiarization phase (T1), thus indicating that the absence of Eps8 does not compromise the explorative behavior of Eps8 KO mice. However, when subjected to novel object recognition phase (T2), 120 minutes later, in order to evaluate episodic memory, Eps8 KO mice spent significantly less time exploring the novel object compared to familiar ones, as shown by a decrease in the discrimination index (Fig.15C). This was not due to altered sensorial parameters, as all mice appeared healthy, displaying normal motor activity and sensory ability (Table 1).

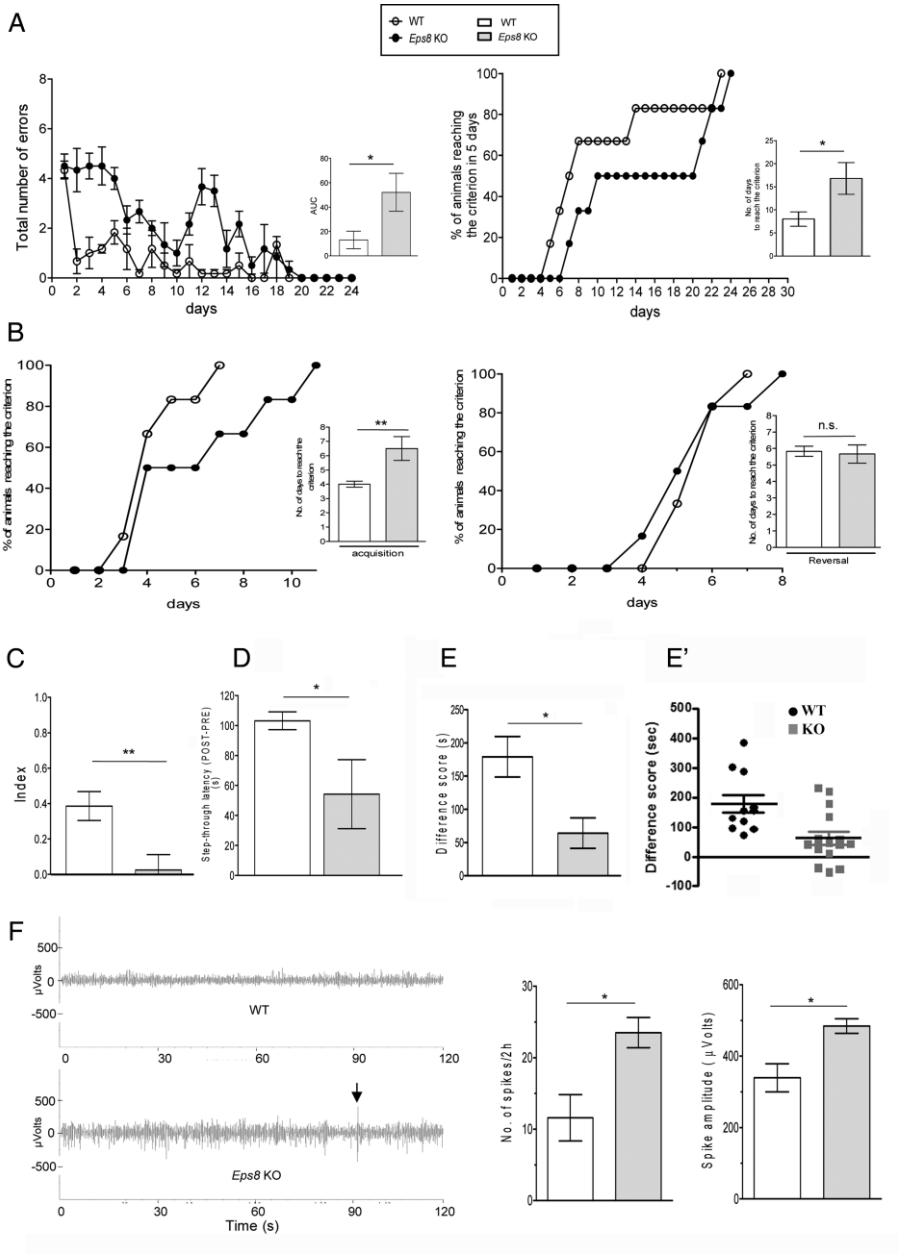

Figure 15. Behavioral characterization of Eps8 KO mice. *(A and B) Eps8 KO mice are impaired in spatial learning. (A) Eight-arm radial maze. (Left) Eps8 KO mice show a delayed learning in terms of increased number of errors statistically evaluated as the area under the curve (AUC). (Right) A lower number of Eps8 KO mice reach the criterion within 5 days evaluated as number of days taken to reach the criterion. (B) T-maze task. During the acquisition phase (left), Eps8 KO mice exhibit a delayed learning, needing more time to reach the criterion. Conversely, mutated mice display normal learning during reversal phase (right). The number of days to reach the criterion during both phases is illustrated in the flanking graph. (C) Novel object recognition test. Eps8 KO mice show a decrease in the discrimination index, meaning no net preference between novel and familiar objects. (D) Passive avoidance task. Mutant mice show reduced step-through latency compared to wt animals. (E, E0) Sociability test. Eps8 KO mice show reduced social interaction, as indicated by significantly lower difference score in a social choice paradigm. Mutant animals spend significantly less time exploring a conspecific than an empty cage. (F) EEG. Abnormal EEG profile was recorded in Eps8 KO mice. (Left) representative traces of EEG recordings of wt and KO mice for 120 s are shown. KO mice show higher spike activity both in term of frequency and amplitude. The frequency of spikes calculated in 2 h recording traces is significantly higher compared to wt (centre). Mean spike amplitude of mutant mice was also larger than wt (right). Increments above a threshold determined according to the increments distribution through an unsupervised approach (Manfredi et al, 2009) and whose amplitude was greater than twice the background were considered as*

*spikes. Data are shown as mean±s.e.m. of ten animals for each genotype and each test. Statistical assessments were performed by Student's t-test comparing wt and KO mice (*P<0.05, **P<0.01). n.s., not significant.*

Then long term memory was examined by passive avoidance task. In this test, subjects learn to avoid an environment in which an aversive stimulus, usually a foot-shock, was previously delivered. The time taken to enter the dark compartment (retention latency) is used as an indicator of the strength of the association between the shock and the above-mentioned compartment. As shown in Fig.15D, Eps8 mice displayed a significant reduction of the mean value of step through latency, indicating impairment in long-term memory.

Moreover, also social behavior was found altered in Eps8 KO mice. Indeed, differently from wt animals, which spent longer time to explore the compartment with the stranger mouse than empty cage, Eps8 KO mice were significantly less social, spending the same amount of time in the two compartments (Fig.15E).

Finally, 2-h cortical EEG recordings revealed that Eps8 KO mice displayed frequent spikes of high amplitude (Fig.15F) although no epileptiform activity was detected and mice did not show seizures, either spontaneously or even after mice handling. Moreover, the mean number and mean amplitude of spikes were significantly higher than wt mice (Fig.15F).

Collectively, these data indicate that Eps8 KO mice show defects in learning and memory, social behavior and cortical activity. Those alterations were no due to abnormal development of brain structures (e.g. cortical displacement of neurons, lamination defects…). Indeed, no obvious alteration of the brain anatomical structures of mutant mice has been found (Fig.16).

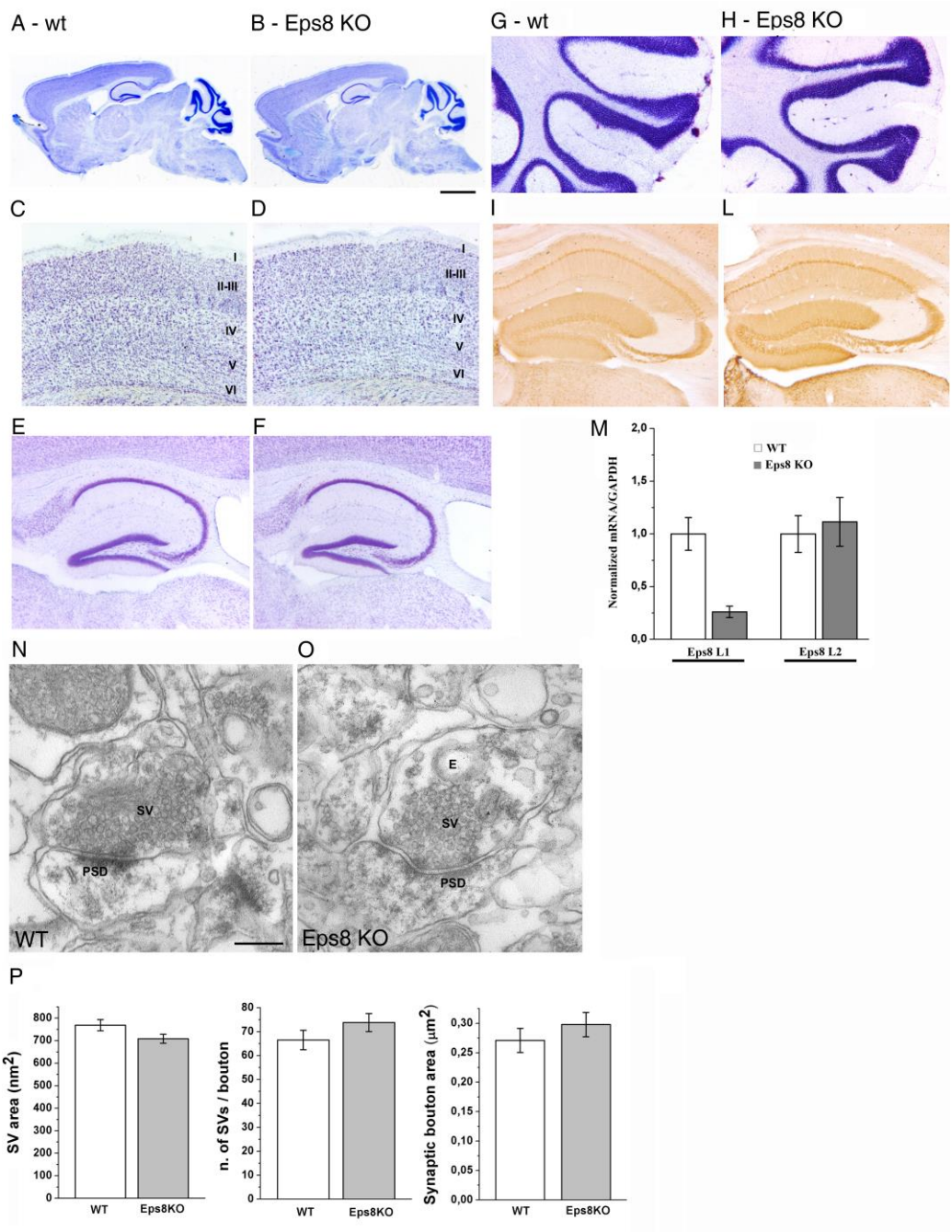

Figure 16. Brain architecture and ultrastructure of presynaptic terminals are normal in Eps8 KO mice. *(A-L) Detailed brain morphological analysis. Sagittal sections through the entire CNS (A, B) or coronal sections of cortex (C,D), hippocampus (E,F) and cerebellum (G,H) of wt (A,C,E,G) and Eps8 KO mice (B,D,F,H) were analyzed by staining with thionine. The thickness and layering of the cerebral cortex, the architecture of the hippocampal formation and cerebellum are undistinguishable between wt and Eps8 KO mice. The cytoarchitectural organization of the CA subfields and dentate gyrus of the hippocampus are evaluated by immunostaining for the calcium binding protein Calbindin. No difference can be detected between wt and mutant mice (I wt, L Eps8 KO). (M) Normalized expression of Eps8L family members in hippocampus from wt and KO adult mice. Expression profiles of Eps8L1, Eps8L2 and Eps8L3 mRNAs were determined by quantitative RT-PCR. Data are expressed as the ratio of mRNA levels of each Eps8L family member relative to that of GAPDH mRNA levels, normalized on the mRNA levels in wt. Bars show the mean±sd (n=3) of three independent experiments. **, P < 0.01 (L1 vs KO). Eps8L3 mRNA was not detected either in wt or in KO samples (not shown). Scale bars, A,B=200 μm; C,D= 220 μm; E,F=450 μm; G,H= 320 μm; I,L= 400 μm. (N-O) Electron micrographs of excitatory synapses of neurons*

from hippocampal sections of wt and Eps8 KO mice. No difference in the size and organization of the synaptic vesicle pool (SV) can be observed in the presynaptic terminals. (E): endosome; PSD: post-synaptic density (Scale bar N,O=200nm). P. Synaptic vesicles area (left graph) (wt, n=3732; Eps8 KO, n=4003), SV abundance, evaluated with respect to the presynaptic bouton profiles (middle graph), and synaptic bouton area (right graph) (wt, n=53; Eps8KO, n=54) are unchanged in wt and KO animals.

Furthermore, we verified whether a change of the mRNAs codifying for the other Eps8L family members (e.i Eps8L1, Eps8L2 and Eps8L3) might occur in the hippocampus. mRNA expression profiles of Eps8 family members were then carried out by quantitative RT-PCR in the hippocampus of wt and Eps8 KO adult mice (Fig.16M). No significantly increase of neither Eps8L1 nor Eps8L2 was found, ruling out that compensatory mechanisms take place. Eps8L3 was not detected in our conditions.

Excessive synaptic growth and abnormal spine morphology in the hippocampus of Eps8 KO mice

We have previously demonstrated that Eps8 negatively regulates filopodium formation during neuronal development. Indeed, Eps8 null neurons display an increased formation of protrusion from both axon and dendrites in culture [1]. Then, since filopodia represent the precursors of pre- and postsynaptic compartments during the process of hippocampal synaptogenesis [177], we investigated whether Eps8 KO adult hippocampus is characterized by a higher numbers of synaptic contacts compared to wt.

Figure17A shows the CA1 hippocampal region of Eps8 KO and wt mouse brain, stained for the synaptic vesicle protein synaptobrevin/VAMP2 and the glutamatergic postsynaptic protein PSD-95. A significantly higher number of both pre- and postsynaptic puncta

was detected within the hippocampi of Eps8 KO mice relative to control (Fig.17A,B).

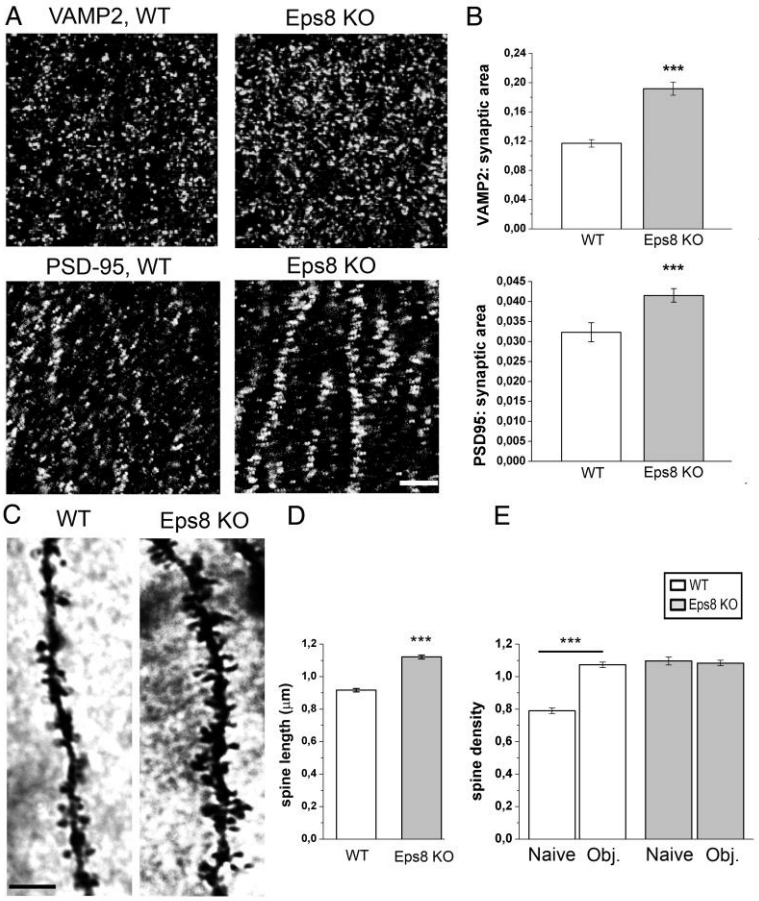

Figure 17. Increased excitatory synapse number and spine abnormalities in the hippocampus of Eps8 KO animals. *(A, B) Representative fields of the CA1 hippocampal region of a wt and Eps8 KO mouse brains, immunostained for the synaptic vesicle protein synaptobrevin/VAMP2 and the glutammatergic postsynaptic protein, PSD-95. Eps8 KO hippocampus display a larger number of synaptic contacts analyzed in term of either pre- or postsynaptic areas. Scale bar, 5 μm. (C) Details of CA1 apical dendrites from wt and Eps8 KO hippocampi subjected to Golgi-Cox staining. Scale bars, 10 μm. (D, E) Quantitation of spine length and density in naïve animals or trained animals 24 h after exposure to novel object recognition test (obj.) Eps8 null animals displayed an increased number of dendritic spines per unitary length of parental dendrites (density, E, wt naive=0.789±0.017 spines per μm of parent dendrite; wt obj.=1.07±0.016 spines per μm; KO naive=1.09±0.024 spines per μm; KO obj.=1.08±0.016 spines per μm total number of examined dendritic branches: 321wt ctr, 242 wt obj, 105 KO ctr, 361 KO obj; number of independent experiments: 3). Notice that Eps8 null spines are longer compare to control and moreover fail to undergo further increase in number after the object recognition (length, D, wt spines=0.91±0.010 μm; KO spines=1.12±0.012 μm; total number of examined spines: 551, wt and 506, Eps8 KO; number of independent experiments: 3). Mann–Whitney rank sum test P<0.001. All data are expressed as mean±s.e.m. Six animals for each condition have been analyzed.*

Ultrastructural analysis, performed in collaboration with Dr. Maura Francolini (University of Milan), revealed normal number and dimension of synaptic vesicles and normal size of synaptic boutons, thus indicating that the lack of Eps8, although affecting synapse number, does not prominently impact the ultrastructural organization of presynaptic compartment (Fig.16N-P). However, analysis of the fine morphology of CA1 pyramidal neurons performed with Golgi-Cox staining revealed that Eps8 KO mice display a severe alteration in the morphology of dendritic spines (Fig.17C-E). In fact, they appeared thinner and significantly longer compared to wt (Fig.17C,D). Moreover, a significantly higher number of dendritic protrusions per unit length was detected on secondary branches of CA1 apical dendrites in Eps8 KO animals relative to wt (Fig.17E, compared the first and the third column). Interestingly, aberrant dendritic spine morphology and density were reported in patients suffering of autism spectrum disorders, schizophrenia and intellectual disabilities [31, 132, 135].

Given that mutant mice are impaired in learning and memory and in consideration of abnormal spine features, we investigated whether learning-dependent spinogenesis occurs properly in Eps8 KO mice. To address this issue wt and mutant animals were subjected to object recognition test and processed for Golgi-Cox staining 24 h after training. The results showed that mutant mice did not show any increase in spine number, which was instead clearly detectable in wt animals (Figure17E)

These results indicate that Eps8 null mice present a defect in spine formation and in the processes of learning-dependent spinogenesis within the hippocampus.

Excessive synaptic growth and abnormal spine morphology in Eps8 KO hippocampal culture

To understand the cellular and molecular mechanisms underlying the abnormal dendritic spine morphology and structural plasticity defects occurring in Eps8 KO mice, we established primary hippocampal cultures from wt and Eps8 null embryos. Primary cultures allowed us to deeply analyze synapse density and spine morphology in neurons mutated for Eps8.

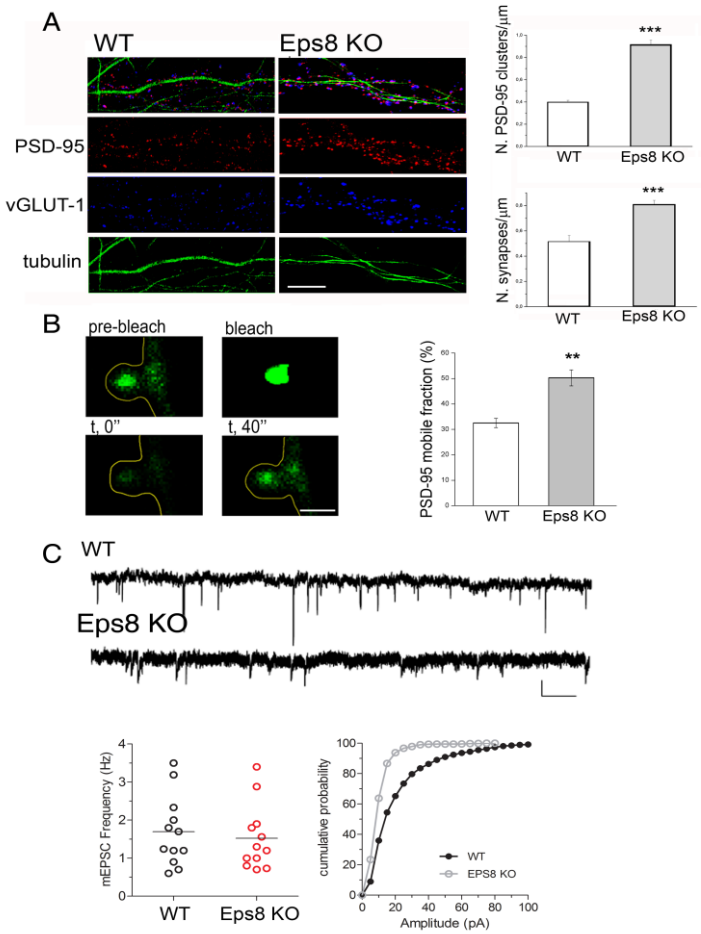

Figure 18. Increased excitatory synapse density and altered PSD-95 mobility in Eps8 KO neurons. *(A) 21 DIV old wt or KO cultures stained for beta III tubulin (green), vGLUT1 (blue) and PSD-95 (red). Quantitation of the PSD-95 positive (top histogram) or PSD-95 and vGLUT1 positive (bottom histogram) puncta per unit length reveals higher number of synaptic contacts in Eps8 KO neurons relative to wt. Scale bar, 20 µm. (B) FRAP experiments in wt or Eps8 KO neurons transfected with PSD-95-GFP. Selected spines are bleached with a high-power 488 laser and the fluorescence recovery is recorded during time. The recovery of fluorescence is expressed as mobile fraction percentage. A faster recovery of PSD-95*

fluorescence occurs in Eps8 null dendirtic spines. Mann-Whitney rank sum test p<0.001. Data are normalized and expressed as mean±s.e.m. Scale bar, 2 μm. (C) Eps8 KO neurons display significantly lower mEPSC amplitude when compare to wt. No difference in mEPSC frequency can be detected in KO neurons. Number of cell examined: 12 wt and 12 KO. Number of independent experiments: 3. Scale bars depict 10pA and 250 ms.

Quantification of pre- and postsynaptic puncta in 21 DIV (day *in vitro*) cultures revealed that, consistently with *in vivo* data, Eps8 KO cultures displayed a significantly higher number of vGLUT1 and PSD-95 puncta per unit length of parent dendrite, meaning that synaptic density was significantly increased in null cultured (Fig.18A). In addition, in line with *in vivo* data, ultrastructural analysis of mature 21 DIV neuronal cultures did not reveal any gross morphological alteration in Eps8 KO presynaptic compartment, including SVs number and size (data not shown). Conversely, Eps8 KO neurons transfected with a vector coding for red fluorescence protein (RFP), which fills all neuronal processes allowing the direct examination of dendritic spines, were characterized by a significantly higher spine density and these protrusions appears also significantly longer than wt ones (Fig.19A). Consistently, the spine morphology shifted toward thin type, while the percentage of mushroom spine was decreased (Fig.19A). However, in spite of the immature feature of the majority of Eps8 null spines, such dendritic protrusions displayed PSD-95 and Bassoon (Bsn) or vGLUT1 immunoreactivity, thus indicating that they represent *bona fide* synaptic contacts (Fig.19A). In summary Eps8 null neurons in culture fully recapitulate the phenotypic features observed *in vivo*.

PSD-95 is a major organizer of the postsynaptic density, playing a crucial role in determining spine size and morphology [55, 98, 244, 245]. Dynamics of synaptic PSD-95 may reflect spine maturity [246]. We therefore set out to examine PSD-95 mobility in Eps8 null spines, using

fluorescence recovery after photobleaching (FRAP) analysis. Mutant spines displayed a significantly higher PSD-95 mobile fraction compared to wt (Fig.18B), suggesting that morphological alteration of dendritic spine may be associated with functional defects. Consistent with this possibility, miniature excitatory postsynaptic currents (mEPSC) recorded in the presence of TTX displayed significantly reduced amplitude in Eps8 KO neurons with the respect to wt (Fig.18C). Moreover, despite the increase in synaptic density, no changes in mEPSC frequency were detected in mutated cultures (Fig.18C). A possible explanation could come from the reduced mEPSC amplitude, which would cause many events falling below detection limit. Nevertheless, we cannot rule out a role of Eps8 in reducing presynaptic release probability.

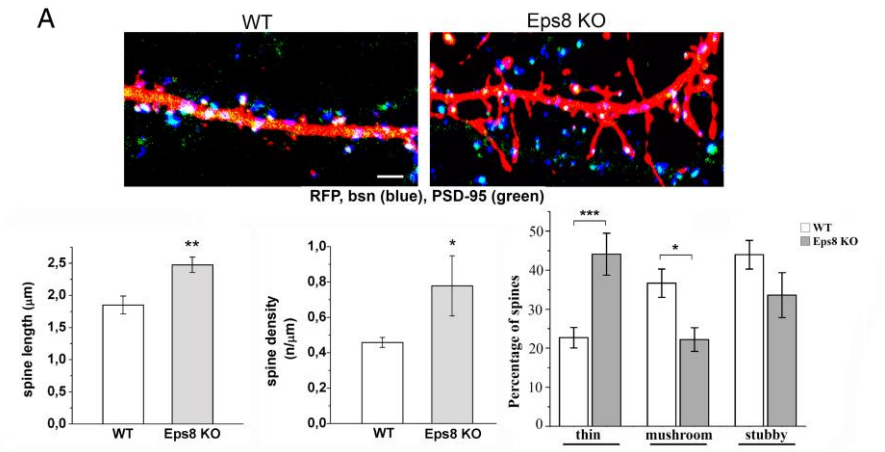

Figure 19. Increased excitatory synapse number and altered spine morphology in Esp8 KO neurons. *(A) Eps8 wt and KO neurons transfected with RFP and stained for the presynaptic protein Bassoon (Bsn, blue) and for the postsynaptic marker PSD-95 (green). Eps8 KO neurons display an increased number of spines per unit length of parental dendrites. Notice also that Eps8 null spines are longer compared to wt ones. (Total number of examined protrusions: 260 wt, 146 Eps8 KO; number of independent experiments: 3). Scale bars depict 5 μm.*

From the structural point of view, dendritic spines are characterized by a highly branched actin filament network containing the Arp2/3 complex and capping proteins [38], the conventional

lamellipodial markers. Consequently, it has been proposed that a fine regulation of capping and branching activities may be required for spine head enlargement during development and plasticity phenomena [154]. We have therefore hypothesized that the ability of Eps8 to cap actin filaments in the spine head may be required for spine formation. It has been previously demonstrated that the capping activity of Eps8 is principally mediated by the amphypathic H1 helix, while H2-H3 core is responsible for bundling [197]. Taking advantage of the Eps8 capping mutant Eps8H1, 10-11 DIV cultured neurons were transfected with wt or mutant protein. Figure 20A shows that overexpression of Eps8 induced a potent increase of spine density, also promoting the formation of larger spines. Conversely, the expression of H1 capping mutant did not result in spine enlargement, clearly indicating that the actin capping activity of Eps8 is necessary for this process. No changes in spine length were observed (data not shown). Notably, Eps8-induced spines were coupled to Bassoon-positive puncta (Fig.20B) and interestingly they also displayed significantly larger PSD-95 puncta compared to neurons transfected with either RFP or H1 mutant, as indicated by immunofluorescence staining and IMARIS reconstruction (Fig.20B, right panel).

Collectively these results clearly indicate that the capping activity of Eps8 is required for proper mushroom-type spine formation, although we cannot exclude that the bundling activity might play a role in the filopodial protrusion from the dendritic shaft, a step that precedes the transition from filopodia to mature spines.

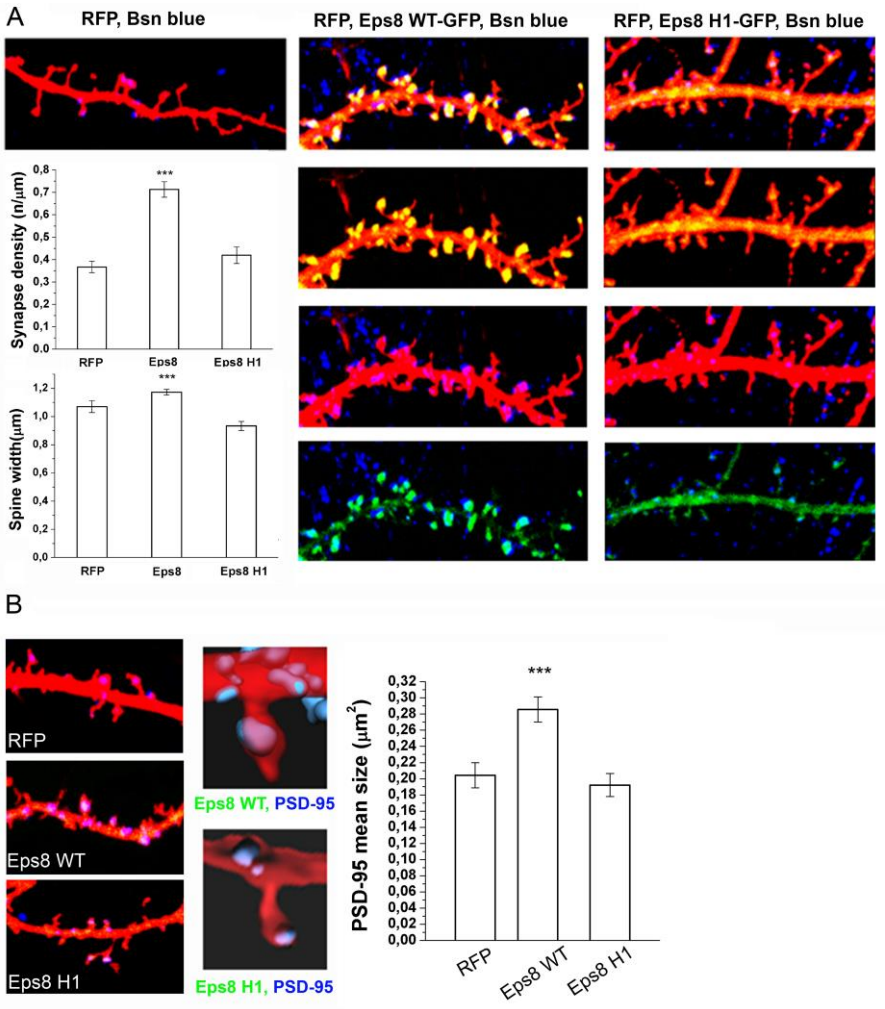

Figure 20. The actin capping activity of Eps8 is required for dendritic spine formation. *(A) Analysis of spine width and density in neurons transfected with RFP, with the cDNA for wt Eps8 (Eps8WT-EGFP) or with the construct for Eps8 devoid of capping activity (Eps8 H1-EGFP). EPS8WT-GFP, but not Eps8H1-EGFP, expressing neurons display increases spine number and size (total number of examined neurons: 15 for RFP, 29 for Eps8 wt and 18 for Eps8 H1; total number of examined spines: 145 for RFP, 553 for Eps8 wt and 105 for Eps8 H1; number of independent experiments: 5). (B) Dendrites of rat hippocampal neurons transfected with RFP, Eps8WT fused to GFP or the actin capping mutant Eps8H1 fused to GFP and stained for PSD-95 (left). 3D reconstruction with Imaris of selected dendritic spines (right). Quantitation of the size of PSD-95 positive puncta is illustrated the flanking graph. Note the increased mean size upon transfection of Eps8WT-EGFP but not Eps8H1-EGFP. Scale bar, 5 µm.*

The lack of Eps8 precludes synaptic potentiation in hippocampal cultures

Given the learning and memory defects of Eps8 KO mice, we investigated whether null cultures are able to undergo proper synaptic potentiation or, like their *in vivo* counterpart show defects in synaptic

plasticity. To address this issue a chemical-induced LTP was applied to both wt and mutant cultures. In more details, selective activation of NMDA receptor has been achieved by a brief (3 minutes) application of high doses (100 μM, [247]) of the NMDA receptor co-agonist glycine. The potential activation of glycine receptor was avoided by including strychnine in all of the solutions. Following washout of glycine, insertion of AMPA receptor occurs in association with mEPSC potentiation [247]. In line with previous reports, application of glycine to wt neurons resulted in a significant increase in both the density and the size of PSD-95 positive puncta and the density of synaptic contacts (Fig.21A,B). Furthermore, upon chemical LTP induction a significant increase in the extent of colocalization between PSD-95 and vGLUT1 staining was detected, in agreement with synaptic strengthening occurring during potentiation phenomena [248]. Notably, in neurons devoid of Eps8, the application of the same protocol did not induce any significant increase in either density or size of PSD-95 positive puncta, or any increase of the colocalization extent of pre- and postsynaptic markers (Fig.21A,B). Patch clamp electrophysiology carried out in parallel revealed that both wt and Eps8 KO cultures displayed normal input resistance before and after chemical-induced LTP, thus excluding the possibility that the protocol affects neuronal health (input resistance: wt=224±7MΩ; KO=210±3MΩ; access resistance: wt=15±2MO; KO=13±2MO; membrane capacitance: wt=42±3 pF; KO=41±10 pF. Number of cells examined, 12 wt and 10 KO).

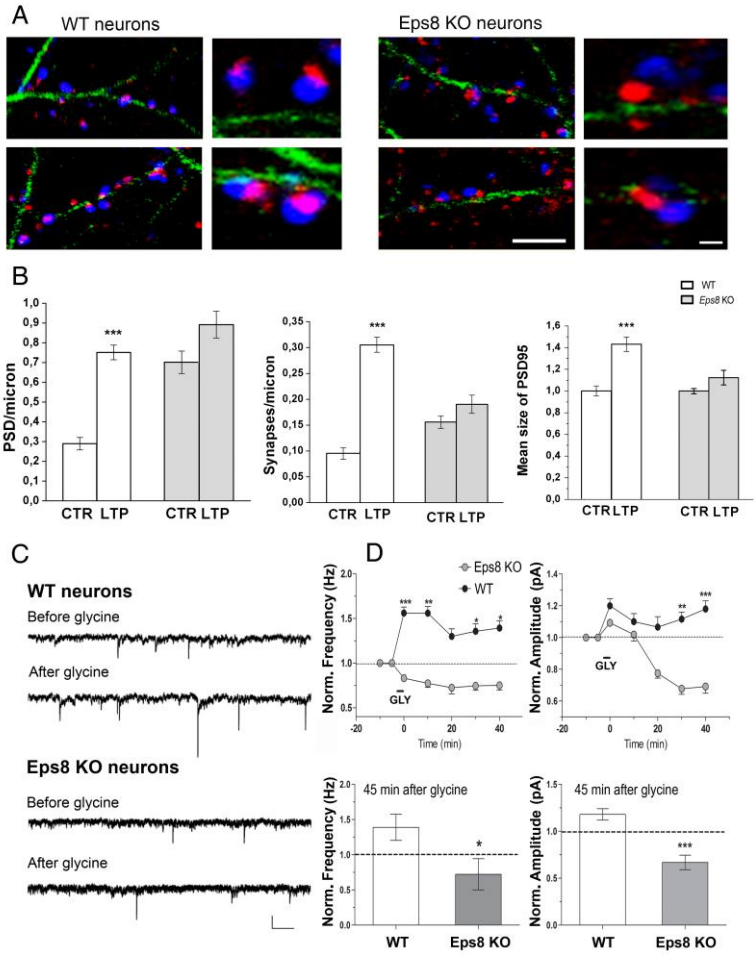

Figure 21. Lack of Eps8 impairs long-term potentiation induced by a chemical LTP protocol. *(A) Representative images of wt and KO cultured neurons before and after application of chemical LTP. Neurons are stained for tubulin (green), PSD-95 (red) and vGLUT1 (blue). Scale bars 10 and 2 μm for higher-magnification images. (B) Quantification of potentiation, expressed as number of PSD-95 puncta per unit length (left), synapse density (middle), mean size of PSD-95 (right). Potentiation occurs in wt but not Eps8 KO cultures, which do not display any increase in the analyzed parameters (Mann–Whitney rank sum test, P<0.001). Data are expressed as mean±s.e.m.; normalized values (total number of examined neurons for analysis of PSD-95 or synapse density: 35 wt ctr and 36 wt LTP; 33 KO ctr and 75 KO LTP; total number of fields for analysis of PSD-95: 46 wt ctr and 59 wt LTP; 72 KO ctr and 90 KO LTP; size number of independent experiments 5). (C,D) Electrophysiological analysis of neuronal cultures exposed to chemical LTP. (C) Representative mEPSCs traces before and after the induction of chemical LTP, in wt and Eps8 null neurons. (D) Time course analysis (5 min before LTP application, 5, 10, 20, 30 and 40 min after LTP application) of mEPSC frequency and amplitude show that KO neurons are unable to undergo LTP (upper). mEPSC mean frequency and amplitude 45 min after the application of LTP are shown in the underlying graphs (bottom). Scale bars, 10 pA and 250ms (total number of examined neurons: 13 wt and 16 KO; number of independent experiments: 5).*

The lack of potentiation in Eps8 KO neurons was also confirmed by electrophysiological recordings of mEPSCs after the application of glycine. As shown in Figure21C,D whereas wt neurons display a significant increase of mEPSC frequency and amplitude, mutant neurons

fail to undergo proper potentiation upon glycine stimulation. Moreover, the lack of potentiation is also confirmed by two independent pair recordings experiments, where stimulation of presynaptic neuron (three 50 Hz, 2 s trains of depolarization at 20 s intervals) during brief perfusion with Mg^{2+}-free solution [249] induced a potentiation of excitatory current in wt but not Eps8 KO neurons (evoked-EPSC amplitude, wt=1.350±0.05; Eps8 KO=0.7750±0.0125 pA). In addition, acute downregulation of Eps8 expression by siRNA similarly prevented synaptic potentiation (Fig.22, right panel).

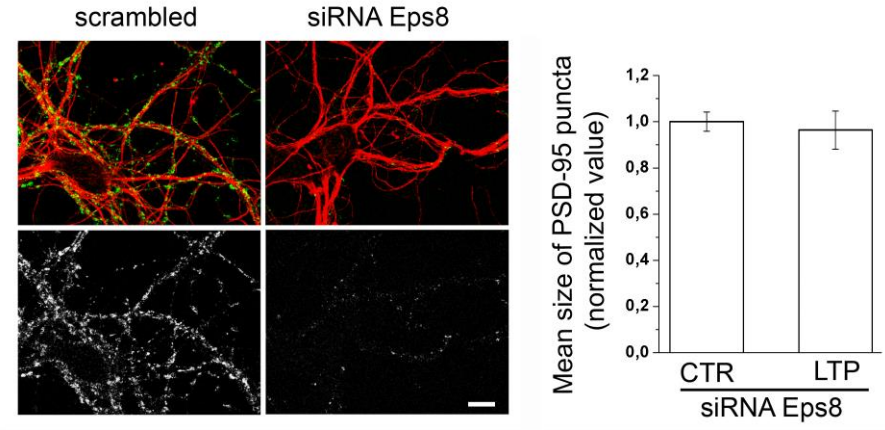

Figure 22. Reduced Eps8 expression impairs synaptic potentiation. *(Left) treatment of mouse hippocampal cultures with Eps8 siRNA potently reduces the expression of the protein (red: tubulin; green: Eps8). (Right) Neurons in which Eps8 is acutely down regulates by siRNA are no longer able to undergo synaptic potentiation in term of increased mean size of PSD-95 after chemical LTP. Scale Bar, 5 µm.*

These data indicate that Eps8 is required for LTP expression in hippocampal cultures and suggest that the protein may be involved in stabilization of actin cytoskeleton during spine remodeling. In further support of this hypothesis, endogenous Eps8 is recruited to spine head upon application of chemical LTP, as indicated by increased immunostaining for the protein in RFP-labelled dendritic protrusions (Fig.22A,B).

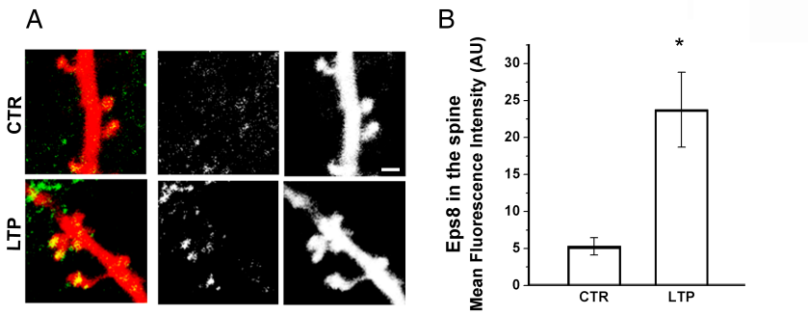

Figure 23. Endogenous Eps8 is recruited to spine head upon application of chemical LTP *(A) Representative examples of dendrites of mice hippocampal neurons transfected with RFP, exposed to chemical LTP and stained for Eps8. Note the increased Eps8 immunoreactivity within stimulated spine head after potentiation. Scale bar, 2 μm. (B) Quantitation of Eps8 immunofluorescence at the spine head in vehicle-treated and glycine-treated (100 μM) neurons (Mann–Whitney Rank Sum Test, P=0.013) (total number of examined neurons: 16 untreated neurons and 12 gly-treated neurons; number of independent experiments: 3).*

Inhibition of Eps8 capping activity impairs spine enlargement and plasticity

Given the demonstration that Eps8 is recruited to spine head after chemical-LTP induction and the capping activity of the protein is required for proper spine formation and morphogenesis during neuronal development (Fig.23 and Fig.19,20), we hypothesized that ability of Eps8 to cap the barbed ends of actin filaments preventing their further extension is crucial for the process of structural plasticity. Therefore we tested the ability of either an Eps8- or Eps8H1- transfected neuron to undergo synaptic potentiation upon chemical LTP. As clearly shown by quantification (Fig.24D), overexpression of Eps8WT but not of Eps8H1 prevents spine enlargement upon LTP, probably because the excess of capping activity ends up in an alteration of actin dynamics in the spine. In fact, expression of actin-capping mutant protein Eps8H1, which has no effects on actin polymerization [197], allows a proper spine remodeling (Fig.24A-D).

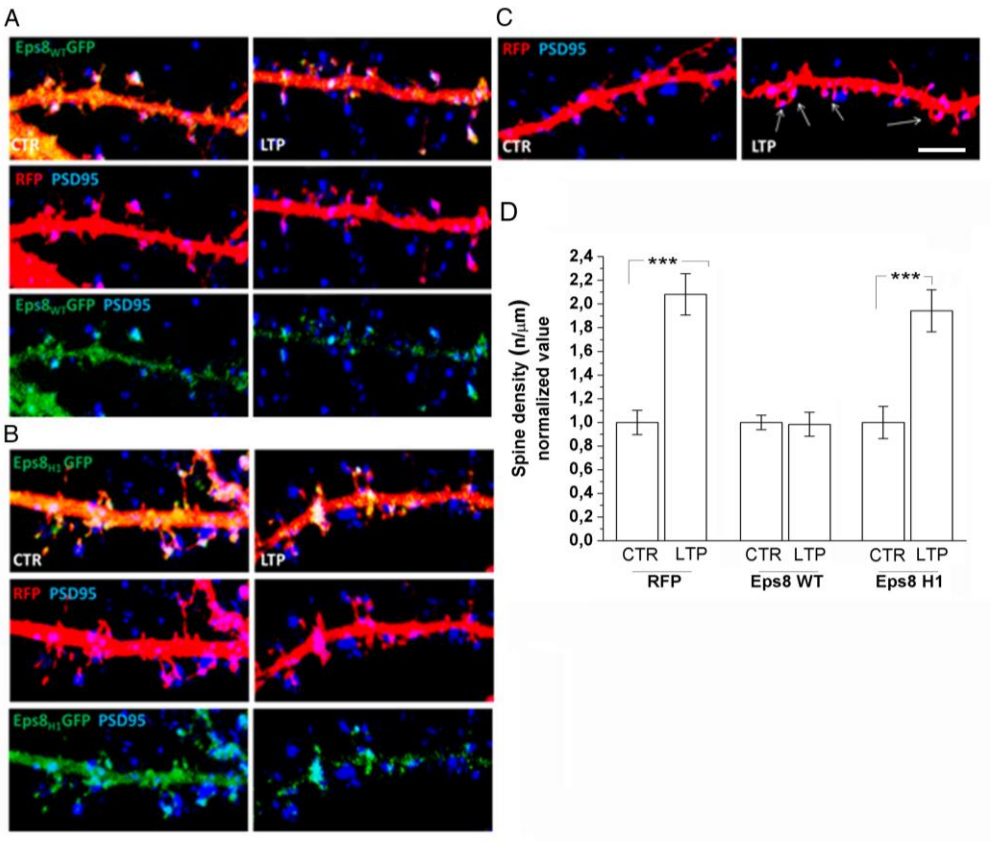

Figure 24. Saturation of actin capping by overexpression of Eps8, but not of its actin capping mutant, preclude LTP. *(A-C) 14-16 DIV rat hippocampal neurons transfected with RFP (A), Eps8WT-EGFP cDNA (B) or cDNA coding for the actin capping mutant Eps8H1-EGFP. (C). Representative images of Eps8WT-EGFP and Eps8H1-EGFP expressing neurons before and after application of chemical LTP and stained for PSD-95 (blue). (D) Quantitation of spine density in RFP transfected neurons and in Eps8WT or H1 expressing neurons. Potentiation is prevented by overexpression of Eps8 but not by its actin-capping mutant H1, meaning that an excess of capping activity precludes potentiation (number of cell examined: 18, RFP; 25, Eps8 wt; 24, Eps8 H1. Number of spines analyzed: 179, RFP; 372, Eps8 wt; 286, Eps8 H1. Number of independent experiments: 5.) Scale bars, 8 µm.*

To further demonstrate the requirement of Eps8 capping activity during spine plasticity, we injected the postsynaptic neuron, through the patch pipette, with a synthetic peptide (blocking peptide), which prevents Eps8 from capping actin filaments by competing with Abi1 for binding to Eps8 [250]. Direct competition could be observed in *in vitro* binding assay using recombinant purified proteins (Fig.25A). LTP was then induced 10 minutes after blocking peptide injection, while mEPSC was electrophysiological recorded during the entire procedure. As clearly

demonstrated by quantitative analysis shown in Figure25B,C the injection of the blocking peptide but not of the scramble peptide impaired synaptic potentiation induced by glycine stimulation. To notice, injection of either blocking or scramble peptides in Eps8 KO neurons following glycine administration did not have any effect (Fig.25D,E). Furthermore the same peptides do not alter *per se* mEPSC frequency or amplitude in wt and null cultures (Fig252F,G).

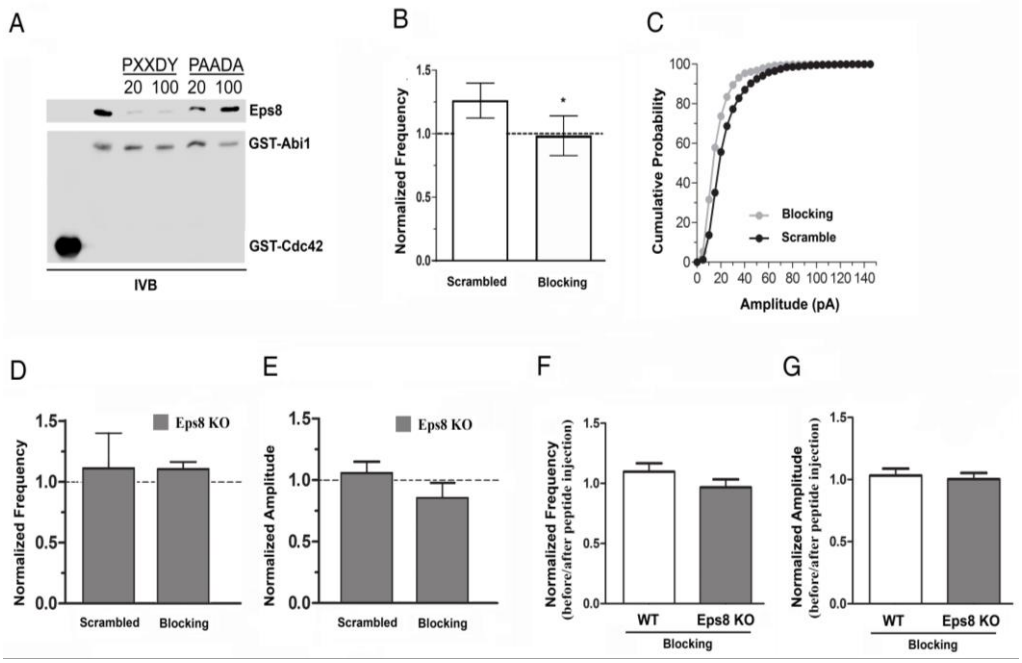

Figure 25. Neurons in which Eps8 actin capping activity was acutely inhibited are no longer able to undergo synaptic potentiation. *(A) The proline rich consensus site of Abi1 (PXXDY) competes with Abi1 for binding to Eps8. Equal amounts of His-Eps8 (0.2 μM) were incubated with 0.2 μ M immobilized GST-Abi1 in the absence or in the presence of 20 and 100 μM of either PXXDY or PAADA synthesized peptides. 2 μM GST-Cdc42 was used as a control. Proteins were analyzed by immunoblotting with the indicated antibodies. (B,C) mEPSC frequency (B) and amplitude (C) in neurons exposed to chemical LTP and intracellularly perfused via the patch pipette with either the scrambled or the blocking peptide (the blocking peptide competes with Abi1 for binding to Eps8 and therefore inhibits the Eps8 capping activity). Note that neurons intracellularly perfused with the blocking peptide (grey column, white dots) are defective in potentiation, measured as mEPSC frequency or amplitude. Synaptic potentiation occurs properly in neurons intracellularly perfused with a scramble peptide (black dots) (total number of examined neurons: 6 for both conditions; number of independent experiments: 3). (D,E) mEPSC frequency (D) and amplitude (E) in Eps8 KO neurons exposed to chemical LTP and intracellularly perfused with either the scrambled or the blocking peptide. Note that mEPSC frequency and amplitude of KO neurons do not change upon glycine administration with or without injection of the blocking peptide. (F,G) Normalized mEPSC frequency (F) and amplitude (G) in wt and KO neurons before and after blocking peptide injection. Note that injection of the blocking peptide does not affect per se basal synaptic activity.*

Finally, the lack of Eps8 had no effects on Rac activity in 15 DIV cultured hippocampal neurons (Fig.26) and, as already demonstrated, in the brain [1], thus suggesting that Eps8 functions mainly as actin capper in the CNS [215]. Moreover this data rule out the possibility that the LTP impairment in Eps8 KO neurons could be due to a missregulation of Rac activity or its downstream effectors, such as WAVE and Arp2/3 complex.

Altogether, these results univocally demonstrated that the capping activity of Eps8 is essential for LTP-mediated synapse formation and strengthening.

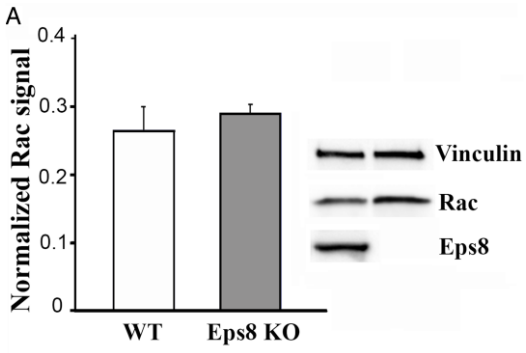

Figure 26. Eps8 removal does not affect Rac-GTP levels. *(A) The levels of Rac-GTP is not affected in Eps8 null hippocampal cultured neurons (P=0,19). Equal amounts of cell protein extract were processed to determine Rac in wt and mutated coltures (see Material and Methods section for details). The results obtained were normalized on the total level of Rac. Equal amounts of lysates from wt and Eps8 KO neurons were processed for western blotting with the indicated antibodies (right panel).*

Eps8 is expressed at lower levels in brains of autistic patients

Eps8 capping activity is regulated by the neurotrophic factor BDNF in a MAP kinase dependent way [1]. BDNF has been demonstrated to be required for spine maturation and dendritic LTP [198, 251], since is a critical factor for synaptogenesis, synaptic plasticity and memory formation [213, 252].

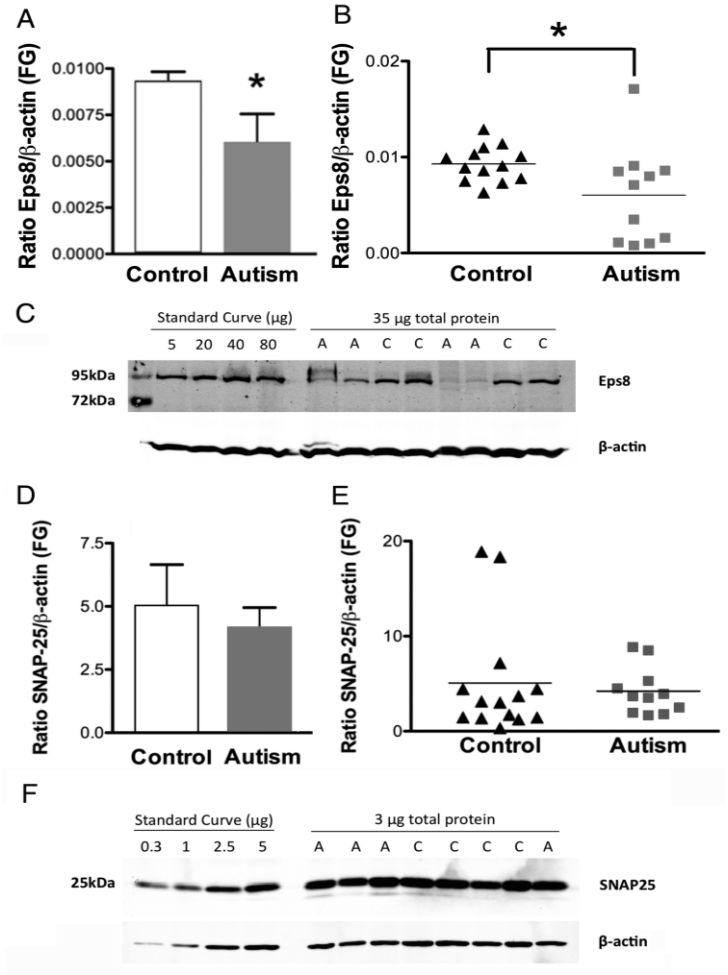

Figure 27. Eps8 expression levels are reduced in brains of patients affected by autism. *(A, B) Quantification of Eps8 protein expression in fusiform gyrus (FG) of autistic patients and control samples by quantitative Western blotting. Each sample was normalized to ß-actin. *P<0.05, two-tailed Student's t-test. Bars indicate mean±s.me. Autism, n=11; control, n=13. (C) Representative western blot of fusiform gyrus showing autism (A) and control (C) cases. Lanes 2–5: standard curve consisting of different amounts of total protein from a single normal human cortex sample. Lanes 6–13: 35 μg of total protein from each autistic patient and control sample. Blots were run twice with two different Eps8 antibodies and gave similar results. (D,E) No change in SNAP-25 levels in fusiform gyrus of autistic subjects compared to controls. Quantification of SNAP-25 protein expression in fusiform gyrus (FG) of autism and control samples determined by western blotting. Each sample was normalized to b-actin. P=0.67, two-tailed t-test. Bars indicate mean±s.e. Autism, n=11; control, n=13. (F) Representative western blot of fusiform gyrus showing autism (A) and control (C) cases. Lanes 1–4: standard curve consisting of different amounts of total protein from a single normal human cortex sample. Lanes 5–12: 3 μg of total protein from each autism and control sample.*

Furthermore, the balance between the BDNF precursor, proBDNF, and the mature BDNF, which controls spine formation [169], has been found to be disrupted in the brain tissue of autistic patients [209]. Thus, given the established spine pathology affecting autistic subjects [2, 13], in

collaboration with Prof. Margaret Fahnestock (McMaster University, Canada) we examined Eps8 levels by quantitative western blot in the fusiform gyrus of the brain; this area is indeed involved in face perception and it is known to be altered in ADS patients [253, 254]. Tissues were collected from 11 patients with autism and 13 control subjects, respectively. Interestingly, we found a substantial reduction of Eps8 in autistic patients compared to controls (Fig.27A-C). Conversely, no difference in the expression of the SNARE protein, SNAP-25, has been detected in the same samples (Fig.27D-F), supporting the specificity of Eps8 deficit.

By leading to changes in spine density and dynamics, a decrease in Eps8 expression in the brain of autistic patients could contribute to the morphological, cognitive and behavioral defects which characterize this disorder. The cognitive and social impairments and the alteration in spine number and morphology we observed in Eps8 KO animals further support this hypothesis.

Table 1.

Phenotypic characteristics of male WT and *Eps8* null mice

General Health			
Weight (g)	26.45±1.08	26.12±0.77	0.81
Fur condition (3-point scale)	3.0±0.0	3.0±0.0	-
Piloerection (%)	0	0	-
Body Tone (3-point scale)	3.0±0.0	3.0±0.0	-
Skin colour (%)	100	100	-
Physical abnormalities (%)	0	0	-
Empty cage behaviour			
Nesting building (5-point scale)	4.80±0.2	4.75±0.25	0.87
Reflexes			
Righting reflexes (4-point scale)	0	0.01±0.01	-
Corneal (8-point scale)	4±0.3	3.9±0.2	0.78
Pinna (8 point scale)	4±0	3.9±0.2	0.62
Tail pinch (8-point scale)	3.9±0.04	4±0.2	0.63
Motor function			
Locomotor activity			
Horizontal counts (n)	3869±141	3963±204	0.76
Vertical counts (n)	921.5 ±56.01	824.5±56.2	0.24
Motor coordination			
Rotarod (%)	60	50	0.89
Wire hanging (s)	260.2±10.8	277.2±15.4	0.37
Sensory abilities			
Hearing (%)	100	100	-
Visual acuity (%)	100	100	-
Emotional-like reactivity			
Anxiety:			
Elevated plus maze			
Open arm entries %	43.7±6.54	44.05±10.49	0.97
Open arm time %	26.18±6.75	37.08±16.82	0.53

Mice were assessed on general health, empty cage behaviour, reflexes, sensory abilities, motor coordination. N = 8-10 per group.

DISCUSSION

Substantial evidences support the role of actin cytoskeleton remodeling in spine structural changes and memory stabilization [154, 255]. For instance, it is known that perturbation of actin dynamics by drugs treatments or due to mutation in key actin regulating proteins affect both synaptic strengthening and spine formation and modifications. Indeed, inhibition of actin filament polymerization suppresses long term potentiation [112, 126, 149, 152] whereas LIMK null mice, which lose the ability to regulate the activity of the actin severing protein cofilin, exhibits enhanced hippocampal LTP [52, 53]. Furthermore, mice lacking the actin-regulating protein WAVE-1 display changes in spine density and defects in synaptic plasticity [256] while Abi2 KO animals present abnormal dendritic spine morphology and density associated with severe deficits in short- and long-term memory [167].

During my PhD we have provided direct demonstration that the actin binding and regulating protein Eps8 not only regulates the formation of axonal and dendritic filopodia in developing neurons [1] but it is also required at the mature synapse for proper spine morphology and synaptic plasticity.

Immature features of Eps8 null dendritic spines

Synaptogenesis and in particular dendritic spine formation start with the protrusion of thin and highly motile actin-based structures, the filopodia [51]. Those structures are more abundant at early developmental stages, when they play a role to sample potentially presynaptic partners, eventually mediating synaptic contact formation [176-180]. The establishment of synaptic contact is associated with the transition from filopodium to a more stable structure, the dendritic spine

[154, 166, 177, 183]. However, dendritic spines are not static structures exhibiting both transitory fluctuation in size and shapes and dynamic changes during synaptic potentiation, supporting and matching functional modifications [99, 109, 120]. These phenomena constantly reshape adult brain circuitry in response to external stimuli, allowing learning processes and memory formation [75, 77, 257]. It is known that the morphology of dendritic spines is tightly linked to functional properties of harbored synaptic contacts. In fact, spine head size positively correlates to the PSD area and AMPA receptors density, and finally to synaptic strength [51, 73, 108, 131, 258, 259]. Accordingly, immature spines are characterized by highly mobile and less stable synaptic PSD-95 clusters [260, 261]. Notably, the loss of Eps8 leads to the formation of thinner and longer dendritic protrusions moreover characterized by a decrease synaptic strength and less stable synaptic PSD-95 clusters, thus suggesting that the capping protein Eps8 is required for spine maturation and proper synaptic function involving both scaffolding proteins and receptors. Given that immature spines have impaired synaptic signaling and defective synaptic plasticity, perturbations of the ratio between mature to immature spines could play a crucial role in neuronal function and connectivity. Consistently, Eps8 null dendritic spines are impaired in activity-dependent structural modifications. These alterations are also associated with cognitive impairment in null mice.

Capping activity: dendritic spine building up and plasticity

It has been recently proposed that the spine head expansion that occurs during synaptic plasticity and developmental dependent maturation may be governed by the same mechanisms that regulates lamellipodium formations, thus involving the concomitant action of actin

capping proteins and Arp2/3 complex, which nucleates branched actin filaments from pre-existent ones (Hootulainer and hoongraad 2010). However, so far no direct evidence supports the involvement of actin-capping activity in activity dependent spine enlargement and in synaptic plasticity. Concurrently to the revision of our manuscript, a paper has been published showing that Eps8 capping activity regulates actin dynamics within dendritic spines, thus promoting dendritic spines formation [262]. The Authors have used the Eps8 capping mutant carrying three point mutations (V729A, T731A, and W732A; [1]) that has been recently demonstrated to destroy the tridimensional structure of the C-terminal region of the protein, thus negatively affecting not only the capping activity but also the bundling activity [197] that may play a crucial role in the initial phase of filopodia extension from the dendritic shaft. The other evidence suggesting that actin-capping proteins may regulate synaptic plasticity comes from the study of Kitanashi and coworkers, who identified F-actin protein CapZ [263], previously shown to regulate growth cone morphology and neurite outgrowth [264], among the proteins whose expression is regulated by neuronal activity [160]. In fact CapZ accumulates within dendritic spines in activity-dependent manner, thus suggesting the involvement of the protein in the regulation of actin remodeling induced by synaptic activation and in synaptic plasticity.

The demonstration of Eps8 capping activity as necessary for proper spine morphogenesis comes from two lines of evidence. First of all, the expression of the well-characterized mutant Eps8H1, selectively avoid of actin-capping activity, is not capable to support proper spine formation while the wt protein increases the density of dendritic spines which are further characterized by a larger head and PSD-95 cluster. In this way, we

were able to specifically study the involvement of capping function distinguishing it from the bundling activity of Eps8. In fact, while the bundling activity is mainly mediated by a compact four-helix bundle, which contacts three actin subunits along filaments, the actin-capping activity is principally sustained by a amphipathic helix that bind within the hydrophobic pocket at the barbed end of actin filaments [197]. In Eps8H1 mutant hydrophobic residues critical for actin-capping activity has been mutated, although actin bundling is unaffected [197]. As a further support, the injection of a blocking peptide designed to acutely inhibit Eps8 in postsynaptic neurons resulted in impairment of synaptic potentiation, thus univocally demonstrating that Eps8 is required for spine formation and for both structural and functional plasticity phenomena through the capping of actin filaments.

Recently, Stamatakou and coworkers have shown that acute downregualtion of Eps8 in primary neuronal cultures affects spine formation and plasticity, the former in particular through its capping activity [262]. However they did not observed any impairment in mEPSC amplitude upon LTP induction, leading them to conclude that Eps8 is required for LTP-mediated synapse formation but not for LTP-induced synaptic strengthening. Conversely, our *in vivo* and *in vitro* data support the involvement of Eps8 also in synaptic strengthening that occurs during synaptic plasticity. The difference observed may be due to residual Eps8 levels in the experimental conditions of Stamatakou's study.

Eps8 has been detected in many brain regions, including the olfactory bulb, anterior olfactory nuclei, basal forebrain, cerebral cortex, hippocampus, septal nuclei, amygdala, thalamus, hypothalamus, colliculi, pontine nuclei, cerebellum cochlear nuclear complex and inferior olive, while the white matter in generally unstained [203]. Interestingly, Eps8 is

highly expressed in layer II and III neurons of cerebral cortex and in the hippocampus, two areas classically implicated in higher cognitive functions [203]. In particular, Eps8 has been found in synaptosomal preparation from hippocampus [1] and cerebellum. Furthermore, the protein has been localized postsynaptically in dendrites articulations of cerebellum granule cells [203, 204] and it is also expressed in axon of cultured hippocampal neurons [1] and of granule cells in situ [204]. Then, Eps8 seems to be in the right place to play a pivotal role in controlling synapse architecture and functions. In line with this hypothesis, mice lacking Eps8 displayed aberrant spine morphology and alteration of dendritic protrusion density associated with impairment in cognitive functions.

Eps8, a new ASD related gene?

The binding of barbed end actin filaments is a key mechanisms for regulating filaments' elongation and disassembly, and as a consequence of the final architecture of actin networks [186, 188, 189]. From this point of view, it is therefore conceivable that the lack of Eps8 would be result in impairment of actin dynamics and organization within dendritic spines and as a consequence of synaptic function and plasticity. Indeed, a variety of evidence supports the existence of a strong link between actin remodeling and functional changes of synaptic contacts [51]. Actin regulating proteins have been found mutated or misexpressed in subjects suffering of ASD, schizophrenia and intellectual disability [18, 38, 39, 171-175], pathologies known to be characterized by altered dendritic spine structures and dynamics [13, 14, 132-135]. In particular, mutations in synaptic genes including Akt/mTOR pathway [265, 266] involved in the regulation of spine protein synthesis, the Neurexin-Neuroligin-SHANK pathway [15, 39] associated with aberrant synaptogenesis and

E/I imbalance, and Ras/Rho GTPase pathway [267] implicated in spine formation and stabilization have been identified in ASD patients. Taken together, these findings suggest a major role of dendritic spines abnormalities in the pathogenesis of these diseases. We have shown that reduced levels of Eps8 occur in fusiform gyrus of patients affected by autism. Together with previous evidence that CP levels are significantly lower in fetal brains of Down syndrome than in control [268], our data suggest that reduced levels of capping activity may characterize or may concurr to the cognitive impairment associated with spine defects. Interestingly, alteration in levels of mature BDNF has been described in autistic subjects [209]. Since the actin-capping activity of Eps8 is regulated in neurons by BDNF [1, 206] and the well characterized role of this neurothrophin in synaptogenesis and spine remodeling [205-207], it is possible speculate that BDNF controls actin capping and spine morphogenesis via Eps8 during synaptic plasticity and learning and that defects in this pathway may be involved in the pathogenesis of autism.

Bibliography

1. Menna, E., et al., *Eps8 regulates axonal filopodia in hippocampal neurons in response to brain-derived neurotrophic factor (BDNF).* PLoS Biol, 2009. **7**(6): p. e1000138.
2. Penzes, P., et al., *Dendritic spine pathology in neuropsychiatric disorders.* Nat Neurosci, 2011. **14**(3): p. 285-93.
3. Penzes, P., et al., *Developmental vulnerability of synapses and circuits associated with neuropsychiatric disorders.* J Neurochem, 2013. **126**(2): p. 165-82.
4. Toro, R., et al., *Key role for gene dosage and synaptic homeostasis in autism spectrum disorders.* Trends Genet, 2010. **26**(8): p. 363-72.
5. van Spronsen, M. and C.C. Hoogenraad, *Synapse pathology in psychiatric and neurologic disease.* Curr Neurol Neurosci Rep, 2010. **10**(3): p. 207-14.
6. Won, H., W. Mah, and E. Kim, *Autism spectrum disorder causes, mechanisms, and treatments: focus on neuronal synapses.* Front Mol Neurosci, 2013. **6**: p. 19.
7. Matson, J.L. and M. Shoemaker, *Intellectual disability and its relationship to autism spectrum disorders.* Res Dev Disabil, 2009. **30**(6): p. 1107-14.
8. Guerrini, R. and E. Parrini, *Epilepsy in Rett syndrome, and CDKL5- and FOXG1-gene-related encephalopathies.* Epilepsia, 2012. **53**(12): p. 2067-78.
9. Mulligan, C.K. and D.A. Trauner, *Incidence and Behavioral Correlates of Epileptiform Abnormalities in Autism Spectrum Disorders.* J Autism Dev Disord, 2013.
10. Edvardson, S., et al., *Mutations in SLC35A3 cause autism spectrum disorder, epilepsy and arthrogryposis.* J Med Genet, 2013.
11. Vivanti, G., et al., *Intellectual development in autism spectrum disorders: new insights from longitudinal studies.* Front Hum Neurosci, 2013. **7**: p. 354.
12. Penzes, P. and C. Remmers, *Kalirin signaling: implications for synaptic pathology.* Mol Neurobiol, 2012. **45**(1): p. 109-18.
13. Hutsler, J.J. and H. Zhang, *Increased dendritic spine densities on cortical projection neurons in autism spectrum disorders.* Brain Res, 2010. **1309**: p. 83-94.
14. Irwin, S.A., et al., *Abnormal dendritic spine characteristics in the temporal and visual cortices of patients with fragile-X syndrome: a quantitative examination.* Am J Med Genet, 2001. **98**(2): p. 161-7.
15. Jamain, S., et al., *Mutations of the X-linked genes encoding neuroligins NLGN3 and NLGN4 are associated with autism.* Nat Genet, 2003. **34**(1): p. 27-9.
16. Kim, H.G., et al., *Disruption of neurexin 1 associated with autism spectrum disorder.* Am J Hum Genet, 2008. **82**(1): p. 199-207.
17. Berkel, S., et al., *Mutations in the SHANK2 synaptic scaffolding gene in autism spectrum disorder and mental retardation.* Nat Genet, 2010. **42**(6): p. 489-91.
18. Durand, C.M., et al., *SHANK3 mutations identified in autism lead to modification of dendritic spine morphology via an actin-dependent mechanism.* Mol Psychiatry, 2012. **17**(1): p. 71-84.
19. Sato, D., et al., *SHANK1 Deletions in Males with Autism Spectrum Disorder.* Am J Hum Genet, 2012. **90**(5): p. 879-87.
20. von Bohlen Und Halbach, O., *Dendritic spine abnormalities in mental retardation.* Cell Tissue Res, 2010. **342**(3): p. 317-23.
21. Kaufmann, W.E. and H.W. Moser, *Dendritic anomalies in disorders associated with mental retardation.* Cereb Cortex, 2000. **10**(10): p. 981-91.
22. Fiala, J.C., J. Spacek, and K.M. Harris, *Dendritic spine pathology: cause or consequence of neurological disorders?* Brain Res Brain Res Rev, 2002. **39**(1): p. 29-54.
23. Newey, S.E., et al., *Rho GTPases, dendritic structure, and mental retardation.* J Neurobiol, 2005. **64**(1): p. 58-74.
24. Harrison, P.J. and D.R. Weinberger, *Schizophrenia genes, gene expression, and neuropathology: on the matter of their convergence.* Mol Psychiatry, 2005. **10**(1): p. 40-68; image 5.

25. Owen, M.J., N. Craddock, and M.C. O'Donovan, *Schizophrenia: genes at last?* Trends Genet, 2005. **21**(9): p. 518-25.
26. Kantrowitz, J.T. and D.C. Javitt, *N-methyl-d-aspartate (NMDA) receptor dysfunction or dysregulation: the final common pathway on the road to schizophrenia?* Brain Res Bull, 2010. **83**(3-4): p. 108-21.
27. Bergeron, R. and J.T. Coyle, *NAAG, NMDA receptor and psychosis.* Curr Med Chem, 2012. **19**(9): p. 1360-4.
28. Janssen, M.J., E. Leiva-Salcedo, and A. Buonanno, *Neuregulin directly decreases voltage-gated sodium current in hippocampal ErbB4-expressing interneurons.* J Neurosci, 2012. **32**(40): p. 13889-95.
29. Andersson, R.H., et al., *Neuregulin and dopamine modulation of hippocampal gamma oscillations is dependent on dopamine D4 receptors.* Proc Natl Acad Sci U S A, 2012. **109**(32): p. 13118-23.
30. Shamir, A., et al., *The importance of the NRG-1/ErbB4 pathway for synaptic plasticity and behaviors associated with psychiatric disorders.* J Neurosci, 2012. **32**(9): p. 2988-97.
31. Yu, W. and B. Lu, *Synapses and dendritic spines as pathogenic targets in Alzheimer's disease.* Neural Plast, 2012. **2012**: p. 247150.
32. Selkoe, D.J., *Alzheimer's disease is a synaptic failure.* Science, 2002. **298**(5594): p. 789-91.
33. Sudhof, T.C., *Neuroligins and neurexins link synaptic function to cognitive disease.* Nature, 2008. **455**(7215): p. 903-11.
34. Jacob, T.C., S.J. Moss, and R. Jurd, *GABA(A) receptor trafficking and its role in the dynamic modulation of neuronal inhibition.* Nat Rev Neurosci, 2008. **9**(5): p. 331-43.
35. Paluszkiewicz, S.M., B.S. Martin, and M.M. Huntsman, *Fragile X syndrome: the GABAergic system and circuit dysfunction.* Dev Neurosci, 2011. **33**(5): p. 349-64.
36. Pizzarelli, R. and E. Cherubini, *Alterations of GABAergic signaling in autism spectrum disorders.* Neural Plast, 2011. **2011**: p. 297153.
37. Yizhar, O., et al., *Neocortical excitation/inhibition balance in information processing and social dysfunction.* Nature, 2011. **477**(7363): p. 171-8.
38. Svitkina, T., et al., *Regulation of the postsynaptic cytoskeleton: roles in development, plasticity, and disorders.* J Neurosci, 2010. **30**(45): p. 14937-42.
39. Durand, C.M., et al., *Mutations in the gene encoding the synaptic scaffolding protein SHANK3 are associated with autism spectrum disorders.* Nat Genet, 2007. **39**(1): p. 25-7.
40. Moessner, R., et al., *Contribution of SHANK3 mutations to autism spectrum disorder.* Am J Hum Genet, 2007. **81**(6): p. 1289-97.
41. Gauthier, J., et al., *De novo mutations in the gene encoding the synaptic scaffolding protein SHANK3 in patients ascertained for schizophrenia.* Proc Natl Acad Sci U S A, 2010. **107**(17): p. 7863-8.
42. Bozdagi, O., et al., *Haploinsufficiency of the autism-associated Shank3 gene leads to deficits in synaptic function, social interaction, and social communication.* Mol Autism, 2010. **1**(1): p. 15.
43. Peca, J., et al., *Shank3 mutant mice display autistic-like behaviours and striatal dysfunction.* Nature, 2011. **472**(7344): p. 437-42.
44. Wang, X., et al., *Synaptic dysfunction and abnormal behaviors in mice lacking major isoforms of Shank3.* Hum Mol Genet, 2011. **20**(15): p. 3093-108.
45. Bockers, T.M., et al., *Differential expression and dendritic transcript localization of Shank family members: identification of a dendritic targeting element in the 3' untranslated region of Shank1 mRNA.* Mol Cell Neurosci, 2004. **26**(1): p. 182-90.
46. Schmeisser, M.J., et al., *Autistic-like behaviours and hyperactivity in mice lacking ProSAP1/Shank2.* Nature, 2012. **486**(7402): p. 256-60.

47. Verpelli, C., et al., *Importance of Shank3 protein in regulating metabotropic glutamate receptor 5 (mGluR5) expression and signaling at synapses.* J Biol Chem, 2011. **286**(40): p. 34839-50.
48. Arber, S., et al., *Regulation of actin dynamics through phosphorylation of cofilin by LIM-kinase.* Nature, 1998. **393**(6687): p. 805-9.
49. Tassabehji, M., et al., *LIM-kinase deleted in Williams syndrome.* Nat Genet, 1996. **13**(3): p. 272-3.
50. Racz, B. and R.J. Weinberg, *Spatial organization of cofilin in dendritic spines.* Neuroscience, 2006. **138**(2): p. 447-56.
51. Cingolani, L.A. and Y. Goda, *Actin in action: the interplay between the actin cytoskeleton and synaptic efficacy.* Nat Rev Neurosci, 2008. **9**(5): p. 344-56.
52. Meng, Y., et al., *Abnormal spine morphology and enhanced LTP in LIMK-1 knockout mice.* Neuron, 2002. **35**(1): p. 121-33.
53. Meng, Y., et al., *Regulation of ADF/cofilin phosphorylation and synaptic function by LIM-kinase.* Neuropharmacology, 2004. **47**(5): p. 746-54.
54. Tsai, N.P., et al., *Multiple autism-linked genes mediate synapse elimination via proteasomal degradation of a synaptic scaffold PSD-95.* Cell, 2012. **151**(7): p. 1581-94.
55. El-Husseini, A.E., et al., *PSD-95 involvement in maturation of excitatory synapses.* Science, 2000. **290**(5495): p. 1364-8.
56. Fan, Y., et al., *Actin capping protein is required for dendritic spine development and synapse formation.* J Neurosci, 2011. **31**(28): p. 10228-33.
57. Carrie, A., et al., *A new member of the IL-1 receptor family highly expressed in hippocampus and involved in X-linked mental retardation.* Nat Genet, 1999. **23**(1): p. 25-31.
58. Pavlowsky, A., et al., *A postsynaptic signaling pathway that may account for the cognitive defect due to IL1RAPL1 mutation.* Curr Biol, 2010. **20**(2): p. 103-15.
59. Valnegri, P., et al., *The X-linked intellectual disability protein IL1RAPL1 regulates excitatory synapse formation by binding PTPdelta and RhoGAP2.* Hum Mol Genet, 2011. **20**(24): p. 4797-809.
60. Yoshida, T., et al., *IL-1 receptor accessory protein-like 1 associated with mental retardation and autism mediates synapse formation by trans-synaptic interaction with protein tyrosine phosphatase delta.* J Neurosci, 2011. **31**(38): p. 13485-99.
61. Gambino, F., et al., *IL1RAPL1 controls inhibitory networks during cerebellar development in mice.* Eur J Neurosci, 2009. **30**(8): p. 1476-86.
62. Mukai, J., et al., *Palmitoylation-dependent neurodevelopmental deficits in a mouse model of 22q11 microdeletion.* Nat Neurosci, 2008. **11**(11): p. 1302-10.
63. Stark, K.L., et al., *Altered brain microRNA biogenesis contributes to phenotypic deficits in a 22q11-deletion mouse model.* Nat Genet, 2008. **40**(6): p. 751-60.
64. Ho, G.P., et al., *S-nitrosylation and S-palmitoylation reciprocally regulate synaptic targeting of PSD-95.* Neuron, 2011. **71**(1): p. 131-41.
65. Chuang, S.C., et al., *Prolonged epileptiform discharges induced by altered group I metabotropic glutamate receptor-mediated synaptic responses in hippocampal slices of a fragile X mouse model.* J Neurosci, 2005. **25**(35): p. 8048-55.
66. Restivo, L., et al., *Simultaneous olfactory discrimination elicits a strain-specific increase in dendritic spines in the hippocampus of inbred mice.* Hippocampus, 2006. **16**(5): p. 472-9.
67. Slutsky, I., et al., *Enhancement of learning and memory by elevating brain magnesium.* Neuron, 2010. **65**(2): p. 165-77.
68. Meredith, R.M., R. de Jong, and H.D. Mansvelder, *Functional rescue of excitatory synaptic transmission in the developing hippocampus in Fmr1-KO mouse.* Neurobiol Dis, 2011. **41**(1): p. 104-10.
69. Garner, C.C., C.L. Waites, and N.E. Ziv, *Synapse development: still looking for the forest, still lost in the trees.* Cell Tissue Res, 2006. **326**(2): p. 249-62.

70. Rollenhagen, A. and J.H. Lubke, *The morphology of excitatory central synapses: from structure to function.* Cell Tissue Res, 2006. **326**(2): p. 221-37.
71. Alvarez, V.A. and B.L. Sabatini, *Anatomical and physiological plasticity of dendritic spines.* Annu Rev Neurosci, 2007. **30**: p. 79-97.
72. Harms, K.J. and A. Dunaevsky, *Dendritic spine plasticity: looking beyond development.* Brain Res, 2007. **1184**: p. 65-71.
73. Holtmaat, A. and K. Svoboda, *Experience-dependent structural synaptic plasticity in the mammalian brain.* Nat Rev Neurosci, 2009. **10**(9): p. 647-58.
74. Hofer, S.B. and T. Bonhoeffer, *Dendritic spines: the stuff that memories are made of?* Curr Biol, 2009. **20**(4): p. R157-9.
75. Hofer, S.B., et al., *Experience leaves a lasting structural trace in cortical circuits.* Nature, 2009. **457**(7227): p. 313-7.
76. Yang, G., F. Pan, and W.B. Gan, *Stably maintained dendritic spines are associated with lifelong memories.* Nature, 2009. **462**(7275): p. 920-4.
77. Xu, T., et al., *Rapid formation and selective stabilization of synapses for enduring motor memories.* Nature, 2009. **462**(7275): p. 915-9.
78. Boeckers, T.M., *The postsynaptic density.* Cell Tissue Res, 2006. **326**(2): p. 409-22.
79. McAllister, A.K., *Dynamic aspects of CNS synapse formation.* Annu Rev Neurosci, 2007. **30**: p. 425-50.
80. Schoch, S. and E.D. Gundelfinger, *Molecular organization of the presynaptic active zone.* Cell Tissue Res, 2006. **326**(2): p. 379-91.
81. Bourne, J.N. and K.M. Harris, *Balancing structure and function at hippocampal dendritic spines.* Annu Rev Neurosci, 2008. **31**: p. 47-67.
82. Nikonenko, I., et al., *Integrins are involved in synaptogenesis, cell spreading, and adhesion in the postnatal brain.* Brain Res Dev Brain Res, 2003. **140**(2): p. 185-94.
83. Shapiro, L., J. Love, and D.R. Colman, *Adhesion molecules in the nervous system: structural insights into function and diversity.* Annu Rev Neurosci, 2007. **30**: p. 451-74.
84. McGeachie, A.B., L.A. Cingolani, and Y. Goda, *Stabilising influence: integrins in regulation of synaptic plasticity.* Neurosci Res, 2011. **70**(1): p. 24-9.
85. Rosenmund, C., J. Rettig, and N. Brose, *Molecular mechanisms of active zone function.* Curr Opin Neurobiol, 2003. **13**(5): p. 509-19.
86. Sudhof, T.C., *The synaptic vesicle cycle.* Annu Rev Neurosci, 2004. **27**: p. 509-47.
87. Matteoli, M., et al., *Vesicle turnover in developing neurons: how to build a presynaptic terminal.* Trends Cell Biol, 2004. **14**(3): p. 133-40.
88. Shupliakov, O. and L. Brodin, *Recent insights into the building and cycling of synaptic vesicles.* Exp Cell Res, 2010. **316**(8): p. 1344-50.
89. Sudhof, T.C. and J. Rizo, *Synaptic vesicle exocytosis.* Cold Spring Harb Perspect Biol, 2011. **3**(12).
90. Becherer, U. and J. Rettig, *Vesicle pools, docking, priming, and release.* Cell Tissue Res, 2006. **326**(2): p. 393-407.
91. Dingledine, R., et al., *The glutamate receptor ion channels.* Pharmacol Rev, 1999. **51**(1): p. 7-61.
92. Ferraguti, F. and R. Shigemoto, *Metabotropic glutamate receptors.* Cell Tissue Res, 2006. **326**(2): p. 483-504.
93. Gurevich, V.V. and E.V. Gurevich, *GPCR monomers and oligomers: it takes all kinds.* Trends Neurosci, 2008. **31**(2): p. 74-81.
94. Rao, V.R., et al., *AMPA receptors regulate transcription of the plasticity-related immediate-early gene Arc.* Nat Neurosci, 2006. **9**(7): p. 887-95.
95. Kohr, G., *NMDA receptor function: subunit composition versus spatial distribution.* Cell Tissue Res, 2006. **326**(2): p. 439-46.
96. Anggono, V. and R.L. Huganir, *Regulation of AMPA receptor trafficking and synaptic plasticity.* Curr Opin Neurobiol, 2012. **22**(3): p. 461-9.
97. Mohler, H., *GABA(A) receptor diversity and pharmacology.* Cell Tissue Res, 2006. **326**(2): p. 505-16.

98. Sala, C., I. Cambianica, and F. Rossi, *Molecular mechanisms of dendritic spine development and maintenance.* Acta Neurobiol Exp (Wars), 2008. **68**(2): p. 289-304.
99. von Bohlen Und Halbach, O., *Structure and function of dendritic spines within the hippocampus.* Ann Anat, 2009. **191**(6): p. 518-31.
100. Huang, Z.J. and P. Scheiffele, *GABA and neuroligin signaling: linking synaptic activity and adhesion in inhibitory synapse development.* Curr Opin Neurobiol, 2008. **18**(1): p. 77-83.
101. Fritschy, J.M., P. Panzanelli, and S.K. Tyagarajan, *Molecular and functional heterogeneity of GABAergic synapses.* Cell Mol Life Sci, 2012. **69**(15): p. 2485-99.
102. Zheng, C.Y., et al., *MAGUKs, synaptic development, and synaptic plasticity.* Neuroscientist, 2011. **17**(5): p. 493-512.
103. Iasevoli, F., C. Tomasetti, and A. de Bartolomeis, *Scaffolding proteins of the post-synaptic density contribute to synaptic plasticity by regulating receptor localization and distribution: relevance for neuropsychiatric diseases.* Neurochem Res, 2013. **38**(1): p. 1-22.
104. Alonso, M., J.H. Medina, and L. Pozzo-Miller, *ERK1/2 activation is necessary for BDNF to increase dendritic spine density in hippocampal CA1 pyramidal neurons.* Learn Mem, 2004. **11**(2): p. 172-8.
105. Patterson, M.A., E.M. Szatmari, and R. Yasuda, *AMPA receptors are exocytosed in stimulated spines and adjacent dendrites in a Ras-ERK-dependent manner during long-term potentiation.* Proc Natl Acad Sci U S A, 2010. **107**(36): p. 15951-6.
106. Shioda, N., et al., *Aberrant calcium/calmodulin-dependent protein kinase II (CaMKII) activity is associated with abnormal dendritic spine morphology in the ATRX mutant mouse brain.* J Neurosci, 2011. **31**(1): p. 346-58.
107. El Gaamouch, F., et al., *Interaction between alphaCaMKII and GluN2B controls ERK-dependent plasticity.* J Neurosci, 2012. **32**(31): p. 10767-79.
108. Tada, T. and M. Sheng, *Molecular mechanisms of dendritic spine morphogenesis.* Curr Opin Neurobiol, 2006. **16**(1): p. 95-101.
109. Ethell, I.M. and E.B. Pasquale, *Molecular mechanisms of dendritic spine development and remodeling.* Prog Neurobiol, 2005. **75**(3): p. 161-205.
110. Dillon, C. and Y. Goda, *The actin cytoskeleton: integrating form and function at the synapse.* Annu Rev Neurosci, 2005. **28**: p. 25-55.
111. Yoshihara, Y., M. De Roo, and D. Muller, *Dendritic spine formation and stabilization.* Curr Opin Neurobiol, 2009. **19**(2): p. 146-53.
112. Ramachandran, B. and J.U. Frey, *Interfering with the actin network and its effect on long-term potentiation and synaptic tagging in hippocampal CA1 neurons in slices in vitro.* J Neurosci, 2009. **29**(39): p. 12167-73.
113. Nakamura, Y., et al., *PICK1 inhibition of the Arp2/3 complex controls dendritic spine size and synaptic plasticity.* EMBO J, 2011. **30**(4): p. 719-30.
114. Murakoshi, H., H. Wang, and R. Yasuda, *Local, persistent activation of Rho GTPases during plasticity of single dendritic spines.* Nature, 2011. **472**(7341): p. 100-4.
115. Knott, G.W., et al., *Spine growth precedes synapse formation in the adult neocortex in vivo.* Nat Neurosci, 2006. **9**(9): p. 1117-24.
116. Honkura, N., et al., *The subspine organization of actin fibers regulates the structure and plasticity of dendritic spines.* Neuron, 2008. **57**(5): p. 719-29.
117. Korobova, F. and T. Svitkina, *Molecular architecture of synaptic actin cytoskeleton in hippocampal neurons reveals a mechanism of dendritic spine morphogenesis.* Mol Biol Cell, 2010. **21**(1): p. 165-76.
118. Kennedy, M.J. and M.D. Ehlers, *Organelles and trafficking machinery for postsynaptic plasticity.* Annu Rev Neurosci, 2006. **29**: p. 325-62.
119. Ostroff, L.E., et al., *Polyribosomes redistribute from dendritic shafts into spines with enlarged synapses during LTP in developing rat hippocampal slices.* Neuron, 2002. **35**(3): p. 535-45.

120. Knott, G. and A. Holtmaat, *Dendritic spine plasticity--current understanding from in vivo studies.* Brain Res Rev, 2008. **58**(2): p. 282-9.
121. Bloodgood, B.L. and B.L. Sabatini, *Ca(2+) signaling in dendritic spines.* Curr Opin Neurobiol, 2007. **17**(3): p. 345-51.
122. Bosch, M. and Y. Hayashi, *Structural plasticity of dendritic spines.* Curr Opin Neurobiol, 2012. **22**(3): p. 383-8.
123. Chen, Y. and B.L. Sabatini, *Signaling in dendritic spines and spine microdomains.* Curr Opin Neurobiol, 2012. **22**(3): p. 389-96.
124. Engert, F. and T. Bonhoeffer, *Dendritic spine changes associated with hippocampal long-term synaptic plasticity.* Nature, 1999. **399**(6731): p. 66-70.
125. Kwon, H.B. and B.L. Sabatini, *Glutamate induces de novo growth of functional spines in developing cortex.* Nature, 2011. **474**(7349): p. 100-4.
126. Okamoto, K., et al., *Rapid and persistent modulation of actin dynamics regulates postsynaptic reorganization underlying bidirectional plasticity.* Nat Neurosci, 2004. **7**(10): p. 1104-12.
127. Otmakhov, N., et al., *Forskolin-induced LTP in the CA1 hippocampal region is NMDA receptor dependent.* J Neurophysiol, 2004. **91**(5): p. 1955-62.
128. Matsuzaki, M., et al., *Structural basis of long-term potentiation in single dendritic spines.* Nature, 2004. **429**(6993): p. 761-6.
129. Zhou, Q., K.J. Homma, and M.M. Poo, *Shrinkage of dendritic spines associated with long-term depression of hippocampal synapses.* Neuron, 2004. **44**(5): p. 749-57.
130. Nagerl, U.V., et al., *Bidirectional activity-dependent morphological plasticity in hippocampal neurons.* Neuron, 2004. **44**(5): p. 759-67.
131. Bonhoeffer, J., et al., *Diagnosis of acute haematogenous osteomyelitis and septic arthritis: 20 years experience at the University Children's Hospital Basel.* Swiss Med Wkly, 2001. **131**(39-40): p. 575-81.
132. Pfeiffer, B.E., et al., *Fragile X mental retardation protein is required for synapse elimination by the activity-dependent transcription factor MEF2.* Neuron, 2010. **66**(2): p. 191-7.
133. Roberts, R.C., et al., *Reduced striatal spine size in schizophrenia: a postmortem ultrastructural study.* Neuroreport, 1996. **7**(6): p. 1214-8.
134. Ito, H., et al., *Dysbindin-1, a schizophrenia-related molecule, is involved in the regulation of neuronal dendritic development.* Mol Psychiatry, 2010. **15**(10): p. 969.
135. Glausier, J.R. and D.A. Lewis, *Dendritic spine pathology in schizophrenia.* Neuroscience, 2013. **251**: p. 90-107.
136. Matus, A., *Actin-based plasticity in dendritic spines.* Science, 2000. **290**(5492): p. 754-8.
137. Malinow, R., Z.F. Mainen, and Y. Hayashi, *LTP mechanisms: from silence to four-lane traffic.* Curr Opin Neurobiol, 2000. **10**(3): p. 352-7.
138. Gu, J., B.L. Firestein, and J.Q. Zheng, *Microtubules in dendritic spine development.* J Neurosci, 2008. **28**(46): p. 12120-4.
139. Lin, W.H. and D.J. Webb, *Actin and Actin-Binding Proteins: Masters of Dendritic Spine Formation, Morphology, and Function.* Open Neurosci J, 2009. **3**: p. 54-66.
140. Ivanov, A., M. Esclapez, and L. Ferhat, *Role of drebrin A in dendritic spine plasticity and synaptic function: Implications in neurological disorders.* Commun Integr Biol, 2009. **2**(3): p. 268-70.
141. Wang, Z., et al., *Myosin Vb mobilizes recycling endosomes and AMPA receptors for postsynaptic plasticity.* Cell, 2008. **135**(3): p. 535-48.
142. Lei, S., et al., *Regulation of NMDA receptor activity by F-actin and myosin light chain kinase.* J Neurosci, 2001. **21**(21): p. 8464-72.
143. Wyszynski, M., et al., *Competitive binding of alpha-actinin and calmodulin to the NMDA receptor.* Nature, 1997. **385**(6615): p. 439-42.
144. Meril, A.J., *Direct current stimulation of allograft in anterior and posterior lumbar interbody fusions.* Spine (Phila Pa 1976), 1994. **19**(21): p. 2393-8.

145. Pollard, T.D. and G.G. Borisy, *Cellular motility driven by assembly and disassembly of actin filaments.* Cell, 2003. **112**(4): p. 453-65.
146. Kaksonen, M., C.P. Toret, and D.G. Drubin, *Harnessing actin dynamics for clathrin-mediated endocytosis.* Nat Rev Mol Cell Biol, 2006. **7**(6): p. 404-14.
147. Carlier, M.F. and D. Pantaloni, *Control of actin assembly dynamics in cell motility.* J Biol Chem, 2007. **282**(32): p. 23005-9.
148. Ackermann, M. and A. Matus, *Activity-induced targeting of profilin and stabilization of dendritic spine morphology.* Nat Neurosci, 2003. **6**(11): p. 1194-200.
149. Fukazawa, Y., et al., *Hippocampal LTP is accompanied by enhanced F-actin content within the dendritic spine that is essential for late LTP maintenance in vivo.* Neuron, 2003. **38**(3): p. 447-60.
150. Star, E.N., D.J. Kwiatkowski, and V.N. Murthy, *Rapid turnover of actin in dendritic spines and its regulation by activity.* Nat Neurosci, 2002. **5**(3): p. 239-46.
151. Kim, C.H. and J.E. Lisman, *A role of actin filament in synaptic transmission and long-term potentiation.* J Neurosci, 1999. **19**(11): p. 4314-24.
152. Krucker, T., G.R. Siggins, and S. Halpain, *Dynamic actin filaments are required for stable long-term potentiation (LTP) in area CA1 of the hippocampus.* Proc Natl Acad Sci U S A, 2000. **97**(12): p. 6856-61.
153. Lisman, J., *Actin's actions in LTP-induced synapse growth.* Neuron, 2003. **38**(3): p. 361-2.
154. Hotulainen, P. and C.C. Hoogenraad, *Actin in dendritic spines: connecting dynamics to function.* J Cell Biol, 2010. **189**(4): p. 619-29.
155. Hering, H. and M. Sheng, *Activity-dependent redistribution and essential role of cortactin in dendritic spine morphogenesis.* J Neurosci, 2003. **23**(37): p. 11759-69.
156. Racz, B. and R.J. Weinberg, *The subcellular organization of cortactin in hippocampus.* J Neurosci, 2004. **24**(46): p. 10310-7.
157. Neuhoff, H., et al., *The actin-binding protein profilin I is localized at synaptic sites in an activity-regulated manner.* Eur J Neurosci, 2005. **21**(1): p. 15-25.
158. Iki, J., et al., *Bi-directional regulation of postsynaptic cortactin distribution by BDNF and NMDA receptor activity.* Eur J Neurosci, 2005. **22**(12): p. 2985-94.
159. Sekino, Y., et al., *Activation of N-methyl-D-aspartate receptor induces a shift of drebrin distribution: disappearance from dendritic spines and appearance in dendritic shafts.* Mol Cell Neurosci, 2006. **31**(3): p. 493-504.
160. Kitanishi, T., et al., *Activity-dependent localization in spines of the F-actin capping protein CapZ screened in a rat model of dementia.* Genes Cells, 2010. **15**(7): p. 737-47.
161. Seese, R.R., et al., *LTP induction translocates cortactin at distant synapses in wild-type but not Fmr1 knock-out mice.* J Neurosci, 2012. **32**(21): p. 7403-13.
162. Bae, J., et al., *F-actin-dependent regulation of NESH dynamics in rat hippocampal neurons.* PLoS One, 2012. **7**(4): p. e34514.
163. Lamprecht, R., et al., *Fear conditioning drives profilin into amygdala dendritic spines.* Nat Neurosci, 2006. **9**(4): p. 481-3.
164. Feng, J., et al., *Spinophilin regulates the formation and function of dendritic spines.* Proc Natl Acad Sci U S A, 2000. **97**(16): p. 9287-92.
165. Wegner, A.M., et al., *N-wasp and the arp2/3 complex are critical regulators of actin in the development of dendritic spines and synapses.* J Biol Chem, 2008. **283**(23): p. 15912-20.
166. Hotulainen, P., et al., *Defining mechanisms of actin polymerization and depolymerization during dendritic spine morphogenesis.* J Cell Biol, 2009. **185**(2): p. 323-39.
167. Grove, M., et al., *ABI2-deficient mice exhibit defective cell migration, aberrant dendritic spine morphogenesis, and deficits in learning and memory.* Mol Cell Biol, 2004. **24**(24): p. 10905-22.
168. Wu, S.H., et al., *Ankyrin Repeat-rich Membrane Spanning/Kidins220 protein regulates dendritic branching and spine stability in vivo.* Dev Neurobiol, 2009. **69**(9): p. 547-57.

169. Koshimizu, H., et al., *Multiple functions of precursor BDNF to CNS neurons: negative regulation of neurite growth, spine formation and cell survival.* Mol Brain, 2009. **2**: p. 27.
170. Muhia, M., et al., *Disruption of hippocampus-regulated behavioural and cognitive processes by heterozygous constitutive deletion of SynGAP.* Eur J Neurosci, 2010

31(3): p. 529-43.
171. Ramakers, G.J., *Rho proteins, mental retardation and the cellular basis of cognition.* Trends Neurosci, 2002. **25**(4): p. 191-9.
172. Weitzdoerfer, R., M. Fountoulakis, and G. Lubec, *Reduction of actin-related protein complex 2/3 in fetal Down syndrome brain.* Biochem Biophys Res Commun, 2002. **293**(2): p. 836-41.
173. van Galen, E.J. and G.J. Ramakers, *Rho proteins, mental retardation and the neurobiological basis of intelligence.* Prog Brain Res, 2005. **147**: p. 295-317.
174. Maloney, M.T. and J.R. Bamburg, *Cofilin-mediated neurodegeneration in Alzheimer's disease and other amyloidopathies.* Mol Neurobiol, 2007. **35**(1): p. 21-44.
175. Ropers, F., et al., *Identification of a novel candidate gene for non-syndromic autosomal recessive intellectual disability: the WASH complex member SWIP.* Hum Mol Genet, 2011. **20**(13): p. 2585-90.
176. Ziv, N.E. and S.J. Smith, *Evidence for a role of dendritic filopodia in synaptogenesis and spine formation.* Neuron, 1996. **17**(1): p. 91-102.
177. Fiala, J.C., et al., *Synaptogenesis via dendritic filopodia in developing hippocampal area CA1.* J Neurosci, 1998. **18**(21): p. 8900-11.
178. Dunaevsky, A., et al., *Developmental regulation of spine motility in the mammalian central nervous system.* Proc Natl Acad Sci U S A, 1999. **96**(23): p. 13438-43.
179. Tashiro, A., et al., *Bidirectional regulation of hippocampal mossy fiber filopodial motility by kainate receptors: a two-step model of synaptogenesis.* Neuron, 2003. **38**(5): p. 773-84.
180. Evers, J.F., D. Muench, and C. Duch, *Developmental relocation of presynaptic terminals along distinct types of dendritic filopodia.* Dev Biol, 2006. **297**(1): p. 214-27.
181. Luscher, C., et al., *Synaptic plasticity and dynamic modulation of the postsynaptic membrane.* Nat Neurosci, 2000. **3**(6): p. 545-50.
182. Jourdain, P., K. Fukunaga, and D. Muller, *Calcium/calmodulin-dependent protein kinase II contributes to activity-dependent filopodia growth and spine formation.* J Neurosci, 2003. **23**(33): p. 10645-9.
183. Jontes, J.D. and S.J. Smith, *Filopodia, spines, and the generation of synaptic diversity.* Neuron, 2000. **27**(1): p. 11-4.
184. Faix, J., et al., *Filopodia: Complex models for simple rods.* Int J Biochem Cell Biol, 2009. **41**(8-9): p. 1656-64.
185. Faix, J. and K. Rottner, *The making of filopodia.* Curr Opin Cell Biol, 2006. **18**(1): p. 18-25.
186. Korobova, F. and T. Svitkina, *Arp2/3 complex is important for filopodia formation, growth cone motility, and neuritogenesis in neuronal cells.* Mol Biol Cell, 2008. **19**(4): p. 1561-74.
187. Pollard, T.D., *Regulation of actin filament assembly by Arp2/3 complex and formins.* Annu Rev Biophys Biomol Struct, 2007. **36**: p. 451-77.
188. Akin, O. and R.D. Mullins, *Capping protein increases the rate of actin-based motility by promoting filament nucleation by the Arp2/3 complex.* Cell, 2008. **133**(5): p. 841-51.
189. Mogilner, A. and B. Rubinstein, *The physics of filopodial protrusion.* Biophys J, 2005. **89**(2): p. 782-95.
190. Fazioli, F., et al., *Eps8, a substrate for the epidermal growth factor receptor kinase, enhances EGF-dependent mitogenic signals.* EMBO J, 1993. **12**(10): p. 3799-808.
191. Metello Innocenti, E.F., Isabella Ponzanelli, John R. Falck, Saskia M. Brachmann, Pier Paolo Di Fiore and Giorgio Scita, *Phosphoinositide 3-kinase activates Rac by enetering in a complex with Eps8, Abi1 and Sos-1.* The Journal of Cell Biology, 2003

192. Scita, G., et al., *An effector region in Eps8 is responsible for the activation of the Rac-specific GEF activity of Sos-1 and for the proper localization of the Rac-based actin-polymerizing machine.* J Cell Biol, 2001. **154**(5): p. 1031-44.
193. Di Fiore, P.P. and G. Scita, *Eps8 in the midst of GTPases.* Int J Biochem Cell Biol, 2002. **34**(10): p. 1178-83.
194. Heasman, S.J. and A.J. Ridley, *Mammalian Rho GTPases: new insights into their functions from in vivo studies.* Nat Rev Mol Cell Biol, 2008. **9**(9): p. 690-701.
195. Disanza, A., et al., *Eps8 controls actin-based motility by capping the barbed ends of actin filaments.* Nat Cell Biol, 2004. **6**(12): p. 1180-8.
196. Disanza, A., et al., *Regulation of cell shape by Cdc42 is mediated by the synergic actin-bundling activity of the Eps8-IRSp53 complex.* Nat Cell Biol, 2006. **8**(12): p. 1337-47.
197. Hertzog, M., et al., *Molecular basis for the dual function of Eps8 on actin dynamics: bundling and capping.* PLoS Biol, 2010. **8**(6): p. e1000387.
198. Abbott, M.A., D.G. Wells, and J.R. Fallon, *The insulin receptor tyrosine kinase substrate p58/53 and the insulin receptor are components of CNS synapses.* J Neurosci, 1999. **19**(17): p. 7300-8.
199. Oda, K., et al., *Identification of BAIAP2 (BAI-associated protein 2), a novel human homologue of hamster IRSp53, whose SH3 domain interacts with the cytoplasmic domain of BAI1.* Cytogenet Cell Genet, 1999. **84**(1-2): p. 75-82.
200. Proepper, C., et al., *Abelson interacting protein 1 (Abi-1) is essential for dendrite morphogenesis and synapse formation.* EMBO J, 2007. **26**(5): p. 1397-409.
201. Proepper, C., et al., *Heterogeneous nuclear ribonucleoprotein k interacts with Abi-1 at postsynaptic sites and modulates dendritic spine morphology.* PLoS One, 2011. **6**(11): p. e27045.
202. Croce, A., et al., *A novel actin barbed-end-capping activity in EPS-8 regulates apical morphogenesis in intestinal cells of Caenorhabditis elegans.* Nat Cell Biol, 2004. **6**(12): p. 1173-9.
203. Offenhauser, N., et al., *Increased ethanol resistance and consumption in Eps8 knockout mice correlates with altered actin dynamics.* Cell, 2006. **127**(1): p. 213-26.
204. Sekerkova, G., et al., *Postsynaptic enrichment of Eps8 at dendritic shaft synapses of unipolar brush cells in rat cerebellum.* Neuroscience, 2007. **145**(1): p. 116-29.
205. Cohen-Cory, S., et al., *Brain-derived neurotrophic factor and the development of structural neuronal connectivity.* Dev Neurobiol, 2010. **70**(5): p. 271-88.
206. Gottmann, K., T. Mittmann, and V. Lessmann, *BDNF signaling in the formation, maturation and plasticity of glutamatergic and GABAergic synapses.* Exp Brain Res, 2009. **199**(3-4): p. 203-34.
207. Kuczewski, N., C. Porcher, and J.L. Gaiarsa, *Activity-dependent dendritic secretion of brain-derived neurotrophic factor modulates synaptic plasticity.* Eur J Neurosci, 2010. **32**(8): p. 1239-44.
208. Nishimura, K., et al., *Genetic analyses of the brain-derived neurotrophic factor (BDNF) gene in autism.* Biochem Biophys Res Commun, 2007. **356**(1): p. 200-6.
209. Garcia, K.L., et al., *Altered balance of proteolytic isoforms of pro-brain-derived neurotrophic factor in autism.* J Neuropathol Exp Neurol, 2012. **71**(4): p. 289-97.
210. Scattoni, M.L., et al., *Reduced social interaction, behavioural flexibility and BDNF signalling in the BTBR T+ tf/J strain, a mouse model of autism.* Behav Brain Res, 2013. **251**: p. 35-40.
211. Genoud, C., et al., *Altered synapse formation in the adult somatosensory cortex of brain-derived neurotrophic factor heterozygote mice.* J Neurosci, 2004. **24**(10): p. 2394-400.
212. An, J.J., et al., *Distinct role of long 3' UTR BDNF mRNA in spine morphology and synaptic plasticity in hippocampal neurons.* Cell, 2008. **134**(1): p. 175-87.
213. Cunha, C., et al., *Brain-derived neurotrophic factor (BDNF) overexpression in the forebrain results in learning and memory impairments.* Neurobiol Dis, 2009. **33**(3): p. 358-68.

214. Laudes, T., et al., *Impaired transmission at corticothalamic excitatory inputs and intrathalamic GABAergic synapses in the ventrobasal thalamus of heterozygous BDNF knockout mice.* Neuroscience, 2012. **222**: p. 215-27.
215. Vaggi, F., et al., *The Eps8/IRSp53/VASP network differentially controls actin capping and bundling in filopodia formation.* PLoS Comput Biol, 2011. **7**(7): p. e1002088.
216. Falck, S., et al., *Biological role and structural mechanism of twinfilin-capping protein interaction.* EMBO J, 2004. **23**(15): p. 3010-9.
217. Amatruda, J.F., et al., *Effects of null mutations and overexpression of capping protein on morphogenesis, actin distribution and polarized secretion in yeast.* J Cell Biol, 1992. **119**(5): p. 1151-62.
218. Schafer, D.A., M.S. Mooseker, and J.A. Cooper, *Localization of capping protein in chicken epithelial cells by immunofluorescence and biochemical fractionation.* J Cell Biol, 1992. **118**(2): p. 335-46.
219. Huang, C.H., et al., *Extra-cellular signal-regulated kinase 1/2 (ERK1/2) activated in the hippocampal CA1 neurons is critical for retrieval of auditory trace fear memory.* Brain Res, 2010. **1326**: p. 143-51.
220. Kelly, A., S. Laroche, and S. Davis, *Activation of mitogen-activated protein kinase/extracellular signal-regulated kinase in hippocampal circuitry is required for consolidation and reconsolidation of recognition memory.* J Neurosci, 2003. **23**(12): p. 5354-60.
221. Samuels, I.S., et al., *Deletion of ERK2 mitogen-activated protein kinase identifies its key roles in cortical neurogenesis and cognitive function.* J Neurosci, 2008. **28**(27): p. 6983-95.
222. Lee, J.A., et al., *Objective measurement of periocular pigmentation.* Photodermatol Photoimmunol Photomed, 2008. **24**(6): p. 285-90.
223. Deacon, R.M., *Assessing nest building in mice.* Nat Protoc, 2006. **1**(3): p. 1117-9.
224. Irwin, S., *Comprehensive observational assessment: Ia. A systematic, quantitative procedure for assessing the behavioral and physiologic state of the mouse.* Psychopharmacologia, 1968. **13**(3): p. 222-57.
225. Corradini, I., et al., *Epileptiform Activity and Cognitive Deficits in SNAP-25+/- Mice are Normalized by Antiepileptic Drugs.* Cereb Cortex, 2012.
226. Jero, J., D.E. Coling, and A.K. Lalwani, *The use of Preyer's reflex in evaluation of hearing in mice.* Acta Otolaryngol, 2001. **121**(5): p. 585-9.
227. Brandewiede, J., M. Schachner, and F. Morellini, *Ethological analysis of the senescence-accelerated P/8 mouse.* Behav Brain Res, 2005. **158**(1): p. 109-21.
228. Moy, S.S., et al., *Sociability and preference for social novelty in five inbred strains: an approach to assess autistic-like behavior in mice.* Genes Brain Behav, 2004. **3**(5): p. 287-302.
229. Moy, S.S., et al., *Social approach and repetitive behavior in eleven inbred mouse strains.* Behav Brain Res, 2008. **191**(1): p. 118-29.
230. Pitsikas, N., et al., *Effects of molsidomine on scopolamine-induced amnesia and hypermotility in the rat.* Eur J Pharmacol, 2001. **426**(3): p. 193-200.
231. Sala, M., et al., *Pharmacologic rescue of impaired cognitive flexibility, social deficits, increased aggression, and seizure susceptibility in oxytocin receptor null mice: a neurobehavioral model of autism.* Biol Psychiatry, 2011. **69**(9): p. 875-82.
232. DeVito, L.M., et al., *Vasopressin 1b receptor knock-out impairs memory for temporal order.* J Neurosci, 2009. **29**(9): p. 2676-83.
233. Manfredi, I., et al., *Expression of mutant beta2 nicotinic receptors during development is crucial for epileptogenesis.* Hum Mol Genet, 2009. **18**(6): p. 1075-88.
234. Zhang, Y., et al., *Elevated thalamic low-voltage-activated currents precede the onset of absence epilepsy in the SNAP25-deficient mouse mutant coloboma.* J Neurosci, 2004. **24**(22): p. 5239-48.
235. Banker, G.A. and W.M. Cowan, *Rat hippocampal neurons in dispersed cell culture.* Brain Res, 1977. **126**(3): p. 397-42.

236. Bartlett, W.P. and G.A. Banker, *An electron microscopic study of the development of axons and dendrites by hippocampal neurons in culture. I. Cells which develop without intercellular contacts.* J Neurosci, 1984. **4**(8): p. 1944-53.
237. Livak, K.J. and T.D. Schmittgen, *Analysis of relative gene expression data using real-time quantitative PCR and the 2(-Delta Delta C(T)) Method.* Methods, 2001. **25**(4): p. 402-8.
238. Glaser, E.M. and H. Van der Loos, *Analysis of thick brain sections by obverse-reverse computer microscopy: application of a new, high clarity Golgi-Nissl stain.* J Neurosci Methods, 1981. **4**(2): p. 117-25.
239. Frassoni, C., et al., *Analysis of SNAP-25 immunoreactivity in hippocampal inhibitory neurons during development in culture and in situ.* Neuroscience, 2005. **131**(4): p. 813-23.
240. Schultz, R.T., et al., *Abnormal ventral temporal cortical activity during face discrimination among individuals with autism and Asperger syndrome.* Arch Gen Psychiatry, 2000. **57**(4): p. 331-40.
241. Lord, C., M. Rutter, and A. Le Couteur, *Autism Diagnostic Interview-Revised: a revised version of a diagnostic interview for caregivers of individuals with possible pervasive developmental disorders.* J Autism Dev Disord, 1994. **24**(5): p. 659-85.
242. Fahnestock, M., et al., *The precursor pro-nerve growth factor is the predominant form of nerve growth factor in brain and is increased in Alzheimer's disease.* Mol Cell Neurosci, 2001. **18**(2): p. 210-20.
243. Kawaja, M.D., et al., *Nerve growth factor promoter activity revealed in mice expressing enhanced green fluorescent protein.* J Comp Neurol, 2011. **519**(13): p. 2522-45.
244. Sweet, E.S., C.Y. Tseng, and B.L. Firestein, *To branch or not to branch: How PSD-95 regulates dendrites and spines.* Bioarchitecture, 2011. **1**(2): p. 69-73.
245. Sheng, M. and E. Kim, *The postsynaptic organization of synapses.* Cold Spring Harb Perspect Biol, 2011. **3**(12).
246. Gray, N.W., et al., *Rapid redistribution of synaptic PSD-95 in the neocortex in vivo.* PLoS Biol, 2006. **4**(11): p. e370.
247. Lu, W., et al., *Activation of synaptic NMDA receptors induces membrane insertion of new AMPA receptors and LTP in cultured hippocampal neurons.* Neuron, 2001. **29**(1): p. 243-54.
248. Fortin, D.A., et al., *Long-term potentiation-dependent spine enlargement requires synaptic Ca2+-permeable AMPA receptors recruited by CaM-kinase I.* J Neurosci, 2010. **30**(35): p. 11565-75.
249. Arancio, O., et al., *Nitric oxide acts directly in the presynaptic neuron to produce long-term potentiation in cultured hippocampal neurons.* Cell, 1996. **87**(6): p. 1025-35.
250. Mongiovi, A.M., et al., *A novel peptide-SH3 interaction.* EMBO J, 1999. **18**(19): p. 5300-9.
251. Tanaka, J., et al., *Protein synthesis and neurotrophin-dependent structural plasticity of single dendritic spines.* Science, 2008. **319**(5870): p. 1683-7.
252. Chapleau, C.A., et al., *Dendritic spine pathologies in hippocampal pyramidal neurons from Rett syndrome brain and after expression of Rett-associated MECP2 mutations.* Neurobiol Dis, 2009. **35**(2): p. 219-33.
253. Hadjikhani, N., et al., *Activation of the fusiform gyrus when individuals with autism spectrum disorder view faces.* Neuroimage, 2004. **22**(3): p. 1141-50.
254. Schultz, R.T., *Developmental deficits in social perception in autism: the role of the amygdala and fusiform face area.* Int J Dev Neurosci, 2005. **23**(2-3): p. 125-41.
255. Lamprecht, R. and J. LeDoux, *Structural plasticity and memory.* Nat Rev Neurosci, 2004. **5**(1): p. 45-54.
256. Soderling, S.H., et al., *A WAVE-1 and WRP signaling complex regulates spine density, synaptic plasticity, and memory.* J Neurosci, 2007. **27**(2): p. 355-65.
257. Yang, C., et al., *Coordination of membrane and actin cytoskeleton dynamics during filopodia protrusion.* PLoS One, 2009. **4**(5): p. e5678.

258. Nusser, Z., et al., *Cell type and pathway dependence of synaptic AMPA receptor number and variability in the hippocampus.* Neuron, 1998. **21**(3): p. 545-59.
259. Matsuzaki, M., *Factors critical for the plasticity of dendritic spines and memory storage.* Neurosci Res, 2007. **57**(1): p. 1-9.
260. Tsuriel, S., et al., *Exchange and redistribution dynamics of the cytoskeleton of the active zone molecule bassoon.* J Neurosci, 2009. **29**(2): p. 351-8.
261. Zheng, C.Y., et al., *SAP102 is a highly mobile MAGUK in spines.* J Neurosci, 2010. **30**(13): p. 4757-66.
262. Stamatakou, E., et al., *Activity-dependent spine morphogenesis: a role for the actin-capping protein Eps8.* J Neurosci, 2013. **33**(6): p. 2661-70.
263. Schafer, D.A., C. Hug, and J.A. Cooper, *Inhibition of CapZ during myofibrillogenesis alters assembly of actin filaments.* J Cell Biol, 1995. **128**(1-2): p. 61-70.
264. Davis, D.A., et al., *Capzb2 interacts with beta-tubulin to regulate growth cone morphology and neurite outgrowth.* PLoS Biol, 2009. **7**(10): p. e1000208.
265. Kelleher, R.J., 3rd and M.F. Bear, *The autistic neuron: troubled translation?* Cell, 2008. **135**(3): p. 401-6.
266. Bourgeron, T., *A synaptic trek to autism.* Curr Opin Neurobiol, 2009. **19**(2): p. 231-4.
267. Pinto, D., et al., *Functional impact of global rare copy number variation in autism spectrum disorders.* Nature, 2010. **466**(7304): p. 368-72.
268. Gulesserian, T., et al., *Aberrant expression of centractin and capping proteins, integral constituents of the dynactin complex, in fetal down syndrome brain.* Biochem Biophys Res Commun, 2002. **291**(1): p. 62-7.